Multicast and Relay Beamforming in Wireless Multi-User Networks

Vom Fachbereich Elektrotechnik und Informationstechnik
der Technischen Universität Darmstadt
zur Erlangung des akademischen Grades eines
Doktor-Ingenieurs (Dr.-Ing.)
genehmigte Dissertation

von

Ahmed Abdelkader, M.Sc.

Geboren am 11. April 1980 in Alexandria, Ägypten

Referent:	Prof. Dr.-Ing. Marius Pesavento
Korreferent:	Prof. Dr.-Ing. Abdelhak Zoubir
Tag der Einreichung:	20. April 2012
Tag der mündlichen Prüfung:	2. Juli 2012

D17

Darmstadt 2012

"And mankind have not been given of knowledge except a little."

To Allah and my parents

To my family members

And...to wife, my supporter, my inspirer, and my companion in the long journey

Acknowledgments

First and foremost, I would like to express my deepest gratitude to my supervisors, Prof. Dr.-Ing. Marius Pesavento and Prof. Dr. Alex Gershman, for all the support and guidance they have offered me during my PhD study. I am very much grateful for the knowledge they have shared with me throughout the development of my thesis and academic papers. I would also like to gratefully thank and acknowledge my co-supervisor in the Graduate School of Computational Engineering Prof. Dr.-Ing. Abdelhak Zoubir for his trust in me and for his support and encouragement. Many thanks to Prof. Dr. Shahram Shahbazpanahi for his contribution to this work and all the interesting discussions and helpful comments and suggestions. Special thanks to all the members of the Communication Systems Group who contributed in one way or another in the successful completion of this work. I would like to thank the Graduate School of Computational Engineering for the prestigious scholarship that I received during my Ph.D. study. Finally, I am grateful to my family members for their support and encouragement.

Ahmed

Zusammenfassung

Zahlreiche Anwendungen wie mobiles Fernsehen und Podcasts erfordern die parallele Verbreitung von Daten an mehrere Nutzer. Drahtlose Multicast-Verfahren ermöglichen dies in einer effizienten Weise, indem die für eine Gruppe von Nutzern bestimmten Daten und Services diesen simultan zugestellt werden. Aus diesem Grund spielen drahtlose Multicast-Verfahren eine wichtige Rolle für zukünftige zellulare Mobilfunksysteme. In modernen Mobilfunksystemen werden Mehrantennensysteme eingesetzt, um eine hohe spektrale Effizienz zu erreichen. Im Fall von Mehrantennensystemen können Beamformingverfahren verwendet werden, um unterschiedlicher Nachrichten gleichzeitig jedoch räumlich unterschiedlich abgestrahlt werden.

In dieser Arbeit entwickeln wir recheneffiziente Beamformingalgorithmen für Multicast-Systeme. Die vorgeschlagenen Algorithmen erreichen einen verbesserten Kompromiss zwischen Sendeleistung und Rechenkomplexität im Vergleich mit existierenden Verfahren.

Zuerst untersuchen wir Single-Group Multicast-Systeme, in denen alle Nutzer dieselben Daten empfangen. Wir entwickeln ein neues Verfahren zur näherungsweisen Minimierung der Sendeleistung unter Nebenbedingungen für die Signal-zu-Rauschverhältnisse an den Empfängern. Das vorgeschlagene Verfahren beruht auf der Orthogonalisierung der Kanalsignaturen einzelner Nutzer. Es erreicht einen verbesserten Kompromiss zwischen Sendeleistung und Rechenkomplexität im Vergleich mit existierenden Algorithmen für Single-Group Multicast-Systeme.

Als nächstes betrachten wir Multi-Group Multicast-Systeme, bei denen unterschiedliche Daten an mehrere Gruppen von Nutzern gesendet werden. Wir schlagen ein neues Multicast-Verfahren vor, bei dem eine geringe Sendeleistung mittels einer hierarchischen Modulation erreicht wird. Das vorgeschlagene Verfahren hat einen geringeren Rechenaufwand und führt zu einer niedrigeren Sendeleistung im Vergleich zu existierenden Verfahren.

Danach erweitern wir das für Mehrantennensysteme vorgeschlagene Kanal-Orthogonalisierungsverfahren auf nicht triviale Weise für den Einsatz in kooperative Relaynetze. Auch in dieser Anwendung lsst sich mit dem vorgeschlagenen Verfahren eine geringe Rechenkomplexität und eine niedrigere Sendeleistung als die bekannten Verfahren für kooperative Relaynetze erzielen.

Schließlich entwickeln wir verteiltes Beamformingverfahren für nicht synchronisierte kooperativen Relaynetzen. Wir verwenden ein orthogonale Frequenzmultiplexverfahren, um die Intersymbolinterferenz am Empfänger zu vermeiden, ohne Verzögerungsglieder an den Relays zu benötigen. Dadurch wird der für vollständig synchronisierte Relaynetze ansonsten erforderliche Signalisierungsoverhead vermieden. Wir vergleichen dann die erforderliche Sendeleistungen für das vorgeschlagene Verfahren mit der Sendeleistung für ein vollständig synchronisiertes Relaynetzwerk.

Abstract

Many of the current and future Internet and digital multimedia applications such as Internet TV, streaming media, and localized services rely on the concept of mass content distribution. Wireless multicasting enable this in an efficient way, since it allows the provision of data and services to a group of users simultaneously using the same frequency band. In this context, wireless multicasting has emerged as a key technology for the next generation cellular and indoor/outdoor wireless networks. Several techniques have been proposed to enhance the spectral efficiency of the wireless multicast network while meeting the quality of service requirements of the network users. One of the most promising techniques is transmit beamforming, since it allows the exploitation of space as a resource at the transmitter in addition to the conventional resources such as time and frequency.

In this thesis, we develop computationally efficient techniques to solve the beamforming problem for single-group and multi-group multicast networks. Our proposed techniques offer improved trade-off between performance in terms of transmitted power and computational complexity.

First, the beamforming problem for single-group multicasting is considered, where all users receive the same datastream. The design approach is based on power minimization subject to individual signal-to-noise-ratio constraints at each user. We propose a channel orthogonalization and local refinement technique to efficiently solve

this problem in an approximate way. The proposed techniques are shown to offer an attractive performance-to-complexity tradeoff as compared to state-of-the-art multiple-antenna multicasting algorithms.

Next, we consider the beamforming problem for multi-group multicasting, where different datastreams are sent to multiple groups of users. A new approach is proposed to solve the power minimization problem using hierarchical modulation. The proposed approach enjoys a significantly reduced computational complexity and achieves a better performance in terms of the total transmitted power compared to the conventional approaches.

Then, a non trivial extension of the channel orthogonalization-based approach, which was developed to approximately solve the beamforming problem for conventional single-group multicasting is proposed to the beamforming problem in single-group multicasting in cooperative relay networks. Similarly as in the previous network, the proposed technique has a small computational complexity and achieves a better performance in terms of transmitted power compared to other existing techniques.

Finally, we propose a solution to the relay synchronization problem in cooperative relay networks with large delay spread. The proposed approach uses orthogonal frequency division multiplexing techniques to eliminate the effects of inter-symbol interference at the destination without applying artificial delays at the relays. In this approach, the additional traffic requirements of a fully synchronized relay network is completely avoided. The performance of the proposed scheme in terms of transmitted power is then compared to the performance of a fully synchronized relay network.

Table of Contents

List of Figures

List of Tables

Notations

a	the scalar a
$\mathbf{a}$	the vector $\mathbf{a}$
$\mathbf{A}$	the matrix $\mathbf{A}$
$[\mathbf{a}]_i$	the ith entry of $\mathbf{a}$
$[\mathbf{A}]_{ij}$	the (i,j)th entry of $\mathbf{A}$
$\mathbf{A} \succeq 0$	$\mathbf{A}$ is positive semi-definite
$a \sim \mathcal{NC}(\mu, \sigma^2)$	a is circular complex Gaussian distribution random variable with mean μ and variance σ^2
$\text{diag}(\mathbf{A})$	the diagonal matrix composed of the diagonal entries of $\mathbf{A}$
$E\{\cdot\}$	the statistical expectation operator
$\text{rank}\{\cdot\}$	the rank of of a matrix
$\mathcal{P}\{\cdot\}$	the normalized principal eigenvector of a matrix
$\|\cdot\|$	the L-2 norm of a vector or Frobenius norm of a matrix
$\|\cdot\|$	the absolute value of a complex variable
$\mathbf{I}_n$	the $n \times n$ identity matrix
$\text{trace}\{\cdot\}$	the trace of a matrix
$\otimes$	the Kronecker matrix product
$\odot$	the Hadamard matrix product
$(\cdot)^T$	the transpose operator
$(\cdot)^*$	the complex conjugate operator
$(\cdot)^H$	the transpose complex conjugate (Hermitian) operator
$\text{Re}(\cdot)$	the real part of a complex value

$\mathrm{Im}(\cdot)$	the imaginary part of a complex value
$\in$	membership in a set
$\lvert \cdot \rvert_S$	the cardinality of a set
$\log_{10}(\cdot)$	the logarithm to the base 10
$\hat{(\cdot)}$	the estimated value
$\mathcal{O}(\cdot)$	the big O notation
$\delta(t)$	the Kronecker delta function

Acronyms

3G	third generation of mobile systems
3GGP	the third generation partnership project
4G	fourth generation of mobile systems
AF	amplify-and-forward
AWGN	additive white Gaussian noise
BD	block diagonalization
BER	bit error rate
BS	base station
CDMA	code-division multiple access
CP	cyclic prefix
CSI	channel state information
DF	decode-and-forward
dL	damped Lozano
dLLI	damped Lozano with Lopez Initialization
DPC	dirty paper coding
eMBMS	enhanced media broadcast/multicast services
FDMA	frequency-division multiple access
FFT	fast Fourier transform
FIR	finite impulse response
GSM	Global System for Mobile communications
i.i.d	independent and identically distributed
ISD	iterative spatial diagonalization

ISI	inter-symbol-interference
LOS	line-of-sight
LTE	Long Term Evolution
MA	multiple access
MAI	multiple access interference
MBMS	media broadcast/ multicast services
MIMO	multiple-input multiple-output
MMSE	minimum mean square error
MSE	mean square error
MS	mobile station
OFDM	orthogonal frequency-division multiplexing
p.d.f.	probability density function
QAM	quadrature amplitude modulation
QCQP	quadratic constraint quadratic problem
QoS	quality of service
QP	quadratic programming
RF	radio frequency
SDMA	space division multiple access
SDP	semi-definite programming
SDR	semi-definite relaxation
SINR	signal-to-interference-plus-noise ratio
SNR	signal-to-noise ratio
SOCP	second-order cone programming
SQP	sequential quadratic programming
s.t.	subject to
STC	space-time coding
TDMA	time division multiple access
UMTS	universal mobile telecommunications system
WiMAX	Worldwide interoperability for Microwave Access

Commonly used symbols

α_p	wireless channel path loss exponent
B_c	wireless channel coherence bandwidth
B	transmitted symbol bandwidth
$\mathbf{F}$	fast Fourier Transform matrix
f_d	Doppler frequency
$\mathbf{f}$	forward channel vector in AF relay networks
$\mathbf{g}$	backward channel vector in AF relay networks
k^2	Rician factor of Rician fading channels
L_p	number of paths in multipath propagation channels
L	number of multicast groups
M	number of users
N	number of transmit antennas
$\mathbf{n}$	received noise vector
N_s	number of samples to compute the sample channel covariance matrix
N_c	number of subcarriers
N_{cp}	length of cyclic prefix
$\hat{\mathbf{R}}_i$	the sample channel covariance matrix of the ith user
R	number of relays
s	complex infromation symbol

σ^2	received noise variance
T_c	wireless channel coherence time
T_m	wireless channel delay spread
T_s	transmitted symbol duration
$\mathbf{w}$	beamforming weight vector

Chapter 1

Introduction

Recent advances in Internet and digital multimedia have promoted a variety of applications based on multicast services, where a common message is broadcasted to a mass audience. Examples of these applications are digital audio/video streaming, mobile TV, localized services, and messaging. The ever growing demand and the wide popularity of these applications require next generation wireless systems to support multicast services on the network layer level and also on the physical layer level.

The radio transmission of a datastream to a group of receivers is typically referred to as physical layer multicasting [97]. Based on the number of datastreams which are transmitted simultaneously in the same frequency band, physical layer multicasting is further classified into two classes: single-group multicasting, where a single datastream is transmitted to a single group of users and multi-group multicasting, where multiple datastreams are transmitted simultaneously on the same frequency resource and each datastream is intended to one group of users. In a wireless multicast network, the choice between these two strategies is based on how well each strategy fulfills a number of objectives, while taking into account the resource limitations of this particular network such as the power allocated for transmission and the licensed radio frequency (RF) spectrum. One important objective is maximizing the efficiency of utilization of the available resources, which is achieved by increasing the number of accommodated users in the network. However, in single-group multicasting, for

example, for a fixed transmit power budget, the quality of service (QoS) provided for each user decreases as the number of users in the multicast group increases, since it is no longer possible to fully adapt the spatial transmission to the individual channel conditions of each user. Furthermore, if multiple multicast groups are admitted, more users will be served but the QoS at each user will be affected by the interference arising from the reception of undesired datastreams. Taking into consideration that the provision of high QoS to each user is another important objective, it is clear that striking a balance between these two objectives is a quite challenging task which has triggered numerous research activities, see [11], [34], [65], [75], and references therein.

Several of these activities focused on adaptive techniques specifically designed for multicast networks to avoid the reduction of QoS for the receivers. Examples of these techniques include power control [66] and error control mechanisms [88], macro-diversity [9], and non-uniform modulation [85]. Beside these techniques, the deployment of multiple antennas at the transmitter was recognized as one of the most effective means for improving the performance of wireless multicast networks significantly without additional power and RF spectrum requirements. By deploying multiple antennas at the transmitter, it is possible to consider space as an additional resource which can be exploited. In this context, several techniques have been proposed, such as antenna subset selection [82], precoded orthogonal space-time block coding [120], and transmit beamforming [10], [11], [12], [24], [25], [26], [30], [31], [34] [42], [50], [51], [52], [53], [62], [63], [65] [75], [77], [90], [91], [97], [105], [106], [108], [126].

In transmit beamforming, it is assumed that the transmitter has some knowledge about the channel conditions of each user, which is a valid assumption in modern subscription-based multicast networks, in which the basestation can, e.g., acquire spatial information about the geographical location of the users , or more generally, the instantaneous or statistical channel state information (CSI) of each subscribed user via feedback channels during the subscription phase. Using this information, the transmitter designs the beamforming weights at every transmit antenna to transmit

the datastream(s) in a spatially selective manner so that, in the best case, each user only receives its intended datastream at the desired QoS. In the literature, several approaches have been proposed to solve the beamforming problem by considering different optimization criteria, which will be summarized in the following. Note that a more detailed overview of state-of-the-art techniques which were developed to solve these optimization problems for single-group and multi-group multicasting is provided at the beginning of Chapter 3 and Chapter 4, respectively.

For single-group multicasting, the beamforming problem was first considered with the objective of maximizing the average signal-to-noise-ratio (SNR) perceived by all users subject to a constraint on the maximum allowable transmit power [62], [77]. Using the average SNR as an objective function does not promote fairness among users. For this reason, the problem of maximizing the minimum SNR was proposed in [108] in order to guarantee fairness among users. In [126], the problem of minimizing the transmitted power subject to satisfying the individual SNR requirement of each user was proposed and in [97] it was proved that this problem is equivalent to the SNR maximization problem up to a scaling factor. The authors also proved that both problems are non-convex and NP-hard, thus requiring efficient suboptimal algorithms which can provide good approximate solutions in polynomial runtime. One of the most successful approaches to approximately solve both problems was suggested in [97] and was based on the popular and well established semi-definite relaxation (SDR) procedure.

Similarly, for multi-group multicasting, the beamforming problem was investigated by taking several objectives into account. In [62], the idea of designing the beamformers to completely suppress the interference at each user was briefly introduced, where the design was based on the assumption that the number of multicast groups and the number of users per group is relatively smaller than the number of transmit antennas. In [53], a design based on the sum-rate maximization was proposed, which is generally highly unbalanced with respect to the individual QoS of each user. In [31], [50], and [51], a more fair design which is also suitable for networks with large number

of users was considered. The idea is to minimize the total transmitted power subject to satisfying the individual signal-to-interfere-plus-noise-ratio (SINR) requirement of each user. In [31] and [52], it was shown that the solution of the previous problem can be obtained from solving the problem of maximizing the SINR of the worst user subject to a power constraint by means of a bisection method.

Over the last decade, cooperative communication has emerged as a new trend in wireless communications and currently, it is an active topic of research due to the potential of performance improvement of numerous existing wireless communication systems with requiring additional infrastructure. The main idea of cooperative communication is that the users in a wireless network act as relays that mutually assist each other in transmitting data through the network.

One of several cooperative relaying strategies which have been proposed is distributed beamforming [5], [13], [14], [19], [27], [28], [38], [39], [40], [48], [92], [93], where multiple single-antenna devices together with the source node act as a virtual transmitter with multiple-antennas. In this way, the users in the network can enjoy similar benefits as in conventional multiple-antenna networks without the need for the deployment of multiple antennas at each user. This is important for many wireless applications such as wireless sensor networks, where the communicating devices are required to be small and inexpensive. In [13], the concept of distributed beamforming was applied to multi-group multicasting for the first time. Based on the CSI, the beamforming weight of each single-antenna relay was designed in [13] so that the total power transmitted by all the relays is minimized subject to individual SINR constraints at each user. In this case, high QoS, expressed in the SINR at the receiver of each user, is maintained without the need for a multiple-antenna transmitter as in the case of conventional multiple-antenna multicast networks. However, distributed beamforming has a major drawback: As it is based on coherent processing of the antenna signals, it requires all the relays to be synchronized on the symbol level in order to a provide constructive superposition of the desired signals and destructive superposition of the undesired signals and noise components at the receivers. Global

synchronization of the relays requires the exchange of information among the relays. This represents a signaling overhead and processing power which consumes a part of the available resources in the network. Furthermore, synchronization typically requires each relay to apply an artificial delay to the signal it receives so that in the transmission phase, the signals transmitted from all relays are synchronized and add up coherently at the users. Based on the artificial delay applied at each relay, the storage capacity required for the delaying process can become prohibitively large and expensive.

1.1 Thesis Contributions and Overview

In this thesis, advanced techniques for solving the beamforming problem for single-group and multi-group multicasting in conventional multicast networks and cooperative relay networks are developed. The proposed techniques, which are based on channel orthogonalization and local refinement provide good approximate solutions to the non-convex NP-hard beamforming problem and offer an attractive performance-to-complexity trade-off compared to state-of-the-art techniques. The outline and contributions of the thesis are as follows:

Chapter 2: Background

In this chapter, a brief overview of the wireless channel characteristics and the concepts of multicasting and beamforming are provided. Moreover, the multiple-antenna multicast networks are introduced and the different transmission modes existing in these networks such as single-group and multi-group multicasting are presented. A generalized system model for multicast networks is then developed. Based on this model and by properly adjusting its parameters, the single-group and multi-group multicasting transmission modes are considered in Chapter 3 and Chapter 4, respectively. Finally, cooperative relay networks are introduced with an emphasis on distributed beamforming techniques. A system model for distributed beamforming

in cooperative relay networks is also presented.

Chapter 3: Transmit Beamforming for Single-Group Multicasting

In this chapter we examine the beamforming problem for single-group multicasting. Several optimization problems which were proposed in other works based on different optimization criteria are surveyed. Subsequently, the optimization problem based on power minimization subject to SNR constraints is formulated and our proposed techniques are introduced. We show via simulations and real measured data that our proposed techniques outperform state-of-the-art techniques in terms of transmitted power and enjoy a smaller and in some cases the same computational complexity as the SDR-based technique, which achieves the best performance among the existing techniques. This chapter is based on the following publications:

- A. Abdelkader, I. Wajid, A. B. Gershman, and N. D. Sidiropoulos, "Transmit beamforming for wireless multicasting using channel orthogonalization and local refinement," *Proceedings of the IEEE International Conference on Acoustics, Speech and Signal Processing (ICASSP'09)*, pp. 2281-2284, Taipei, Taiwan, April 2009.

- A. Abdelkader, A. B. Gershman, and N. D. Sidiropoulos, "Multiple-antenna multicasting using channel orthogonalization and local refinement," *IEEE Transactions on Signal Processing*, vol. 58, no. 7, pp. 3922-3927, July 2010.

Chapter 4: Transmit Beamforming for Multi-Group Multicasting

In this chapter we examine the beamforming problem for multi-group multicasting. The optimization problems which were proposed in other works and state-of-the-art techniques which were developed to solve these problems are first introduced. Then, the power minimization problem is formulated and the SDR-based technique, which was proposed in [52] to solve this problem is explained. A modification to the SDR-based technique is introduced in order to reduce its computational complexity,

while maintaining the same performance. Moreover, a novel approach based on hierarchical modulation is developed to solve the power minimization problem. This approach enjoys a significantly reduced computational complexity and achieves a better performance in terms of the total transmitted power compared to the conventional approaches. Another important advantage of the proposed approach is that it avoids solving the beamforming problem for multi-group multicasting, which often becomes infeasible if the number of users in the network is large. Instead, the QoS targets are satisfied by solving a beamforming problem for single-group multicasting, which is always feasible.

Chapter 5: Distributed Beamforming in Cooperative Amplify-and-Forward Relay Networks

In this chapter, we consider the distributed beamforming problem in cooperative relay networks. The channel orthogonalization-based approach, which was developed in [4] to approximately solve the beamforming problem for conventional single-group multicasting is extended to solve the beamforming problem for single-group multicasting in cooperative relay networks. We show via simulations that the proposed technique outperforms the existing state-of-the-art techniques in the scenarios under consideration. Moreover, a practical solution to the relay synchronization problem in distributed beamforming with large delay spread is developed. The solution is based on applying orthogonal frequency division multiplexing (OFDM) at the source and the destination nodes, while jointly optimizing the complex weights applied at the relays and the power allocation for each subcarrier of the OFDM transmission. This chapter is based on the following publications:

- A. Abdelkader, S. Shahbazpanahi, and A. B. Gershman, "Joint subcarrier power loading and distributed beamforming in OFDM-based asynchronous relay networks," *Proceedings of the Fourth International Workshop on Computational Advances in Multi-Sensor Adaptive Processing (CAMSAP2009)*, pp. 105-108, Aruba, December 2009.

- A. Abdelkader, M. Pesavento, and A. B. Gershman, "Orthogonalization techniques for single group multicasting in cooperative amplify-and-forward networks," *Proceedings of the Fourth International Workshop on Computational Advances in Multi-Sensor Adaptive Processing (CAMSAP2011)*, pp. 225-228, San Juan, Puerto Rico, December 2011.

Chapter 2

Background

Wireless communication has experienced huge advances over the last few decades and today it is, by far, the most vibrant segment of the communication industry [113]. This fast growth was driven mainly by two complementary factors. The first factor is the technological advances in the large scale integrated circuits which opened the door for digital wireless communications and within few years, efficient and sophisticated digital signal processing techniques were already implemented on small-sized and energy-saving communication platforms. This revolutionary step, accompanied by the outstanding success of the global system for mobile communications (GSM), the first mobile cellular system with digital services, has increased the interest of the public and the media in wireless communication. Ever since, the growing demand for mobility, higher data rates, and better QoS has been another important factor for driving the industry and shaping the future of wireless communication. Fig. 2.1 shows the growth in the data rates in mobile cellular systems over the last two decades.

In wireline communications, the transmitter and the receiver can be thought of as a pair of communicating terminals connected through a copper wire and isolated from their surroundings. This is not the case in wireless communication, where electromagnetic waves propagate freely in space. Due to free space propagation, the communicating terminals are significantly less isolated from their surroundings and

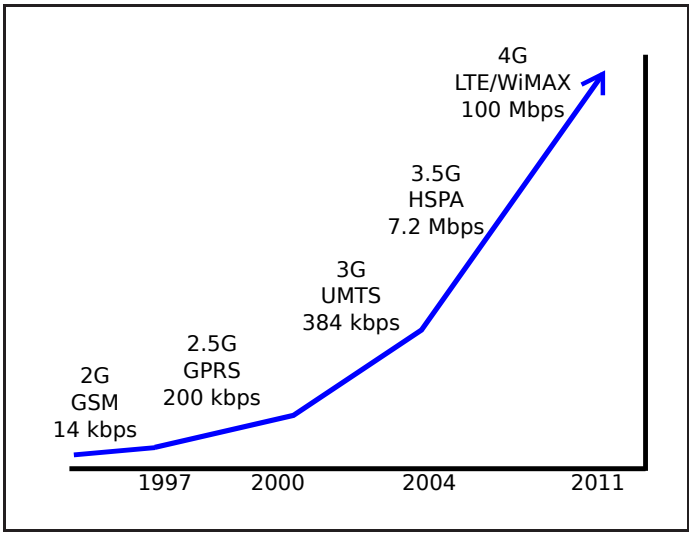

Figure 2.1: Data rates of different generations of mobile cellular systems.

the impact of the wireless communication channel has to be taken into consideration. This makes the design of wireless communication systems more challenging. One main advantage of the wireless channel is its broadcasting nature which allows transmitting the same signal to multiple receivers simultaneously. On the other hand, this may lead to interference, for example, if multiple transmitters are transmitting simultaneously to a single receiver as in the uplink of systems [113]. How to benefit from the characteristics of the wireless channel and avoid its drawbacks is the target of numerous research activities. The answer to this question clearly requires a deep understanding of the characteristics of the channel and the development of realistic channel models. In the next section, we describe the main characteristics of the wireless channel and introduce a statistical channel model.

2.1 Wireless Channel Model

One of the important characteristics of the wireless channel is fading. It accounts for the variation in the strength of the signal at the receiver due to the channel and can be divided into three main components: path loss, large scale, and small scale fading.

2.1.1 Path Loss Fading

In perfect conditions, the signal arrives at the receiver via the direct path propagation of the transmitted electro-magnetic wave, which is commonly known as the line-of-sight (LOS) component. The power of this received signal, P_R, is inversely proportional to the square of the distance d between the transmitter and the receiver, i.e., $P_R \propto d^{-2}$. However, in the presence of obstacles such as buildings between the transmitter and the receiver, the LOS component vanishes and the power of the received signal usually drops off at a rate higher than d^{-2}. As a result, the path loss is assumed to vary as $d^{-\alpha_p}$ where α_p denotes the path loss exponent which is typically between 2.5 for rural areas and 4.5 for urban areas where the density of obstacles is higher [55].

2.1.2 Large Scale Fading

This type of fading, which is also known as "log-normal fading", occurs due to the shadowing effect of the obstacles which lie in the propagation path of the signal from the transmitter to the receiver. It is modeled based on the assumption that each obstacle between the transmitter and the receiver attenuates the signal by a factor of $10^{-\xi_n}$, where ξ_n is a random value. If there are N_0 randomly located obstacles, the overall fading term varies as $\propto 10^{-\sum_{n=1}^{N_0}\xi_n} = 10^{-\xi}$, where $\xi \triangleq \sum_{n=1}^{N_0}\xi_n$. From the central limit theorem, if N_0 is assumed to be very large, the exponent ξ can be considered as a random variable with normal (Gaussian) distribution of mean μ and variance σ^2, i.e., $\xi \sim \mathcal{N}(\mu, \sigma^2)$. This explains the term "log-normal", which means that the *logarithm* of the fading term, i.e., ξ is normally distributed.

2.1.3 Small Scale Fading

In the presence of many obstacles, the transmitted wave is subject to reflection, refraction, diffraction, and scattering as shown in Fig. 2.2. This leads to the generation of multiple waves propagating in multiple different paths. The arrival of multiple

copies of the transmitted signal at the receiver, each with a slightly different path length, is known as multipath fading or small scale fading. The term "small scale fading" comes from the fact that huge fluctuations in the signal strength can occur if the location of the receiver is slightly changed, i.e., sensitive to small scale movements. Since most wireless communications occur in the 1-3 GHz band, i.e., the wave length $\lambda \sim 30-10$ cm, a variation in the location of the receiver as small as $\lambda/2$ can cause two waves coming from two different paths to add destructively rather than constructively, thus reducing the strength of the total received signal significantly. In order to model the small scale fading term, we make use of the baseband equivalent signal model [41] which is used to model the communication signals of limited bandwidth.

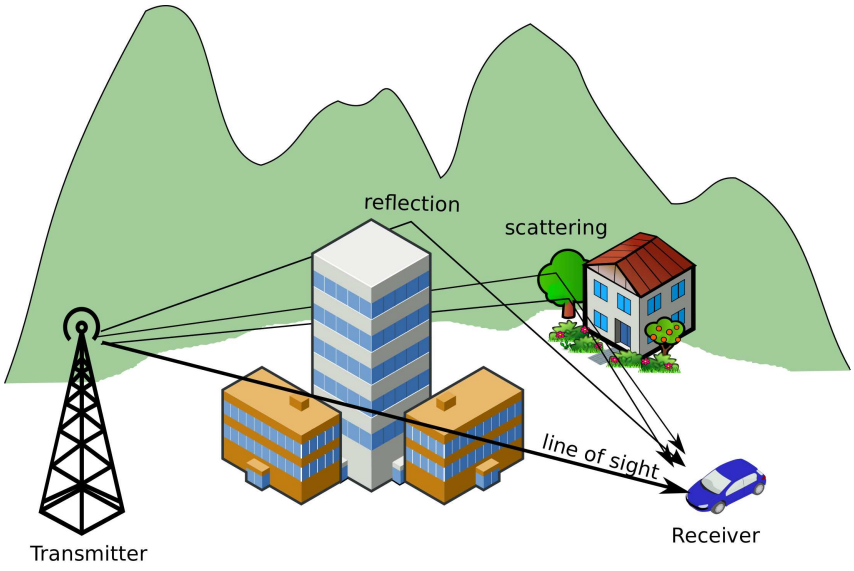

Figure 2.2: Multipath propagation scenario.

Assuming P random paths over which the signal arrives at the receiver, the received signal at time instant t can be written as

$$y(t) = s(t) \sum_{i=1}^{P} a_i e^{j\phi_i} \tag{2.1}$$

where $s(t)$, a_i, and $e^{j\phi_i}$ denote the complex baseband representation of the transmitted signal, the attenuation factor due to the ith path, and the random phase shift

due to the ith path, respectively. The *Rayleigh fading* channel model assumes that the attenuation over all P paths is equal, i.e., $a_1 = \cdots = a_P$. Based on this assumption and using the central limit theorem, as P increases, the received signal can be written as

$$y(t) = s(t)h(t) \tag{2.2}$$

where $h(t)$ has a circularly symmetric complex Gaussian distribution with zero mean and variance σ_h^2 ,i.e., $h(t) \sim \mathcal{CN}(0, \sigma_h^2)$. Its magnitude $|h(t)|$ in this case is a Rayleigh random variable with the p.d.f.

$$p_{|h(t)|}(x) = \frac{x}{\sigma_h^2} e^{-\frac{x^2}{2\sigma_h^2}} \quad , \quad x \geq 0. \tag{2.3}$$

If the LOS component exists and has a non-negligible power, the channel coefficient $h(t)$ is distributed as $\mathcal{CN}(\mu_h, \sigma_h^2)$, where μ_h denotes the channel gain associated with the LOS component. Its magnitude $|h(t)|$ in this case is a Rician random variable with the p.d.f.

$$p_{|h(t)|}(x) = \frac{x}{\sigma_h^2} e^{-\frac{x^2+|\mu_h|^2}{2\sigma_h^2}} I_0\left(\frac{|h\mu_h|}{\sigma_h^2}\right) \quad , \quad x \geq 0, \tag{2.4}$$

where $I_0(\cdot)$ denotes the modified Bessel function of the first kind of zero-order [55]. This is known as the *Rician fading* model and the factor $k^2 = \dfrac{|\mu_h|^2}{2\sigma_h^2}$, which is known as the *Rician factor*, is used to define the ratio of the power received via the LOS path to the power received via the other paths [113].

So far, we have considered the channel model when the signals arriving at the receiver over different paths have slight differences in their path lengths, which leads to a variation in their phases at the receiver. If the path differences increase significantly such that they exceed the symbol duration T_s, the channel becomes *frequency selective* and another characteristic of the wireless channel becomes more pronounced, namely, *inter-symbol interference* (ISI). In the following section, we describe the frequency selective channels and introduce their channel model.

2.1.4 Frequency Selectivity

The *delay spread* of a wireless communication channel T_m is defined as the delay difference between the longest and the shortest paths over which the signal is received with significant power. If $T_m < T_s$, then the signals from all paths arrive within one symbol duration and individual paths can not be resolved. Therefore, the fading effect appears as a single multiplicative coefficient $h(t)$ as in (2.2).
On the other hand, if $T_m > T_s$, the signals from all paths arrive over multiple symbol durations creating ISI. The fading effect can therefore be resolved into multiple coefficients and the time domain representation of the channel can be written as [41]

$$h(t) = \sum_{i=1}^{L_p} h_i \delta(t - \tau_i) \tag{2.5}$$

where L_p and $\delta(t)$ denote the total number of paths that can be resolved and the Kronecker delta function, respectively. If we assume Rayleigh fading, each coefficient h_i in (2.5) has a complex Gaussian distribution, i.e., $h_i \sim \mathcal{CN}(0, \sigma_{h_i}^2)$, $i = 1, \ldots, L_p$.
In the frequency domain, the *coherence bandwidth* of the channel is defined as the bandwidth over which the channel's frequency response is considered to be approximately constant and is given by the relation

$$B_c \simeq \frac{1}{T_m}. \tag{2.6}$$

Given that the bandwidth B required in any efficient transmission scheme is approximately equal to $1/T_s$ [41], if $T_m < T_s$, it directly follows that $B_c > B$ and the channel response is approximately constant over the entire transmission bandwidth, i.e., the channel is frequency *flat*. However, if $B_c < B$, different frequency components of the transmitted signal will experience different frequency responses of the channel. In this case, the channel is frequency *selective* and its impulse response is given in (2.5).

2.1.5 Time Selectivity

Another important characteristic of the wireless communication channel is the rate with which the channel impulse response is changing with time. This divides the

channels into two groups: *fast fading* and *slow fading* channels. If either the transmitter or the receiver or both are moving, the characteristics of the multipath fading channel will change. The rate of change depends on the wavelength λ and the relative velocity v between the transmitter and the receiver. This is commonly referred to as the *Doppler frequency* which is given as

$$f_d = \frac{v}{\lambda}. \tag{2.7}$$

The *channel coherence time*, T_c, is defined as the time over which the channel is approximately constant, i.e., $T_c \simeq \frac{1}{f_d}$. If $T_c > T_s$, the channel is considered constant over the entire symbol duration. This is known as *slow fading*. On the other hand, if $T_c < T_s$, the channel changes within one symbol duration and has to be modeled as a linear time varying system [55]. This is known as *fast fading*. In this work, we will assume slow fading channels where $T_c \gg T_s$. This is a valid assumption for fixed wireless networks or if the symbol duration is relatively very small due to high data rate requirements.

2.2 Multiple-Antenna Multi-User Networks

In the previous section, we considered the effect of the surrounding medium, such as reflectors, scatterers and the motion of the communicating terminals on the reliability of the wireless communication. We showed that the channel suffers from fading, frequency selectivity (ISI in time domain), and time selectivity. This channel model is only valid if we assume that a single datastream is transmitted over a given frequency band. However, this assumption is impractical since the RF spectrum which is suitable for wireless communication is limited and must be shared among different network operators. Additionally, the demand for wireless communication services is steadily increasing, which means that more users have to be accommodated within the available RF spectrum. Therefore, multiple access (MA) techniques are required to improve the spectral efficiency of the wireless networks by serving multiple users simultaneously and in the same frequency band.

Efficient MA techniques allow the transmission of multiple datastreams while maintaining their separability at the receivers. This is achieved by orthogonal allocation of the available resources, such as time and frequency, to each of the intended receivers. However, the orthogonality is not always preserved at the receivers side due to the influence of the channel. This introduces another type of interference to the wireless channel which known as *multiple access interference* (MAI). A common way of quantifying the MAI is to express the SINR at the receivers, which is the ratio of the power of the desired signal to the power of the unwanted signals or interferers plus noise. The SINR is an important measure of the QoS at each receiver in MA networks. Increasing the number of users in the wireless network may lead to reduction of the SINR at some receivers due to the increase in MAI. In order to maintain a high QoS, the transmitter may need to invest more power in the signals intended to receivers suffering from MAI. This reduces the power efficiency of the network.

Traditional MA techniques include time division multiple access (TDMA), frequency division multiple access (FDMA), and code division multiple access (CDMA). These techniques which are based on exploiting three resources or degrees of freedom: time, frequency, and spreading code, have been implemented and used for many years [56], [113]. Also recently, multiple-input multiple-output (MIMO) antenna systems have been identified as one of the key technologies which can increase the reliability of communication and support higher data rates without additional bandwidth or transmit power. MIMO systems can also facilitate another type of MA to the wireless system, which can be easily combined with other MA techniques. As MIMO exploits space as an additional degree of freedom, this MA scheme is generally termed space division multiple access (SDMA). Through the deployment of multiple antennas at the transmitter, it is possible design a particular beam pattern and to steer it in a way which creates multiple spatial channels, one channel in the direction of each user.

The process of steering the beam pattern of a transmitter with multiple antennas in the direction of the intended receivers is commonly known as *transmit beamforming*. Beamforming is a powerful tool which allows transmission as well as reception of single

or multiple signals of interest in a spatially selective manner [34]. Beamforming can be regarded as a spatial filtering mechanism where a spatial filter or a *beamformer* is designed for each datastream.

In conventional transmit beamforming for narrow band signals, for each datastream, a single filter coefficient or a *beamforming weight* is applied at each antenna-element [115]. These coefficients change the phase and the amplitude of the signal at each antenna-element in order to create a pattern of constructive and destructive interferences in the wavefront. By careful adjustment of the coefficients of each beamformer based on the CSI of each user, it is possible to create peaks in the desired directions and nulls in the undesired directions for each user in order to reduce MAI. However, in practice it is not always possible to perfectly adjust the beamformers to avoid MAI at all users due to several reasons: Normally, the CSI is measured at the receiver and fed back to the transmitter. For wireless networks with fading channels where the channel is continuously changing, the CSI used in the design of the beamformer may not be the actual CSI due to the feedback delay. Furthermore, the CSI is subject to estimation and quantization errors introduced at the receiver side as well as thermal noise introduced at the transmitter side. For these reasons, the design of the beamformers at the transmitter assuming imperfect CSI has been proposed which is known as *robust* beamforming [18], [75], [110], [117], [118]. In addition to imperfect CSI, the distribution of the users in different spatial directions is random and is possibly changing with time. As a result, it might occur that users requesting different datastreams are in close proximity of each other such that their complete spatial separation is impossible. This leads to the reduction of the SINR and consequently the QoS at these users. Therefore, techniques for *admission control* have been developed [17], [68], [69], [70], [71], [72]. Admission control aims at choosing the largest subset of users to be admitted to the network while preserving a high QoS at each admitted user. It is important to point out that the spatial selectivity of the transmitter can be improved by increasing the number of transmit antennas. However, for technical and

practical considerations, the number of transmit antennas in most wireless applications is limited. In the literature, numerous techniques have been proposed to design the beamforming weights for multiple-antenna multi-user networks. The complexity of the technique depends strongly on the *design criteria* and the *transmission mode* in the network. There are three different modes of transmission which can occur in a multi-user network:

Multi-User Unicast Transmission

This transmission mode corresponds to the conventional multi-user transmission which was explained earlier. Multiple datastreams are transmitted simultaneously and in the same frequency band to multiple users. The CSI of each user is used at the transmitter to design multiple beamformers where each beamformer directs one signal in the direction of its intended receiver. Over the last two decades, numerous advances in this field have promoted spatial multiplexing to become an essential part of the standards of the third generation (3G) and the fourth generation (4G) of mobile cellular networks [22], [23], [24], [25], [26], [56], [73], [90], [91], [105], [106], [116].

Single-Group Multicast Transmission

The term *"multicast"* describes the process of sending the same message to multiple destinations simultaneously, also known as point-to-multipoint communication. Multicast services are expected to become very popular in the next generation wireless systems due to a huge variety of applications which target mass audience. These applications range from audio/video streaming and mobile TV to localized services and messaging. Together with tremendous growth in the number of users, these applications are rapidly changing the nature of the traffic in almost all types of communication systems from the traditional point-to-point to point-to-multipoint. Efforts to support multicast services in mobile cellular networks have taken place and specifications for multimedia broadcast/multicast services (MBMS) were introduced for GSM and UMTS networks [1], [9], [78]. Also recently, enhanced MBMS (eMBMS)

was proposed for LTE and worldwide interoperability for microwave access (WiMax) networks [2], [44].

The eMBMS as well as MBMS services introduce additional functionalities and procedures which have a strong impact on the network architecture. One main objective is to be able to support both point-to-point and multicast connections over multiple hops within the core network or over a single wireless hop between the source and the destinations. The problem of finding the best routes for multi-hop multicast data has been considered in several other works [73], [116]. In this thesis, we focus on *physical layer* multicasting where the multicast connection is assumed to be realized directly over the radio link between the base station (BS) and the mobile stations (MS). The group of MS which belong to the same multicast connection is called *multicast group*. This could be a group of users which have requested the same *multicast service* such as Mobile TV.

In single-group multicasting the BS allocates a single frequency resource for all users belonging to one multicast group, which is an efficient way of frequency resource utilization. Also single-group multicasting reduces the data traffic in the core network significantly, since it avoids the establishment of redundant point-to-point connections if the users requesting the same service were to connect separately. On the other hand, the BS, in case of point-to-multi-point connections, can no longer fully adapt to the conditions of the radio link of each user individually. This limited adaptivity has a negative impact on the QoS perceived by each user. Therefore, a trade-off between the number of admitted users and guaranteeing high QoS for each user has to be met. Note that in part of the wireless communication and signal processing literature, single-group multicasting is also referred to as *broadcasting* transmission, which is intuitive from the previous description [49], [96], [126], [127]. However, in the context of information theory, the term broadcasting generally describes the transmission of multiple independent messages to multiple users. hence, the transmission mode that we have previously introduced as multi-user unicasting [15], [95].

Multi-Group Multicast Transmission

This type of transmission is a combination of multiuser unicasting and multicasting, since multiple datastreams are transmitted simultaneously and in the same frequency band to multiple multicast groups, where each multicast group can have more than one user. In this way, the transmitter is able to allocate a single frequency resource to a large number of users, which is more efficient than single-group multicasting and multi-user unicasting in terms of spectrum utilization. However, multi-group multicasting can suffer from strong MAI in case of large number of multicast groups and large number of users per group.

In general, finding a good operation point of the network is achieved by choosing among the multi-user unicast, single-group multicast, and multi-group multicast transmission modes in order to strike a balance between spectral efficiency, power efficiency and the QoS that has to be delivered to the users [62]. The design of the beamforming filters at the transmitter for the aforementioned transmission modes is the main topic of this thesis and will be discussed in the following chapters in detail. In the following section, we introduce the system model for multiple-antenna multi-user networks and provide the main assumptions which will be used later in this thesis. We consider the multi-group multicasting transmission, since it contains the other two modes as special cases. The proposed model includes the transmission and reception chain and provides the system parameters which can be easily adjusted to represent particular modes of transmission.

2.2.1 System Model

Fig. 2.3 depicts the transmit beamforming scenario in a multi-group multicast network. We consider a wireless communication system, where a single transmitter with N transmit antennas communicates with M users each equipped with one receive antenna. The input of the transmitter are L independent bitstreams which are simultaneously mapped to complex modulation symbols using, e.g., phase shift keying

(PSK) or quadrature amplitude modulation (QAM). Within one symbol duration, L complex symbols $s_1, \ldots, s_L$ are generated. These symbols are precoded before transmission by passing through the beamforming filter. The beamforming filter generates a set of intermediate symbols $x_1, \ldots, x_N$, where each symbol is a linear combination of the input symbols $s_1, \ldots, s_L$. Stacking the input symbols in vector $\mathbf{s} \triangleq [s_1, \ldots, s_L]^T$ and the output symbols in vector $\mathbf{x} \triangleq [x_1, \ldots, x_N]^T$, the input-output relation of the beamforming filter is given as

$$\mathbf{x} = \mathbf{W}^* \mathbf{s} = \sum_{k=1}^{L} \mathbf{w}_k^* s_k \tag{2.8}$$

where $(\cdot)^*$, $\mathbf{W}$, and $\mathbf{w}_k$ denote the complex conjugate operator, the $N \times L$ beamforming matrix, and the kth column vector of $\mathbf{W}$ which is also known as the kth beamforming vector. Each symbol x_i, $i = 1, \ldots, N$, at the output of the linear precoder passes through the analogue RF front-end, where the pulse-shape filtering, upconversion, and amplification are performed. The output signals are then fed to the antennas and transmitted simultaneously over the channel. Each of the M users belongs to one of the L multicast groups denoted by the sets $\mathcal{G}_1, \ldots, \mathcal{G}_L$. Each of the L multicast groups is interested in only one of the L simultaneously transmitted signals.

Assuming slow flat fading channels between all the transmit antennas and all the receivers, the baseband representation of the channel between the nth transmit antenna, $n = 1, \ldots, N$ and the ith receiver, $i = 1, \ldots, M$ can be modeled as in (2.2) by the complex Gaussian random variable $h_{n,i}$. The channel vector $\mathbf{h}_i \triangleq [h_{1,i}, \ldots, h_{N,i}]^T$ can then be used to model the channel between all the transmit antennas and the ith receiver, $i = 1, \ldots, M$. Also, rich local scattering is assumed at the transmitter and the receivers such that the elements of $\mathbf{h}_i$, $i = 1, \ldots, M$ are independent and identically distributed (i.i.d.) random variables. If we denote the received signal at the ith user after the demodulation block as y_i, and assuming that the ith user belongs to the kth multicast group $\mathcal{G}_k$, then using (2.8), the baseband representation

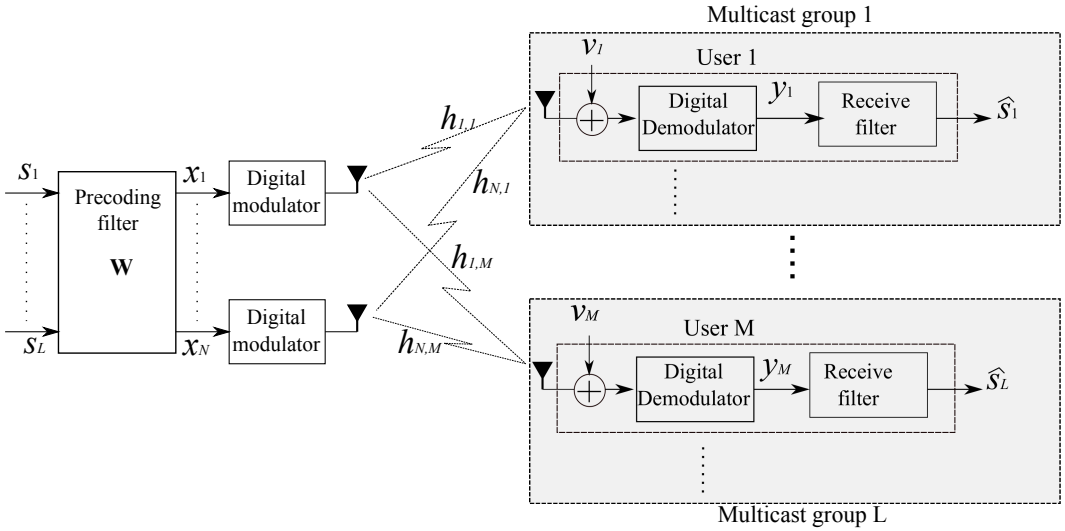

Figure 2.3: Generalized baseband system model for multiple-antenna multicast networks.

of y_i in terms of $\mathbf{s}$ is given as

$$\begin{aligned} y_i =& \sum_{n=1}^{N} x_n h_{n,i} + \nu_i \\ =& \mathbf{x}^T \mathbf{h}_i + \nu_i \\ =& \underbrace{\mathbf{w}_k^H \mathbf{h}_i s_k}_{\text{desired signal}} + \underbrace{\sum_{j \neq k} \mathbf{w}_j^H \mathbf{h}_i s_j}_{\text{MAI}} + \underbrace{\nu_i}_{\text{noise}} \\ & \text{for all } \; i \in \mathcal{G}_k \text{ and } j,k = 1,\ldots,L \end{aligned} \tag{2.9}$$

where ν_i denotes a complex circularly symmetric Gaussian random variable which models the additive white Gaussian noise (AWGN) at the jth receiver. The received signal y_i is processed via a receive filter to obtain an estimate $\hat{s}_k$ of the desired symbol s_k.

Based on the values of the parameters L and M, single-group multicasting and multi-user unicasting transmission modes can be described as special cases of this general model as follows:

- $L = M$ and $|\mathcal{G}|_s = 1$, $k = 1, \ldots, L$, where $|\cdot|_s$ denotes the cardinality of the set. This corresponds to the multi-user unicasting transmission mode where the kth multicast group contains only a single user labeled as user k, $k = 1, \ldots, L$. In this case, equation (2.8) remains the same, while equation (2.9) simplifies to

$$y_i = \underbrace{\mathbf{w}_i^H \mathbf{h}_i s_i}_{\text{desired signal}} + \underbrace{\sum_{j \neq i} \mathbf{w}_j^H \mathbf{h}_i s_j}_{\text{MAI}} + \underbrace{\nu_i}_{\text{noise}} \quad \text{for all} \quad i, j = 1, \ldots, L.$$

- $L = 1$ which corresponds to single-group multicasting. In this case, the transmitter is broadcasting a single datastream, i.e., all users belong to the same multicast group. The transmitted signal vector is given as

$$\mathbf{x} = \mathbf{w}^* s \tag{2.10}$$

where s and $\mathbf{w}$ denote the information symbol and the beamforming weight vector at the transmitter, respectively. Note that in single-group multicasting, no MAI exists and equation (2.9) is given as

$$y_i = \underbrace{\mathbf{w}^H \mathbf{h}_i s_k}_{\text{signal component}} + \underbrace{\nu_i}_{\text{noise}}, \quad \text{for all} \quad i = 1, \ldots, M. \tag{2.11}$$

2.3 Cooperative Relaying Networks

Cooperative communication aims at increasing the data rates and the reliability of the communication in a wireless network by allowing the cooperation between co-located devices. Due to the diversity of technologies used and the different topologies of existing wireless networks, cooperative communication has different forms and strategies. Cooperative communication can be applied in modern multi-user wireless communication systems where the transmitter typically knows the number of subscribers and has some information about the quality of their channels. In many cases, several subscribers temporarily switch to the idle mode since they are inactive and do not wish to exchange information with the transmitter. If another subscriber with poor

channel quality is trying to communicate with the transmitter, it could make use of the existing idle subscribers to *relay* its message to the transmitter. Fig. 2.4 shows an example of cooperative communication in mobile cellular networks.

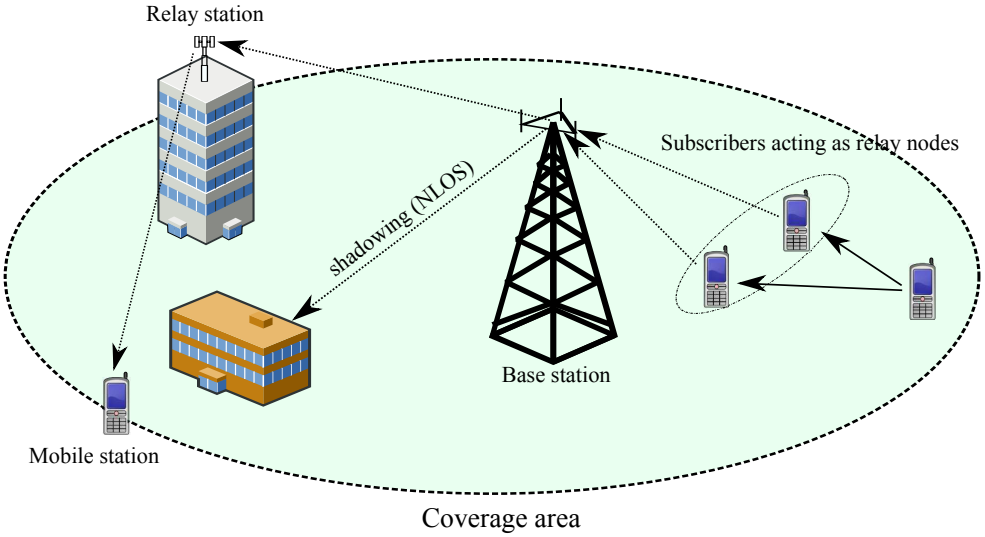

Figure 2.4: Relay stations and cooperative relaying in mobile cellular networks.

Another application is in wireless sensor networks, where several sensors are distributed over a certain geographical area, e.g., in order to perform some measurements. In this case, the communication device in each sensor is limited in size and can not deploy multiple antennas due to the size limitations of the sensor. Also, the devices have a limited transmission range in order to extend the life time of the sensors batteries. A simple strategy to collect the measurement data is to allow the devices to receive the signals from their neighbors and forward them to other devices in the network as shown in Fig. 2.5. After multiple hops, the message arrives at a central processing unit where it could be further processed. This is known as multi-hop cooperative communication which requires joint routing and resource allocation.

In many cases, the communicating devices are required to be cheap and mobile. This imposes some limitations on the cost and size of the devices which makes MIMO communication impractical. One of the applications of cooperative communication

is that a pair of single-antenna devices can communicate through multiple single-antenna relays. The relays act as a *virtual* multiple-antenna transmitter that forwards or "relays" the signal it receives from the source to the destination. In this way, it is possible to provide similar advantages of conventional MIMO communication, such as the higher data rates and the improved reliability of communication for single-antenna systems. In this context, MIMO techniques such as *distributed* beamforming [5], [13], [14], [27], [28], [38], [39], [40], [48], [80], [81], [89], [92], [93], [111] and *distributed* space-time coding (STC) [6], [7], [58], [59], [76], [92], [93] have been developed for cooperative relay networks, where the term "distributed" emphasizes the fact that the processing of the signals is done in a distributed fashion at the relays, hence without mutual exchange of relays received data, in contrast to conventional MIMO techniques, where the data received at all antennas is processed jointly.

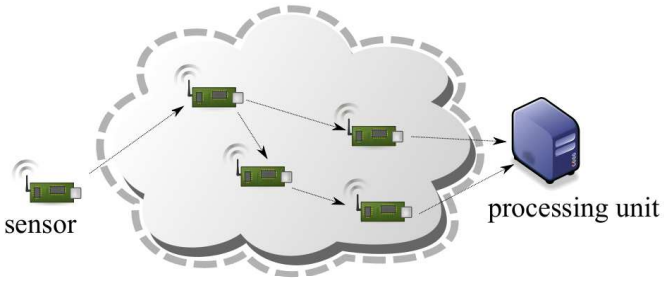

Figure 2.5: Multi-hop relaying in wireless sensor networks.

In the scenarios where the relays act as virtual multiple-antenna transmitter, it is required that the relays are globally synchronized at the symbol level. This type of networks is known as *synchronous* relay networks. Denoting τ_d as the difference in the propagation delay between the shortest path and the longest path relays, i.e., the relays which have the shortest and the longest total propagation delay from the source to the relay and from the relay to the destination, respectively. If $\tau_d << T_s$, this means that the total propagation delays over all the relaying paths are comparable and the relays are assumed to synchronized. However, if $\tau_d >> T_s$, the relays need to perform time synchronization. Since the relays are typically randomly located, the

synchronization procedure requires some information exchange between the relays so that each relay knows its relative delay with respect to the relay of the shortest path. The information exchanged to perform the synchronization represents a *traffic overhead* which is a major disadvantages of synchronous relay networks. For this reason, *asynchronous* relay networks, where the relays are not assumed to be synchronous, have been proposed as an alternative for cooperative relaying [3], [37], [59], [122].

In the literature, several relaying protocols have been proposed. These protocols are classified based on the type of processing at the relays into two main classes: Amplify-and-forward (AF) and decode-and-forward (DF) protocols. In AF protocols, the signal processing at the relays is kept at the minimum level. Every relay node receives the signal from the source in one time slot, multiplies it with a complex coefficient, and forwards it in the next time slot to the destination [5], [13], [14], [27], [28], [38], [39], [40], [48], [80], [81], [92], [93]. The complex coefficient applied at each relay is chosen based on the availability of the CSI. If the CSI of the forward channels from the source to all the relays and the backward channel from all the relays to the destination are known at a centralized processing node, distributed beamforming can be employed at the relays. In this case, the complex coefficients at the relays resemble the beamforming weights of a transmitter with multiple-antennas. If the CSI is not available, distributed STC techniques are considered.

In DF protocols, the relays decode the received signal in the first time slot and forward the newly encoded signals to the destination in the next time slot [6], [7], [58], [92], [93]. Similar to the AF protocols, distributed beamforming techniques can also be applied in DF relay networks by multiplying the decoded signal at each relay with a beamforming coefficient before transmission. In the absence of CSI, distributed STC techniques can be applied.

Note that the AF protocol enjoys a low complexity at the relays, however, it has the disadvantage of forwarding a distorted version of the source signal due to the noise added at the receiver of each relay. Nevertheless, the destination node still benefits from the diversity offered by receiving multiple independently faded replicas

of the source signal. For the DF protocol, the effect of the noise is removed since each relay restores the signal through decoding. However, if the received signal is highly contaminated with noise, i.e., when the receive SNR at the relay is low, decoding errors may occur at the relay and, consequently, at the destination.

Both AF and DF protocols can be used in full duplex or half duplex modes. The type of the duplexing mode used in the relay network is determined based on the capabilities of the relay nodes and the nature of the wireless application. In full duplex scenarios, it is assumed that the relays can transmit and receive simultaneously on two different frequency bands, whereas in the half duplex case, the relays can either transmit or receive in one time slot. In most of the cases, it is assumed that the relays are half-duplex. The reason is that in applications such as sensor networks, the devices are typically of simple architectures which do not support full duplex transmission. Other examples of full-duplex relaying are in mobile cellular networks where fixed relays are deployed as a part of the infrastructure of the network to improve the coverage at cell edges, see Fig. 2.4.

Cooperative relay networks can be further classified based on the number of communicating devices and the direction of the traffic flow in the network. In one-way relaying, it is assumed that the traffic flows in one direction from the source to the relays and from the relays to the destination. In bi-directional relaying, two communicating devices use the relays to exchange infromation, i.e., each device is transmitting and receiving signals over the relays [6], [7], [89], [39], [111]. Networks with multiple sources and multiple destinations, where each source destination pair are communicating with each other through a group of relays, are known as multiple peer-to-peer relay networks [27], [28].

In the next section, we introduce cooperative relaying in the context of multicast networks. We provide the system model and the main assumptions which will be used later in Chapter 5.

2.3.1 System Model

We consider a distributed beamforming scenario for single-group multicasting in one-way half-duplex AF relay networks. Fig. 2.6 depicts a network consisting of a single source node, R relay nodes and M destination nodes, where all nodes are assumed to be single-antenna devices and there is no direct link between the source and the destination nodes. It is also assumed that all the wireless channels between the transmitter and the relays, and between the relays and the receivers are flat fading channels. In the first time slot, the transmitter sends the symbol s to the relays with transmit power P_0. Each of the R relays multiplies its received signal with a complex weight and forwards it to the receivers in the next time slot. Note that we assume that the relays are globally synchronized at the symbol level. This means that in the second time slot, the signals arriving from all the relays will add up coherently at each receiver. If we define f_i as the complex channel coefficients between the transmitter and the ith relay and n_i as the AWGN of the ith relay, respectively, the received signal at the ith relay r_i can be written as

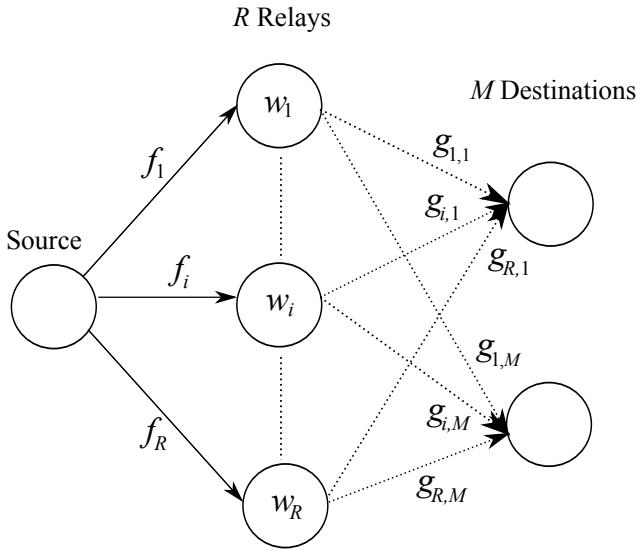

Figure 2.6: System model for distributed beamforming in AF relay networks.

$$r_i = \sqrt{P_0} f_i s + n_i. \tag{2.12}$$

Let w_i^* denote the complex weight at the ith relay. The signal transmitted by the ith relay t_i is given by

$$t_i = \sqrt{P_0} f_i w_i^* s + w_i^* n_i. \tag{2.13}$$

The signal received at the jth receiver is then given by

$$y_j = \sum_{i=1}^{R} t_i g_{i,j} = \sum_{i=1}^{R} \sqrt{P_0} f_i w_i^* g_{i,j} s + \sum_{i=1}^{R} w_i^* n_i g_{ij} + \nu_j \tag{2.14}$$

where $g_{i,j}$ and ν_j are the complex channel coefficients between the ith relay and the jth receiver and the AWGN of the jth receiver, respectively. We define the vectors

$$\begin{aligned} \mathbf{w} &\triangleq [w_1, \ldots, w_R]^T \\ \mathbf{f} &\triangleq [f_1, \ldots, f_R]^T \\ \mathbf{n} &\triangleq [n_1, \ldots, n_R]^T \\ \mathbf{g}_j &\triangleq [g_{1,j}, \ldots, g_{R,j}]^T, \quad j = 1, \ldots, M, \end{aligned} \tag{2.15}$$

as the vector of complex coefficients at the relays, the vector containing the R forward channels from the source to the relays, the vector of AWGN at the relays, and the vector containing the M backward channels from the relays to the jth receiver, respectively. Equation (2.14) can then be written as

$$y_j = \sqrt{P_0} \mathbf{w}^H (\mathbf{f} \odot \mathbf{g}_j) s + \mathbf{w}^H (\mathbf{n} \odot \mathbf{g}_j) + \nu_j \tag{2.16}$$

where $\odot$ denotes the Hadamard product, hence element-wise multiplication. As it was mentioned in Section 2.2.1, a rich scattering environment is assumed such that all channel coefficients are i.i.d. random variables. We also assume that the information symbols are uncorrelated with average power equal to one, i.e., $\mathrm{E}\{|s|^2\} = 1$. If we define $\mathbf{h}_j \triangleq \mathbf{f} \odot \mathbf{g}_j$ as the vector of random coefficients which models the composite channel from the transmitter via the relays to the jth receiver, then the signal power

at the jth receiver P_{s_j} can be written as

$$\begin{aligned} P_{s_j} &= P_0 \mathrm{E}\left\{\mathbf{w}^H(\mathbf{f}\odot\mathbf{g}_j)(\mathbf{f}\odot\mathbf{g}_j)^H\mathbf{w}\right\} \\ &= P_0 \mathrm{E}\left\{\mathbf{w}^H\mathbf{h}_j\mathbf{h}_j^H\mathbf{w}\right\} \\ &= P_0\mathbf{w}^H\mathbf{R}_{h_j}\mathbf{w} \end{aligned} \tag{2.17}$$

where $\mathbf{R}_{h_j} \triangleq \mathrm{E}\left\{\mathbf{h}_j\mathbf{h}_j^H\right\}$ denotes the overall channel covariance matrix for the composite link of the jth receiver. Note that if the instantaneous value of $\mathbf{h}_j$ is known at the transmitter, i.e., $\mathbf{h}_j$ is deterministic, $\mathbf{R}_{h_j}$ becomes a rank-one matrix, otherwise it is generally a full rank matrix. Therefore, we distinguish two types of scenarios depending on the CSI available, either instantaneous CSI or covariance CSI. In instantaneous CSI scenarios, $\mathbf{h}_j$ is assumed to be perfectly known, whereas in covariance CSI scenarios, we assume that some estimate of $\mathbf{R}_{h_j}$ can be obtained, e.g., from the sample covariance matrix.

Assuming that the AWGN at the jth receiver, the AWGN at the relays, and the backward channel coefficients from the relays to the jth receiver are mutually statistically independent and the noise is spatially white, the total noise power at the jth receiver can be written as

$$\begin{aligned} P_{n_j} &= \mathrm{E}\left\{\mathbf{w}^H(\mathbf{n}\odot\mathbf{g}_j)(\mathbf{n}\odot\mathbf{g}_j)^H\mathbf{w}\right\} + \mathrm{E}\left\{\nu_j\nu_j^*\right\} \\ &= \sigma_n^2\mathbf{w}^H\mathbf{D}_{g_j}\mathbf{w} + \sigma_\nu^2 \end{aligned} \tag{2.18}$$

where σ_n^2 and σ_ν^2 denote the variance of the AWGN at the relays and the jth receiver, respectively, and $\mathbf{D}_{g_j} \triangleq \mathrm{diag}(\mathrm{E}\{\mathbf{g}_j\mathbf{g}_j^H\})$ where $\mathrm{diag}(\cdot)$ denotes the diagonal matrix. Similarly, the total transmitted relay power is given by

$$P_t = \sum_{i=1}^{R} \mathrm{E}\{t_i t_i^*\} = \mathbf{w}^H\mathbf{D}_f\mathbf{w} \tag{2.19}$$

where $\mathbf{D}_f \triangleq \mathrm{diag}(\mathrm{E}\left\{\mathbf{f}\ \mathbf{f}^H\right\}) + \sigma_n^2\mathbf{I}$ and $\mathbf{I}$ denotes the $R \times R$ identity matrix.

Chapter 3

Transmit Beamforming for Single-Group Multicasting

In this chapter, we consider the transmit beamforming problem for single-group multicast networks. This problem has been investigated in several works and different solutions have been proposed. In Section 3.1, we present a review of state-of-the-art techniques and the recent advances in single-group multicast beamforming algorithms. The beamforming problem based on minimizing the transmitted power subject to satisfying the minimum SNR requirement of each user is formulated in Section 3.2. This is a quadratic programming (QP) problem with non-convex constraints and it was proved to be NP-hard problem in [97]. In Section 3.3, a computationally efficient technique, which was developed in [97] to solve this problem is explained in detail. The technique uses the semi-definite relaxation (SDR) approach to obtain an approximate solution to the problem. A modified version of the damped Lozano with Lopez Initialization (dLLI) algorithm, which was originally developed in [70] to solve the admission control problem, is proposed in Section 3.4 to solve the power minimization problem. In Section 3.5, we explain our proposed algorithms based on channel orthogonalization techniques. The problem of maximizing the minimum SNR subject

to a power constraint as well as the achievable bit rates in a multicast network are considered in Section 3.6. In Section 3.7, the performance of our proposed techniques is compared to the performance to state-of-the-art techniques based on simulation results and real data experiments. The results show that the proposed techniques outperform the state-of-the-art techniques in terms of transmitted power and offer an attractive performance-to-complexity trade-off. Finally, a conclusion is made in Section 3.8.

3.1 Motivation and Preliminary Work

In multicast networks, a trade-off between the transmitted power and the QoS at the intended receivers has to be met. Finding the best trade-off is achieved by solving an optimization problem, where the beamforming vector (vectors in case of multiple groups) is the optimization variable. Since the single-group multicasting problem can be specified in alternative ways, several optimization problems have been proposed based on different objectives and cost functions [42], [49], [62], [63], [77], [96], [97], [99], [100], [101], [108], [126], [127].

In [62], [77], the first optimization problem for single-group multicasting has been formulated. The objective is to maximize the average of the receive SNR of all users. This approach has a reduced computational complexity, since the solution, also known as the *average* SNR *beamformer*, is obtained directly by solving an eigen-decomposition problem. However, the average SNR approach has the disadvantage of being *unfair* to some users since it maximizes the average but not the individual SNR. This may lead to the existence of users with very poor SNRs. However, in multicasting applications, the worst SNR is an important limiting value, since it determines the *common* information rate. For this reason, several other works have proposed different objectives which guarantee fairness among users.

A reasonable optimization objective which promotes fairness among users is the maximization of the minimum SNR among all users subject to an upper bound on

the transmitted power P_0. This is known as *max-min fair* beamforming and the associated problem and can be written as

$$\max_{\mathbf{w}} \quad \min_{i} \quad \gamma_i \quad \text{s.t.} \quad P_T \leq P_0, \quad i = 1, \ldots, M \tag{3.1}$$

where $\mathbf{w}$, P_T, and γ_i denote the beamforming weight vector, the average transmitted power, and SNR at the ith receiver, respectively. In [126] and [127], Zhang et al. proposed numerical methods to solve the max-min fair beamforming problem based on iterative spatial diagonalization (ISD). The algorithm proposed is restricted to the case where the number of users is less than or equal to the number of antennas at the transmitter.

Another optimization problem which is interesting from the view point of the network operator is to minimize the average transmitted power while satisfying the prescribed QoS requirements of all users. Since the SNR at the ith receiver, denoted as γ_i, can be taken as a good measure of the QoS, the power minimization problem is defined

$$\min_{\mathbf{w}} \quad P_T \quad \text{s.t.} \quad \gamma_i \geq \gamma_{\min,i}, \quad i = 1, \ldots, M \tag{3.2}$$

where $\gamma_{\min,i}$ denotes the minimum required SNR at the ith receiver to achieve the QoS requirement, respectively. This problem was first formulated in [108] and was solved using sequential quadratic programming (SQP). However, the existing SQP solvers have a high computational cost and they require careful selection of the initialization points to avoid local minima. Furthermore, it was shown in [108] that the diversity techniques such as STC, which typically have a much lower complexity and do not require CSI at the transmitter, perform better than beamforming techniques in terms of transmitted power especially in multicasting scenarios with significantly large number of users [120].

In [97], a more computationally efficient approach for solving the max-min fair and the power minimization problems was proposed. The authors first proved that both problems are NP-hard and showed that the optimal solutions to both problems are equivalent to each other up to power scaling. As a result, the authors proposed an

approximate solution based on semi-definite relaxation (SDR) followed by customized randomization techniques. The algorithm developed in [97] was shown to perform substantially well even in the case where the network had more users than transmit antennas. Furthermore, the SDR-based technique, in particular cases, e.g., when the number of users is relatively small, can directly find the optimal solution by solving the relaxed version of the original problem without employing the randomization step that only yields suboptimal solutions. The high performance and relatively low complexity which falls within practical limits have promoted this technique to be considered as a bench-mark technique and for this reason it will be explained in more detail in Section 3.3.

More recently, the traditional beamforming techniques developed for unicast scenarios, such as the matched filter or the zero-forcing techniques, were extended to the multicast case in [99]-[101]. The proposed techniques enjoy a low computational complexity and achieve a performance close to the SDR-based technique especially in the case of small number of users.

Another promising approach that applies to the single-group multicasting problem has been proposed in [63]. The iterative algorithm of [63] is very efficient from the computational point of view, yet in some cases its performance is very sensitive with respect to initialization and it may fail to converge as limit cycles can be easily demonstrated via constructed examples [70], [72]. To improve the performance of the latter approach, the authors of [72] proposed its enhancement using i) the average SNR beamformer of Lopez [62] as initialization; and ii) a step-size damping strategy that was empirically optimized. In [72], the so-obtained technique is referred to as dLLI (damped Lozano with Lopez Initialization) algorithm.

The use of channel orthogonalization in the context of single-group multicasting was originally proposed in [42], which also included a successive *orthogonal* refinement algorithm that is similar in spirit to the one introduced in [63]. The best algorithm in [42] is called *reduced-complexity combine-2* (RCC2) and incorporates successive orthogonal refinements. The simulations in [42] suggest that this combination can

slightly outperform the SDR-based technique of [97] when 100 randomization instances are used. However, this number of instances is an order of magnitude lower than the number suggested in [97] for the given problem size and it is generally known that increasing the number of randomizations significantly improves the performance of the SDR solution.

The performance of the approach in [42] is limited mainly by the suggested order of orthogonalization and scaling in the successive refinement algorithm, as well as by its (RCC2) initialization. In contrast to [42], our proposed approach examines various orthogonalization orders in a pseudo-random way [57] and then chooses the best one based on the criterion of minimum transmitted power.

3.2 Problem Formulation

Consider a single-group multicasting scenario, where the transmitter is broadcasting a single datastream to all users. The users are randomly distributed within a certain coverage area of the transmitter as shown in Fig. 3.1. The objective is to design the beamformer to minimize the total transmitted power subject to individual SNR constraints. Taking into account the system model presented in Section 2.2.1 and assuming that the information symbols at the transmitter are typically uncorrelated and have a variance equal to one, i.e., $E\{s^*s\} = 1$. The average transmitted power can be computed as

$$P_T = E\{\mathbf{x}^H\mathbf{x}\} = E\{s^*s\}\|\mathbf{w}\|^2 = \|\mathbf{w}\|^2. \tag{3.3}$$

From (2.11), the SNR expression of the ith receiver can be written as

$$\gamma_i = \frac{E\{\mathbf{w}^H\mathbf{h}_i ss^*\mathbf{h}_i^H\mathbf{w}\}}{\sigma_i^2}, \quad i = 1, \ldots, M \tag{3.4}$$

where σ_i^2 denotes the variance of noise at the ith receiver. Assuming that the transmitter accurately knows the CSI for all users, i.e., the instantaneous value of the

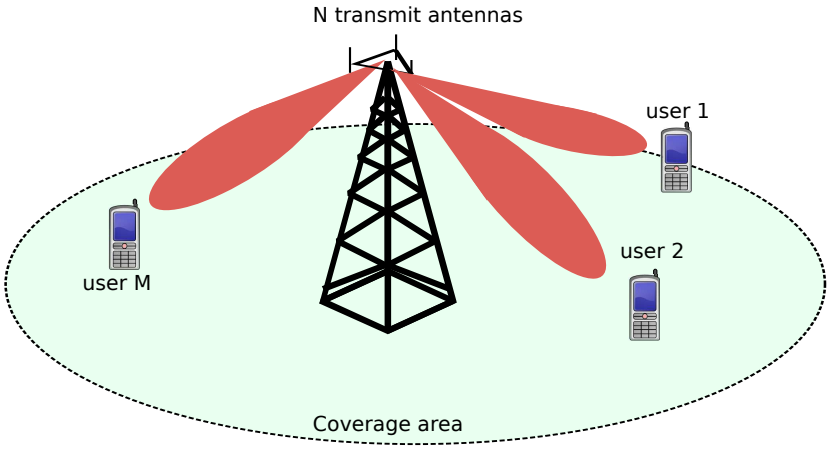

Figure 3.1: A transmitter with multiple-antennas broadcasting to a single multicast group.

random vector $\mathbf{h}_i$, $i = 1, \ldots, M$, is known, (3.4) can be written as

$$\gamma_i = \frac{|\mathbf{w}^H \mathbf{h}_i|^2}{\sigma_i^2}, \quad i = 1, \ldots, M \tag{3.5}$$

and the power minimization problem in (3.2) can be expressed as

$$\begin{aligned} \min_{\mathbf{w}} \quad & \|\mathbf{w}\|^2 \\ \text{s.t.} \quad & |\mathbf{w}^H \tilde{\mathbf{h}}_i|^2 \geq 1, \quad i = 1, \ldots, M \end{aligned} \tag{3.6}$$

where

$$\tilde{\mathbf{h}}_i \triangleq \mathbf{h}_i / \sqrt{\gamma_{\min,i} {\sigma_i}^2}$$

denotes the ith user's normalized downlink channel vector. The problem in (3.6) represents a quadratically constrained quadratic program (QCQP) and the constraints are non-convex since the ith constraint, $i = 1, \ldots, M$, requires the convex quadratic function $\mathbf{w}^H \tilde{\mathbf{h}}_i \tilde{\mathbf{h}}_i^H \mathbf{w}$ to be greater than equal a constant and not smaller or equal, as in convex quadratic constraints.

In the case where $M = 1$, we only have one user in the network and the problem reduces to a matched filter design problem and the optimal beamforming weight vector $\mathbf{w}_{\text{opt}}$ is directly given by

$$\mathbf{w}_{\text{opt}} = \frac{\tilde{\mathbf{h}}}{\|\tilde{\mathbf{h}}\|^2} \tag{3.7}$$

where $\tilde{\mathbf{h}}$ denotes the normalized downlink channel vector. As the number of users increases, the difficulty of the problem increases and a closed form solution as in (3.7) generally does not exist. Although several techniques were developed to provide computationally efficient solutions to the problem in (3.6) in the case where $M \leq N$, in most current MIMO wireless networks, the number N is small due to cost and size limitations. Therefore, restricting the number of admitted users M to be less than N may not allow the full exploitation of the benefits of multiple-antenna transmission. In the following, single-group multicasting networks with $M > N$ are considered, where the constraints in (3.6) form a system of overdetermined inequalities. It was shown in [97] that this problem contains a binary partitioning problem as a special case and therefore, it is NP-hard [32], i.e., solving an arbitrary instance of this problem in polynomial run-time is highly unlikely, hence efficient algorithms are required to obtain suboptimal solutions.

3.3 SDR-Based Technique

SDR is a popular and well established approach which has been commonly used in a number of communications applications, e.g., [67], [98], [114], [128]. Following the same procedure as in [97], let us define the matrices $\mathbf{X} \triangleq \mathbf{w}\mathbf{w}^H$ and $\mathbf{Q}_i \triangleq \tilde{\mathbf{h}}_i\tilde{\mathbf{h}}_i^H$ for all $i = 1, \ldots, M$. Using the fact that $|\mathbf{w}^H\tilde{\mathbf{h}}_i|^2 = \text{trace}\{\mathbf{w}^H\tilde{\mathbf{h}}_i\tilde{\mathbf{h}}_i^H\mathbf{w}\} = \text{trace}\{\mathbf{w}\mathbf{w}^H\tilde{\mathbf{h}}_i\tilde{\mathbf{h}}_i^H\}$, the problem in (3.6) can be rewritten as

$$\begin{aligned} \min_{\mathbf{X}} \quad & \text{trace}(\mathbf{X}) \\ \text{s.t.} \quad & \text{trace}(\mathbf{X}\mathbf{Q}_i) \geq 1, \quad i = 1, \ldots, M \\ & \mathbf{X} \succeq 0 \\ & \text{rank}\{\mathbf{X}\} = 1 \end{aligned} \tag{3.8}$$

where the constraint $\mathbf{X} \succeq 0$ means that $\mathbf{X}$ belongs to the set of positive semi-definite matrices which is convex. Similarly, the trace constraints and the cost function in (3.8) are linear inequalities and a linear function in $\mathbf{X}$, respectively. This motivates

using convex optimization techniques to solve the problem in (3.8). However, the constraint $\text{rank}\{\mathbf{X}\} = 1$ is non-convex. Therefore, the problem is first relaxed by dropping the rank constraint. The resulting convex optimization problem after the relaxation step is written as

$$\begin{aligned} \min_{\mathbf{X}} \quad & \text{trace}(\mathbf{X}) \\ \text{s.t.} \quad & \text{trace}(\mathbf{X}\mathbf{Q}_i) \geq 1, \quad i = 1, \ldots, M \\ & \mathbf{X} \succeq 0 \end{aligned} \tag{3.9}$$

which is a semi-definite programming problem (SDP) that can be easily solved using SDP solvers such as SeDuMi [107] or CVX [36]. Both solvers use the interior point methods to efficiently solve the SDP problem in (3.8) with a worst case computational complexity of $\mathcal{O}((M + N^2)^{3.5})$ [97]. The solution of the problem in (3.9), denoted as $\mathbf{X}_{\text{opt}}$, is generally not a rank-one matrix. In order to obtain a solution to the original problem in (3.8), the rank of $\mathbf{X}_{\text{opt}}$ is determined. If $\text{rank}\{\mathbf{X}_{\text{opt}}\} = 1$, this means that $\mathbf{X}_{\text{opt}} = \mathbf{w}_{\text{opt}}\mathbf{w}_{\text{opt}}^H$ where $\mathbf{w}_{\text{opt}}$ is the optimal solution to the original problem. If $\text{rank}\{\mathbf{X}_{\text{opt}}\} > 1$, randomization techniques are used to generate multiple candidate weight vectors $\{\mathbf{w}_{\text{cand},j}\}_{j=1}^{n_{\text{rand}}}$ from $\mathbf{X}_{\text{opt}}$, where n_{rand} denotes the number of randomizations performed. In [97], three different randomization techniques were considered.

Rand A:

The eigen-decomposition of $\mathbf{X}_{\text{opt}}$ is computed as: $\mathbf{X}_{\text{opt}} = \mathbf{U}\mathbf{S}\mathbf{U}^H$, and the jth candidate vector, $j = 1, \ldots, n_{\text{rand}}$, is chosen as $\mathbf{w}_{\text{cand},j} = \mathbf{U}\mathbf{S}^{\frac{1}{2}}\mathbf{e}_j$, where $\mathbf{e}_j$ is $N \times 1$ vector of complex random variables uniformly distributed on the unit circle of the complex plane. This choice of $\mathbf{e}_j$ satisfies the equality: $\mathbf{w}_{\text{cand},j}^H \mathbf{w}_{\text{cand},j} = \text{trace}(\mathbf{X}_{\text{opt}})$, i.e., the cost function of each candidate weight vector is equal to that of $\mathbf{X}_{\text{opt}}$.

Rand B:

The elements of the jth candidate vector are chosen as: $[\mathbf{w}_{\text{cand},j}]_k = \sqrt{[\mathbf{X}_{\text{opt}}]_{kk}}[\mathbf{e}_j]_k$, where $[\cdot]_m$ and $[\cdot]_{mn}$ denote the mth element of a vector and the element in the mth row and the nth column of a matrix, respectively. This ensures that $|[\mathbf{w}_{\text{cand},j}]_k|^2 = [\mathbf{X}_{\text{opt}}]_{kk}$ [114], which is a stricter condition than that of *Rand A*.

Rand C:
The jth candidate vector is computed as: $\mathbf{w}_{\text{cand},j} = \mathbf{U}\mathbf{S}^{\frac{1}{2}}\mathbf{z}_j$, where $\mathbf{z}_j$ is $N \times 1$ vector of zero mean circularly symmetric complex Gaussian random variables with unit variance. This satisfies $E\{\mathbf{w}_{\text{cand},j}\mathbf{w}_{\text{cand},j}^H\} = \mathbf{X}_{\text{opt}}$ [64]. Note that the previously mentioned randomization techniques are heuristic in nature and were designed such that their computational cost is negligible compared to that of computing $\mathbf{X}_{\text{opt}}$ [97].

For each of the candidate weight vectors generated by *Rand A, Rand B* and *Rand C*, the constraints in (3.6) are checked. If one or several constraints are violated, a minimum scaling of the candidate weight vector is computed by satisfying the most violated constraint with equality. The jth candidate weight vectors is rescaled as

$$\tilde{\mathbf{w}}_{\text{cand},j} = \frac{1}{\min_i |\mathbf{w}_{\text{cand},j}^H \mathbf{h}_i|}\mathbf{w}_{\text{cand},j}, \quad i = 1, \ldots, M. \tag{3.10}$$

Finally, out of the scaled candidate weight vectors, the weight vector with the least norm is selected. The additional computational complexity due to the randomization step is $\mathcal{O}(n_{\text{rand}}MN)$, which, for reasonably small n_{rand}, can be neglected compared to the complexity of the interior point methods. Therefore, the overall computational complexity of the SDR-based technique is determined as $\mathcal{O}((M + N^2)^{3.5})$ [97]. It is important to point out that if the solution of the relaxed problem $\mathbf{X}_{\text{opt}}$ is not rank-one, then trace($\mathbf{X}_{\text{opt}}$) represents a lower bound on the power required to satisfy all the constraints of the original problem in (3.6). This bound is exact if and only if a solution $\mathbf{X}_{\text{opt}}$ with rank equal to one can be obtained. In the simulations section, trace($\mathbf{X}_{\text{opt}}$) is used to assess the efficiency of different techniques which approximately solve the problem in (3.6).

3.4 DLLI-Based Technique

The dLLI is a highly heuristic algorithm, which was originally formulated in [70] to solve the joint beamforming and admission control problem in multi-group multicast networks with limited transmit power. In case of power minimization under prescribed

QoS constraints for single-group multicasting as described in (3.6), the problem is always feasible and no admission control is required. Therefore, a slightly modified version of the dLLI algorithm is developed in this section to solve the problem in (3.6).

The dLLI algorithm computes the beamforming weight vector iteratively. The initialization step starts by computing the weight vector $\mathbf{w}_0$ which maximizes the average SNR of all users. This weight vector is given as the principal eigenvector of the channel pseudo-correlation matrix, i.e., the matrix obtained by computing the ensemble average [62]

$$\mathbf{C}_{\mathbf{h}} = \frac{1}{M} \sum_{i=1}^{M} \tilde{\mathbf{h}}_i \tilde{\mathbf{h}}_i^H. \tag{3.11}$$

The tth iteration of the weight vector, $\mathbf{w}_t$, is computed from the previous value $\mathbf{w}_{t-1}$ by taking a step in the direction of the gradient of the worst SNR while keeping the norm of $\mathbf{w}_t$ equal to one by rescaling. In order to avoid limit cycles and to ensure that the algorithm converges, the step size in the tth iteration is controlled by a back-off factor μ_t which is (aggressively) reduced every 10 iterations [72]. The algorithm stops if the change in the worst SNR is less than or equal to a certain threshold. We remark that this algorithm can be considered as a linearization of the original problem, since in every iteration, a linear approximation of the SNR function of the current worst SNR user is used to update the weight vector. The dLLI algorithm is summarized in Table 3.4. The computational complexity of the dLLI algorithm is of $\mathcal{O}(IMN)$, where I is a bound on the number of iterations that depends only on the initial μ_t.

3.5 The Proposed Orthogonalization Techniques

In this section, we develop a channel orthogonalization with local refinement based approach to solve the problem in (3.6) in an approximate way [4]. As typically the number of users in the network is larger than the number of transmit antennas ($M > N$), hereafter only this case will be considered. In the proposed approach,

Table 3.1: Summary of the dLLI algorithm.

Step 1. Compute $\mathbf{w}_0 = \mathcal{P}\{\mathbf{C_h}\}$ where $\mathbf{C_h}$ is defined in (3.11) and $\mathcal{P}\{\cdot\}$ denotes the principal eigenvector.

Step 2. Rescale $\mathbf{w}_0$ as $\mathbf{w}_0 = \mathbf{w}_0/\|\mathbf{w}_0\|$.

Step 3. Set t=1 and initiate μ_t.

Step 4. If t mod $10 = 0$ then $\mu_t = \frac{\mu_{t-1}}{t/10}$ else $\mu_t = \mu_{t-1}$.

Step 5. Find the user with the worst SNR and denote its index k.

Step 6. Update the weight vector as $\mathbf{w}_t = \mathbf{w}_{t-1} + \mu_t \tilde{\mathbf{h}}_k \tilde{\mathbf{h}}_k^H \mathbf{w}_{t-1}$.

Step 7. Rescale $\mathbf{w}_t$ as $\mathbf{w}_t = \mathbf{w}_t/\|\mathbf{w}_t\|$ and increment t.

Step 8. Repeat Steps 4 to 7 until no significant change in the worst SNR occurs.

Step 9. Scale the final $\mathbf{w}$ to satisfy the worst SNR with equality.

first a subset of N vectors is chosen from the set $\{\tilde{\mathbf{h}}_i\}_{i=1}^M$ to generate N orthonormal vectors $\mathbf{q}_i$, $i = 1, \ldots, N$. As these vectors span the whole N-dimensional space, the desired weight vector $\mathbf{w}$ can be represented as a linear combination:

$$\mathbf{w} = \sum_{i=1}^{N} c_i \mathbf{q}_i, \tag{3.12}$$

where $\mathbf{c} = [c_1, \ldots, c_N]^T$ is the vector of complex coefficients. From the orthonormality property of the vectors $\mathbf{q}_i$, it follows that

$$\|\mathbf{w}\|^2 = \|\mathbf{c}\|^2. \tag{3.13}$$

The key idea of this approach is to choose each component $c_i\mathbf{q}_i$ of $\mathbf{w}$ in (3.12) to satisfy the QoS constraints in (3.6) corresponding to the chosen subset of channel vectors with equality. The remaining $(M - N)$ QoS constraints can be then satisfied by scaling the so-obtained vector $\mathbf{w}$ so that the most violated constraint is satisfied with equality.

3.5.1 The QR Decomposition-Based Beamforming Technique

Consider the $N \times M$ matrix $\mathbf{H} \triangleq [\tilde{\mathbf{h}}_1, \ldots, \tilde{\mathbf{h}}_M]$ whose columns are the vectors $\tilde{\mathbf{h}}_i$, $i = 1, \ldots, M$. Let the $N \times N$ matrix $\mathbf{V}$ be obtained by discarding $(M - N)$ randomly selected columns of $\mathbf{H}$. Applying QR decomposition to $\mathbf{V}$, we obtain

$$\mathbf{V} = [\mathbf{q}_1, \ldots, \mathbf{q}_N] \begin{bmatrix} r_{11} & r_{12} & \cdots & r_{1N} \\ 0 & r_{22} & \cdots & r_{2N} \\ \vdots & \vdots & \ddots & \vdots \\ 0 & \cdots & 0 & r_{NN} \end{bmatrix} \triangleq \mathbf{QR} \tag{3.14}$$

where $r_{ii} > 0$ for all $i = 1, \ldots, N$. Equation (3.12) can be rewritten as

$$\mathbf{w} = \mathbf{Qc} \tag{3.15}$$

and using (3.14), (3.15), and the property $\mathbf{Q}^H\mathbf{Q} = \mathbf{I}_N$, we have

$$\mathbf{w}^H\tilde{\mathbf{h}}_i = \mathbf{c}^H\mathbf{Q}^H\tilde{\mathbf{h}}_i = \mathbf{c}^H\mathbf{Q}^H\mathbf{Q}\mathbf{r}_l = \mathbf{c}^H\mathbf{r}_l \tag{3.16}$$

where it is assumed without any loss of generality that $\tilde{\mathbf{h}}_i$ has been chosen as the lth column of $\mathbf{V}$ and $\mathbf{r}_l$ denotes the lth column of $\mathbf{R}$. Then, using (3.13) and (3.16), and keeping in (3.6) only the N QoS constraints that correspond to the columns of $\mathbf{V}$, the latter problem can be transformed to

$$\begin{aligned} \min_{\mathbf{c}} \quad & \|\mathbf{c}\|^2 \\ \text{s.t.} \quad & |\mathbf{c}^H\mathbf{r}_i|^2 \geq 1, \quad i = 1, \ldots, N. \end{aligned} \tag{3.17}$$

Although the problem (3.17) has the same mathematical form as (3.6), an important difference between these two problems is that the vectors $\mathbf{r}_i$ inherit the upper-triangular structure of the matrix $\mathbf{R}$. Also, as $N < M$, the number of constraints in (3.17) is less than in (3.6). These two facts make it possible to satisfy the constraints in (3.17) with equalities by computing the coefficients c_i, $i = 1, \ldots, N$ successively. In particular, from the first constraint $|\mathbf{c}^H\mathbf{r}_1| = 1$, we obtain that $|c_1 r_{11}| = 1$ and, hence, $|c_1| = 1/r_{11}$. Note that the phase of c_1 can be chosen arbitrarily. Indeed, due

to the successive way of computing the coefficients c_i $(i = 1, \ldots, N)$, any change of $\arg\{c_1\}$ will only cause a rotation of the computed weight vector and, clearly, such a rotation will not alter the cost function. Therefore, without any loss of generality, we can set $\arg\{c_1\} = 0$. That is, the first coefficient can be computed as

$$c_1 = 1/r_{11}. \tag{3.18}$$

From the kth constraint $|\mathbf{c}^H \mathbf{r}_k| = 1$ for any $k = 2, \ldots, N$, we have

$$\left| \sum_{i=1}^{k} c_i^* r_{ik} \right| = 1. \tag{3.19}$$

Defining $\beta_k \triangleq \sum_{i=1}^{k-1} c_i^* r_{ik}$ for $k = 2, \ldots, N$, we can rewrite (3.19) as

$$|c_k^* r_{kk} + \beta_k| = 1. \tag{3.20}$$

Equation (3.20) illustrates the kth step of our proposed successive algorithm to compute the vector $\mathbf{c}$. In this step, all c_i for $i = 1, \ldots, k-1$ have already been computed (that is, the value of β_k is given), and c_k should be obtained from (3.20) so that the increase of the cost function $\|\mathbf{c}\|^2$ caused by c_k is minimized. Obviously, this is equivalent to selecting c_k that satisfies (3.20) with the smallest absolute value c_k. From the fact that r_{kk} is positive, it readily follows that such an optimal value of c_k can be found as

$$c_k = \begin{cases} \frac{1-|\beta_k|}{r_{kk}} \, e^{-j \arg\{\beta_k\}} & , \ |\beta_k| < 1 \\ 0 & , \ |\beta_k| \geq 1. \end{cases} \tag{3.21}$$

Equations (3.18) and (3.21) describe the proposed technique to successively compute the coefficients c_k, $k = 1, \ldots, N$. After computing the whole coefficient vector $\mathbf{c}$ in this way, the associated weight vector can be found from (3.12). The remaining $(M-N)$ QoS constraints to be satisfied correspond to the $(M-N)$ discarded columns of $\mathbf{H}$. To satisfy the latter constraints, we check if any of them is violated and then rescale the resulting weight vector so that the most violated constraint is satisfied with equality.

Since the choice of the columns of $\mathbf{V}$ from $\mathbf{H}$ and their particular order can greatly affect the resulting performance of our technique, multiple candidate values of $\mathbf{w}$ are computed. These candidate weight vectors correspond to different choices of the discarded columns of $\mathbf{H}$ and different orders of the remaining columns of $\mathbf{V}$. Then, from these candidate weight vectors, the vector with the smallest norm, i.e., with the lowest total transmitted power, is finally chosen.

The process of finding the best (in terms of performance) ordered subset of N vectors out of the set of M channel vectors $\{\tilde{\mathbf{h}}_i\}_{i=1}^{M}$ requires generating the weight vector and checking the cost function for all $M!/(M-N)!$ possibilities. Clearly, for large M and N this is prohibitive. Therefore, we propose to consider $J \ll M!/(M-N)!$ random permutations where J is a design parameter that can be used to trade off between computational complexity and performance. As a result, there will be J candidate weight vectors $\{\mathbf{w}_{\text{cand},j}\}_{j=1}^{J}$ and the resulting dominant complexity of our algorithm is given by $\mathcal{O}(J(N^3+MN))$. Therefore, for a reasonably low choice of J, the proposed technique represents a computationally attractive alternative to the SDR-based technique of [97].

3.5.2 The Gram-Schmidt Orthogonalization-Based Beamforming Technique

As the computational complexity of the QR decomposition based technique of Section 3.5.1 can be still considerably high, let us consider a computationally more efficient *ad hoc* approach for selecting the columns of $\mathbf{V}$ and the order in which the columns are selected in the scheme proposed in the previous subsection. Our approach uses the Gram-Schmidt procedure to orthogonalize the selected channel vectors.

We start by choosing an arbitrary initial channel vector $\mathbf{v}_1$ from the set $\{\tilde{\mathbf{h}}_i\}_{i=1}^{M}$. In what follows, we denote the N vectors chosen from this set at the N steps of the Gram-Schmidt procedure as $\mathbf{v}_i$, $i=1,\ldots,N$, so that $\mathbf{V}=[\mathbf{v}_1,\ldots,\mathbf{v}_N]$. The rule for selecting these vectors will be discussed in the sequel. The Gram-Schmidt

orthogonalization procedure can be expressed as

$$\mathbf{b}_k = \mathbf{v}_k - \sum_{i=1}^{k-1} (\mathbf{q}_i^H \mathbf{v}_k)\, \mathbf{q}_i, \quad \mathbf{q}_k = \mathbf{b}_k / \|\mathbf{b}_k\| \tag{3.22}$$

for $k = 2, \ldots, N$ where $\mathbf{q}_1 = \mathbf{v}_1 / \|\mathbf{v}_1\|$. In the kth step of this procedure, the intermediate weight vector can be obtained as

$$\mathbf{w}_k = \sum_{i=1}^{k} c_i \mathbf{q}_i \tag{3.23}$$

where the principle of computing the coefficients c_i is the same as in the QR decomposition based technique of the previous subsection, i.e.,

$$c_k = \begin{cases} \frac{1-|\mu_k|}{\|b_k\|}\, e^{-j \arg\{\mu_k\}} & , \quad |\mu_k| < 1 \\ 0 & , \quad |\mu_k| \geq 1 \end{cases} \tag{3.24}$$

where $\mu_k \triangleq \sum_{i=1}^{k-1} c_i^* (\mathbf{q}_i^H \tilde{\mathbf{v}}_k)$ and $\mathbf{b}_k$ is computed as in (3.22). The key of our approach to select the channel vectors $\mathbf{v}_k$ from $\{\tilde{\mathbf{h}}_i\}_{i=1}^M$ can be described as follows. At the kth step ($k > 1$) of the above Gram-Schmidt procedure, the vector v_k is chosen such that it is the vector which has the smallest magnitude of its inner product with the intermediate weight vector of the previous step $\mathbf{w}_{k-1}$, i.e., the channel vector of worst SNR user. Since the newly added component to the weight vector in the kth step $c_k \mathbf{q}_k$ is orthogonal to all the previously selected channel vectors $\mathbf{v}_1, \ldots, \mathbf{v}_{k-1}$, updating the weight vector with this component will not violate any of the previously satisfied constraints. Finally, (3.12) is used to compute the resulting $\mathbf{w}$. This vector is then rescaled to satisfy the "most violated" of the remaining $(M - N)$ constraints with equality. Note that selecting the channel vectors in the Gram-Schmidt process in the order described previously resembles a special case of QR-decomposition with pivoting, where the permutation matrix for the pivoting in this case is defined such that the channel vector of the worst SNR user is always selected in each orthogonalization step.

The whole orthogonalization process is repeated M times, where each time a new channel vector is chosen as the initial vector $\mathbf{v}_1$ for the Gram-Schmidt procedure.

As a result, we end up with M candidate weight vectors $\{\mathbf{w}_{\text{cand},j}\}_{j=1}^{M}$ and the one having the smallest norm is chosen as the final weight vector. The complexity of this technique is $\mathcal{O}(MN^3 + M^2N)$.

3.5.3 Local Refinement

To further improve the performance of the techniques developed in Subsections 3.5.1 and 3.5.2, we introduce a local search based refinement step. The idea is to perform a norm-constrained local search for any candidate weight vector $\mathbf{w}_{\text{cand},j}$ used in these techniques.

For all values of j, the local refinement algorithm takes $\mathbf{w}_{\text{cand},j}$ as an initial value and then searches for another vector $\tilde{\mathbf{w}}_j$ in its neighborhood that maximizes the worst user SNR and has the same cost function $\|\mathbf{w}_{\text{cand},j}\|$. This can be achieved by finding the local minimum of

$$f(\tilde{\mathbf{w}}_j) = \frac{\|\tilde{\mathbf{w}}_j\|}{\min_i |\tilde{\mathbf{w}}_j^H \tilde{\mathbf{h}}_i|}, \quad i = 1, \ldots, M.$$

The resulting vectors are then treated as the refined candidate weight vectors, which are rescaled such that the worst SNR is satisfied with equality. Note that global maximization of the worst user SNR under a norm(power) constraint is also non-convex, NP-hard, and closely related to our original problem [97]; but what we advocate here is a local optimization in the vicinity of the candidate weight vector $\mathbf{w}_{\text{cand},j}$, which can be easily accomplished using a variety of standard methods. We will use the damped version of Lozano's algorithm [63], as shown in Section 3.4, where the initialization vector $\mathbf{w}_0$ is chosen as $\mathbf{w}_{\text{cand},j}$. Both algorithms of Section 3.5.1 and Section 3.5.2 with local refinement are summarized in Tables 3.2 and 3.3, respectively.

Table 3.2: Summary of the beamforming technique of Section 3.5.1.

Step 1. Obtain the matrix $\mathbf{V}$ by randomly selecting and permuting N columns of $\mathbf{H}$.

Step 2. Obtain the matrices $\mathbf{Q}$ and $\mathbf{R}$ using QR decomposition of $\mathbf{V}$.

Step 3. Compute the candidate weight vector using (3.12), (3.18) and (3.21).

Step 4. Locally refine this weight vector.

Step 5. Rescale the refined vector so that the most violated from all the M constraints in (3.6) is satisfied with equality.

Step 6. Repeat steps 1 to 5 for J times to obtain $\{\tilde{\mathbf{w}}_i\}_{i=1}^{J}$.

Step 7. Select from $\{\tilde{\mathbf{w}}_i\}_{i=1}^{J}$ the vector with the minimum norm to be the final solution.

3.5.4 The Proposed Beamforming Approach in Case of Covariance CSI

The availability of instantaneous CSI at the transmitter requires that the channel variations sensed by the receiver are promptly fed back to the transmitter. This may introduce a huge feedback overhead in the network, especially in the case of fast fading channels. An alternative approach is to design the beamformer based on information about the channel covariance matrix of each user, which is known as covariance CSI. In this case, the CSI is fed back only if major changes in the channel occur and the transmitter takes the expectation over a number of samples and not the exact value of $\tilde{\mathbf{h}}_i\tilde{\mathbf{h}}_i^H$ to evaluate the SNR of the ith user, $i = 1, \ldots, M$. Although this approach has less feedback requirements, it comes at the cost of sacrificing the QoS guarantees. The reason is that the beamformer based on the covariance CSI will only satisfy the SNR constraint of each user on an average basis and the instantaneous values may sometimes be below the average. Furthermore, the channel covariance matrix computed is usually the sample covariance matrix and not the exact one

Table 3.3: Summary of the beamforming technique of Section 3.5.2.

for $j = 1, \ldots, M$

Step 1. Define $\mathcal{H} = \{\tilde{\mathbf{h}}_i\}_{i=1}^{M}$ and select $\mathbf{v}_1 = \tilde{\mathbf{h}}_j$.

Step 2. $\mathcal{H} := \mathcal{H} \setminus \tilde{\mathbf{h}}_j$. Re-index all vectors in $\mathcal{H}$.

Step 3. Compute $\mathbf{q}_1 = \mathbf{v}_1 / \|\mathbf{v}_1\|$.

Step 4. Compute c_1 using (3.18) and obtain $\mathbf{w}_1 = c_1 \mathbf{q}_1$.

Step 5. For $k = 2, \ldots, N$

1. For all current vectors in $\mathcal{H}$, compute $\alpha_i = |\mathbf{w}_{k-1}^H \tilde{\mathbf{h}}_i|,\ i = 1, \ldots, M-k+1$.
2. Select $\mathbf{v}_k = \tilde{\mathbf{h}}_l$ where α_l is the minimum value from $\{\alpha_i\}_{i=1}^{M-k+1}$ and $\tilde{\mathbf{h}}_l$ is the corresponding channel vector.
3. $\mathcal{H} := \mathcal{H} \setminus \tilde{\mathbf{h}}_l$. Re-index all vectors in $\mathcal{H}$.
4. Compute $\mathbf{q}_k$ using (3.22) and c_k using (3.24).

Step 6. Compute the candidate weight vector $\tilde{\mathbf{w}}_j$ using (3.12).

Step 7. Locally refine this weight vector.

Step 8. Rescale the refined vector so that the most violated from all the M constraints in (3.6) is satisfied with equality.

end for

Step 9. Select from $\{\tilde{\mathbf{w}}_j\}_{j=1}^{M}$ the vector with the minimum norm to be the final solution.

which makes it subject to measurement errors as well as errors due to the limited number of samples taken. Nevertheless, this design offers a good trade-off between practicality and system performance.

Let $\hat{\mathbf{R}}_i \triangleq \sum_{n=1}^{N_s} \tilde{\mathbf{h}}_n \tilde{\mathbf{h}}_n^H / N_s$ denote the normalized sample covariance matrix of the ith user where N_s denotes the number of channel samples used for the computation of $\hat{\mathbf{R}}_i$. For a large number of N_s, $\hat{\mathbf{R}}_i$ approaches the exact channel covariance matrix of the ith user $\mathbf{R}_i$, i.e., as N_s increases, $\hat{\mathbf{R}}_i \approx \mathbf{R}_i$. Therefore, the normalized SNR

expression for the ith user computed at the transmitter based on $\hat{\mathbf{R}}_i$ is given as

$$\tilde{\gamma}_i = \mathbf{w}^H \hat{\mathbf{R}}_i \mathbf{w}, \quad i = 1, \ldots, M \tag{3.25}$$

and similar to (3.6), the power minimization problem can be formulated as

$$\begin{aligned} \min_{\mathbf{w}} \quad & \|\mathbf{w}\|^2 \\ \text{s.t.} \quad & \mathbf{w}^H \hat{\mathbf{R}}_i \mathbf{w} \geq 1, \quad i = 1, \ldots, M. \end{aligned} \tag{3.26}$$

For the SDR-based technique, the same algorithm developed to solve the problem in (3.6) is used here to approximately solve the problem in (3.26). Rewriting the problem in (3.26) and dropping rank constraint, we have:

$$\begin{aligned} \min_{\mathbf{X}} \quad & \text{trace}(\mathbf{X}) \\ \text{s.t.} \quad & \text{trace}(\mathbf{X}\hat{\mathbf{Q}}_i) \geq 1, \quad i = 1, \ldots, M \\ & \mathbf{X} \succeq 0 \end{aligned} \tag{3.27}$$

where $\hat{\mathbf{Q}}_i \triangleq \hat{\mathbf{R}}_i$. Note that the only change is that the matrices $\mathbf{Q}_i$ in (3.9) which are rank-one are now replaced by the matrices $\hat{\mathbf{Q}}_i$ which are, per definition, of higher rank.

In order to solve the problem in (3.26) using our proposed techniques of Section 3.5, an additional approximation step has to be introduced, since the orthogonalization techniques can only be applied to SNR constraints in the vector product form as in (3.6). Consider the SNR constraint of the ith user in (3.26), which can be written as

$$\mathbf{w}^H \hat{\mathbf{R}}_i \mathbf{w} = \sum_{k=1}^{r_i} \lambda_{k,i} |\mathbf{w}^H \mathbf{u}_{k,i}|^2 \geq 1 \tag{3.28}$$

where r_i, $\lambda_{k,i}$, $\mathbf{u}_{k,i}$ denote the rank, the non-zero eigenvalues, and the corresponding non-zero eigenvectors of $\hat{\mathbf{R}}_i$, respectively. Note that, per definition, the matrix $\hat{\mathbf{R}}_i$ is a positive semi-definite matrix with non-negative eigenvalues. This allows the approximation of the constraint in (3.28) by r_i separate constraints, one per non-zero

eigenvalue, where each of these constraints has the same vector product form as in (3.6). For the ith user, the approximation is written as

$$|\mathbf{w}^H\mathbf{u}_{l,i}|^2 \geq \frac{1}{\sum_{k=1}^{r_i}\lambda_{k,i}}, \quad l=1,\ldots,r_i. \tag{3.29}$$

If all the constraints in (3.29) are satisfied with equality, the original constraint in (3.28) will also be satisfied with equality but the reverse is not always true. To prove this, let us consider the SNR constraint of the ith user and assume for simplicity that $r_i = 2$, i.e., the approximation in (3.29) will yield two separate constraints. Assuming that the vector $\mathbf{w}$ satisfies both constraints, it follows that

$$|\mathbf{w}^H\mathbf{u}_{1,i}|^2 = \frac{\alpha_1}{\lambda_{1,i}+\lambda_{2,i}}, \quad |\mathbf{w}^H\mathbf{u}_{2,i}|^2 = \frac{\alpha_2}{\lambda_{1,i}+\lambda_{2,i}} \tag{3.30}$$

where α_1, $\alpha_2 \geq 1$. The SNR of the ith user in (3.28) is then given as

$$\mathbf{w}^H\hat{\mathbf{R}}_i\mathbf{w} = \frac{\lambda_{1,i}\alpha_1}{\lambda_{1,i}+\lambda_{2,i}} + \frac{\lambda_{2,i}\alpha_2}{\lambda_{1,i}+\lambda_{2,i}} \geq 1 \tag{3.31}$$

If $\alpha_1 = \alpha_2 = 1$, the constraints in (3.30) and the SNR constraint in (3.31) are all satisfied with equality. However, if we define a small positive value $\beta < 1$ and substitute α_1 and α_2 with $\alpha_1 - \beta$ and $\alpha_2 + \beta(\frac{\lambda_{1,i}}{\lambda_{2,i}})$, respectively, then the SNR constraint in (3.31) will still be satisfied with equality while the first constraint in (3.30) will be violated. This means that the inequalities in (3.29) describe a feasible set that is an inner approximation of the original feasible set for the SNR constraint of the ith user in (3.28). Using (3.29), the power minimization problem in case of covariance CSI can be approximated as

$$\begin{aligned} \min_{\mathbf{w}} \quad & \|\mathbf{w}\|^2 \\ \text{s.t.} \quad & |\mathbf{w}^H\tilde{\mathbf{u}}_{l,i}|^2 \geq 1 \quad l=1,\ldots r_i, \quad i=1,\ldots,M \end{aligned} \tag{3.32}$$

where

$$\tilde{\mathbf{u}}_{l,i} \triangleq \mathbf{u}_{l,i}\sqrt{\sum_{k=1}^{r_i}\lambda_{k,i}} \quad l=1,\ldots r_i, \quad i=1,\ldots,M. \tag{3.33}$$

The problem in (3.32) has the same mathematical form as the problem in (3.26) and the orthogonalization-based techniques can be directly applied. However, the problem in (3.32) is a strict approximation and has more constraints than the original problem in (3.26). Therefore, the orthogonalization techniques are applied with a slight modification.

For the technique based on QR decomposition, the only change is in the rescaling in Step 5 in Table 3.2. After the candidate vectors are computed and locally refined as in Steps 1-4 of Table 3.2, the vectors are rescaled to satisfy the most violated of the M original SNR constraints in (3.26) with equality and not the approximated constraints in (3.32).

For the technique based on the Gram-Schmidt procedure, we first assume without loss of generality that $\lambda_{1,i} \geq \cdots \geq \lambda_{r_i,i} > 0$. Let the matrix $\tilde{\mathbf{U}}_i \triangleq [\tilde{\mathbf{u}}_{1,i}, \ldots, \tilde{\mathbf{u}}_{r_i,i}]$ contain the scaled non-zero eigenvectors of $\hat{\mathbf{R}}_i$, as defined in (3.33), where the vectors of $\tilde{\mathbf{U}}_i$ are sorted based on their respective eigenvalues in descending order. Similar to the procedure in section 3.5.2, the initial vector in the Gram-Schmidt procedure denoted as $\mathbf{v}_1$ is chosen arbitrarily from one of the principal eigenvectors of the matrices $\tilde{\mathbf{U}}_1, \ldots, \tilde{\mathbf{U}}_M$. The first intermediate weight vector $\mathbf{w}_1$ is computed as in (3.23), where $\mathbf{q}_1$ and c_1 are given by equations (3.22) and (3.24) by substituting $k = 1$. Then, the respective column of the matrix from which $\mathbf{v}_1$ is chosen, is discarded. Using $\mathbf{w}_1$, we find the index, η, of the user with the "most violated" SNR constraint, i.e., $\min_i \mathbf{w}_1^H \hat{\mathbf{R}}_i \mathbf{w}_1$, $i = 1, \ldots, M$. The second vector in the Gram-Schmidt procedure, denoted as $\mathbf{v}_2$, is taken as the first column vector in $\tilde{\mathbf{U}}_\eta$ and the coefficient c_2 is computed as in (3.24) to satisfy the constraint corresponding to $\mathbf{v}_2$ in (3.32) with equality. Since the order of the vectors in $\tilde{\mathbf{U}}_\eta$ is based on the decreasing value of their respective eigenvalue, satisfying the constraint of the first vector with equality provides the strongest contribution to the SNR of the ηth user. This strategy gradually satisfies the original SNR constraints on a greedy basis. The matrix $\tilde{\mathbf{U}}_\eta$ is then updated by dropping the vector $\mathbf{v}_2$ and the second intermediate weight vector $\mathbf{w}_2$ is computed as in (3.23). The above routine is repeated in every step of the remaining

$R-2$ steps of the Gram-Schmidt procedure in order to generate a candidate weight vector. The entire orthogonalization process is repeated M times, where each time a different principal eigenvector is chosen as the initial vector $\mathbf{v}_1$ for the Gram-Schmidt procedure. Finally, the local refinement step is performed on each of the M generated candidate weight vectors $\{\mathbf{w}_{\text{cand},j}\}_{j=1}^{M}$ and the vector with the least norm is chosen.

The beamforming algorithms in the case of covariance CSI using and QR decomposition are summarized in Tables 3.4 and 5.1, respectively.

Table 3.4: Summary of the beamforming technique of Section 3.5.1 in case of covariance CSI.

Step 1. Define $\mathbf{U} = [\tilde{\mathbf{U}}_1, \ldots, \tilde{\mathbf{U}}_M]$ and obtain the matrix $\mathbf{V}$ by randomly selecting and permuting N columns of $\mathbf{U}$.

Step 2. Obtain the matrices $\mathbf{Q}$ and $\mathbf{R}$ using QR decomposition of $\mathbf{V}$.

Step 3. Compute the candidate weight vector using (3.12), (3.18) and (3.21).

Step 4. Locally refine this weight vector.

Step 5. Rescale the refined vector so that the most violated from all the M constraints in (3.26) is satisfied with equality.

Step 6. Repeat steps 1 to 5 for J times to obtain $\{\tilde{\mathbf{w}}_i\}_{i=1}^{J}$.

Step 7. Select from $\{\tilde{\mathbf{w}}_i\}_{i=1}^{J}$ the vector with the minimum norm to be the final solution.

3.6 The Max-Min Fair Problem

So far, we have considered the power minimization problem in case of perfect and covariance CSI. In this section, we consider the max-min fair problem. It was proved in [97] that the maximum common information rate C_0 for a given power P_0 is achieved by solving the Lagrangian dual of the problem in (3.6) which is in fact equivalent to

Table 3.5: Summary of the beamforming technique of Section 3.5.2 in case of covariance CSI.

for $j = 1, \ldots, M$

Step 1. Define $\mathcal{U} = \{\tilde{\mathbf{u}}_{1,i}\}_{i=1}^{M}$ and select $\mathbf{v}_1 = \tilde{\mathbf{u}}_{1,j}$.

Step 2. Compute $\mathbf{q}_1 = \mathbf{v}_1/\|\mathbf{v}_1\|$.

Step 3. Compute c_1 using (3.18) and obtain $\mathbf{w}_1 = c_1\mathbf{q}_1$.

Step 4. For $k = 2, \ldots, N$

1. Compute $\mathbf{w}_{k-1}^H \hat{\mathbf{R}}_i \mathbf{w}_{k-1}$, $i = 1, \ldots, M$.
2. Select $\mathbf{v}_k = \tilde{\mathbf{U}}_\eta^{(1)}$ where $\eta = \arg\ \min_i \mathbf{w}_{k-1}^H \hat{\mathbf{R}}_i \mathbf{w}_{k-1}$, $i = 1, \ldots, M$ and $\tilde{\mathbf{U}}_\eta^{(1)}$ is first column vector of the corresponding matrix $\tilde{\mathbf{U}}_\eta$.
3. Update $\tilde{\mathbf{U}}_\eta$ by discarding $\tilde{\mathbf{U}}_\eta^{(1)}$.
4. Compute $\mathbf{q}_k$ using (3.22) and c_k using (3.24).

Step 5. Compute the candidate weight vector $\tilde{\mathbf{w}}_j$ using (3.12).

Step 6. Locally refine this weight vector.

Step 7. Rescale the refined vector so that the most violated from all the M constraints in (3.26) is satisfied with equality.

end for

Step 8. Select from $\{\tilde{\mathbf{w}}_j\}_{j=1}^{M}$ the vector with the minimum norm to be the final solution.

the max-min fair formulation. Hence, the dual problem is given by

$$\begin{aligned} \max_{\mathbf{w}} \quad & \min_{i} \quad |\mathbf{w}^H \tilde{\mathbf{h}}_i|^2, \quad i = 1, \ldots, M \\ \text{s.t.} \quad & \|\mathbf{w}\|^2 \leq P_0. \end{aligned} \tag{3.34}$$

It is clear from (3.34) that the optimal $\mathbf{w}$ is achieved when the inequality constraint is satisfied with equality, otherwise $\mathbf{w}$ can be scaled to increase the minimum SNR and therefore, contradicting with the condition of optimality. Following the same

procedure to write (3.6) and applying SDR, the relaxed problem of (3.34) can then be written as

$$\begin{aligned} \max_{\mathbf{X}} \quad & \min_{i} \quad \text{trace}(\mathbf{X}\mathbf{Q}_i), \quad i = 1, \ldots, M \\ \text{s.t.} \quad & \text{trace}(\mathbf{X}) = P_0 \\ & \mathbf{X} \succeq 0 \end{aligned} \tag{3.35}$$

where the constraint $\text{rank}\{\mathbf{X}\} = 1$ is dropped and the inequality constraint in (3.34) is replaced with equality. The problem in (3.35) can be solved using SDP solvers and the solution $\mathbf{X}'_{\text{opt}}$ is equivalent to the solution of (3.6) up to a scaling and it was shown in [97] that $\mathbf{X}'_{\text{opt}}$, which is generally not rank-one, is the optimal transmit covariance matrix that maximizes the common mutual information rate over the MIMO channel described by the channel matrix $\mathbf{H}$ [46], [97]. Therefore,

$$C_0(\mathbf{H}, P_0) = \log_2\big(1 + P_0(\min_{\mathbf{h}_i} \ \mathbf{h}_i^H \mathbf{X}'_{\text{opt}} \mathbf{h}_i)\big). \tag{3.36}$$

In case of beamforming transmission strategies, the additional rank-one constraint leads to suboptimal performance. The maximum achievable bit rate in this case is given by

$$R_{bf}(\mathbf{H}, P_0) = \log_2\big(1 + P_0(\min_{\mathbf{h}_i} \ |\mathbf{w}^H \mathbf{h}_i|^2)\big) \tag{3.37}$$

where $\mathbf{w}$ denotes the beamforming vector provided by the beamforming algorithm. The general rank technique requires the simultaneous transmission of multiple (possibly N) independent bitstreams from each antenna. This may introduce larger encoding and decoding overheads as compared to beamforming which typically trades off reduction in information rate for implementation simplicity.

3.7 Simulation and Real Data Processing Results

In all our examples, the acronyms QR-dL and GS-dL stand for the proposed QR decomposition based algorithm of Section 3.5.1 and the Gram-Schmidt orthogonalization based technique of Section 3.5.2, respectively, both using damped Lozano's

(dL) local refinement step. The QR-dL and GS-dL techniques are compared with the dLLI technique of [72], the RCC2 algorithm with successive orthogonal refinement of [42] (referred to as RCC2-SOR), the SDR-based approach of [97], and the same SDR-based technique combined with the dL local refinement. The latter technique is referred to as SDR-dL. The choice of the initial step-size μ and the stopping threshold in the dL technique were empirically optimized to achieve fast convergence and good performance. To optimize the parameters of the SDR-based approach, we have followed the guidelines of [97] where three different randomization procedures have been used in parallel, with 1000 randomizations for each. The number of iterations in the successive orthogonal refinement part of the RCC2-SOR technique was chosen equal to the number of randomizations used in the SDR-based technique ($n_{\text{rand}} = 3000$). For the QR-dL technique, $J = 200$ has been selected. This value of J corresponds to nearly equal computational complexities (measured in terms of MATLAB run-times) of the SDR, SDR-dL and QR-dL methods. Note that the run time of the GS-dL technique is substantially smaller than that of the QR-dL, SDR and SDR-dL techniques.

3.7.1 Rayleigh Fading Channels with Instantaneous CSI at the Transmitter

Throughout our simulations, a Rayleigh fading channel with i.i.d. circularly symmetric unit-variance channel coefficients is assumed. We also assume that $\sigma_i^2 = \sigma^2 = 1$ and $\gamma_{\min,i} = \gamma_{\min}$ for all $i = 1, \ldots, M$. All our results are averaged over 1000 Monte Carlo runs.

In the first example, we assume that $\gamma_{\min} = 5$ dB. In Table 3.6, the so-called *boost ratio* [97]

$$\varepsilon = \|\mathbf{w}_{\text{fin}}\|^2 / \text{trace}\{\mathbf{X}_{\text{opt}}\}$$

is used to characterize the performance, where $\mathbf{w}_{\text{fin}}$ is the final beamformer weight vector of each technique tested. The mean and the standard deviation (std) values of

Table 3.6: Comparison of the boost ratios of different multicasting techniques; first simulation example.

M	RCC2-SOR		dLLI		SDR		SDR-dL		GS-dL		QR-dL	
	Mean	Std	Mean	Std	Mean	Std	Mean	Std	Mean	Std	Mean	Std
10	1.41	0.52	1.21	0.25	1.24	0.23	1.11	0.14	1.08	0.08	1.06	0.07
20	1.99	0.73	1.60	0.59	1.71	0.37	1.36	0.29	1.24	0.14	1.21	0.12
30	2.59	1.02	2.04	0.72	2.07	0.45	1.61	0.39	1.40	0.18	1.35	0.16
40	3.05	1.19	2.39	0.98	2.40	0.51	1.87	0.48	1.55	0.21	1.48	0.18
50	3.38	1.25	2.75	1.21	2.75	0.59	2.09	0.57	1.68	0.25	1.60	0.22
60	3.66	1.42	3.14	1.31	3.03	0.65	2.31	0.63	1.83	0.29	1.72	0.24
70	4.10	1.45	3.43	1.50	3.37	0.74	2.52	0.72	1.94	0.30	1.83	0.26
80	4.29	1.57	3.88	1.76	3.66	0.81	2.71	0.79	2.09	0.33	1.96	0.28

the boost ratio are summarized in this table for $N = 4$ and $M = [10, \ldots, 80]$. As it can be observed from the table, the QR-dL and GS-dL techniques have substantially lower values of both the mean and standard deviation as compared to the SDR, SDR-dL, RCC2, and dLLI techniques. This implies that the QR-dL and GS-dL techniques are more power-efficient than the other techniques tested.

In our second example, we illustrate the achievable rates of the different beamformers for fixed transmit power. Fig. 3.3 shows these rates versus the number of users M for P=1. Also, the multicast capacity is shown in the figure as an upper bound on the achievable rate, where both $\mathbf{X}_{\text{opt}}$ and $\mathbf{w}_{\text{fin}}$ are normalized to satisfy the transmit power constraint $\text{trace}\{\mathbf{X}_{\text{opt}}\} = \|\mathbf{w}_{\text{fin}}\|^2 = P$.

It can be observed from this figure that the proposed QR-dL and GS-dL techniques have increased achievable rates over the remaining multicasting algorithms tested. As previously observed, QR-dL performs slightly better than GS-dL. Another interesting observation is that the multicast capacity can be seen as a relatively loose upper bound on the rates that can be achieved via beamforming. This is expected due to the additional rank-one constraint which is imposed on the design of the transmit covariance matrix in the beamforming case.

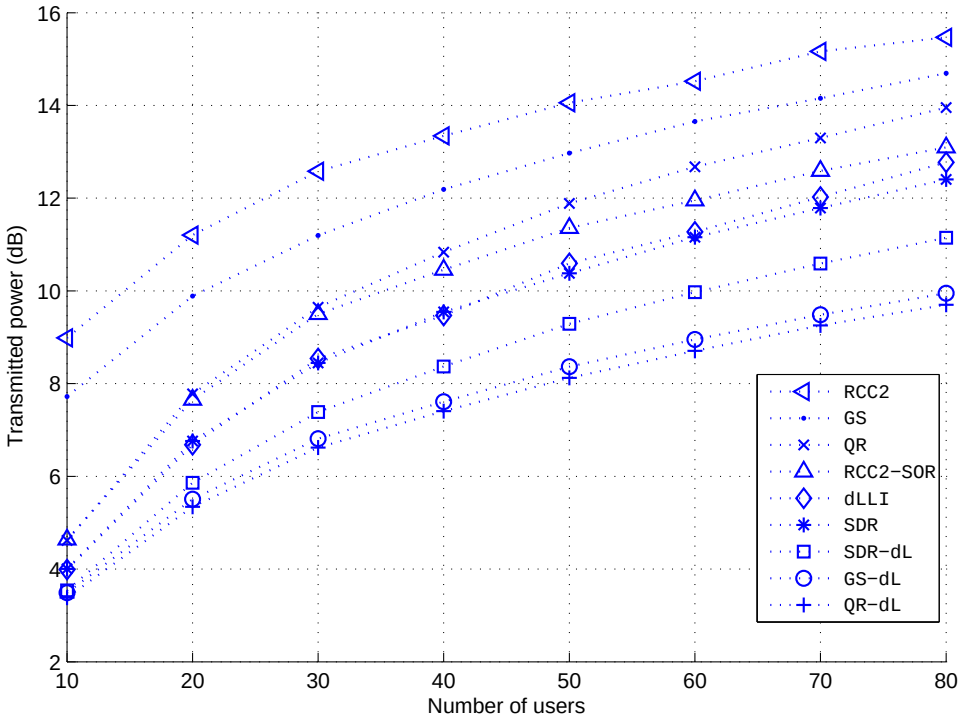

Figure 3.2: Total transmitted power versus number of users; first simulation example.

In our third example, we choose $N = 4$, $M = 80$, and the minimum required SNR is varied. All the other parameters are the same as in the first simulation example. Fig. 3.4 shows the transmitted powers versus the minimum required SNR. As in the first example, we can observe from this figure than the proposed GS-dL and QR-dL techniques perform better in terms of transmitted power than the other techniques tested. Also, as before, the QR-dL beamformer has a slightly better performance than the GS-dL one.

3.7.2 Rayleigh Fading Channels with Covariance CSI at the Transmitter

In our fourth example, we assume that the transmitter uses the sample covariance matrix $\hat{\mathbf{R}}_i$ to design the beamforming vector. We assume the number of samples

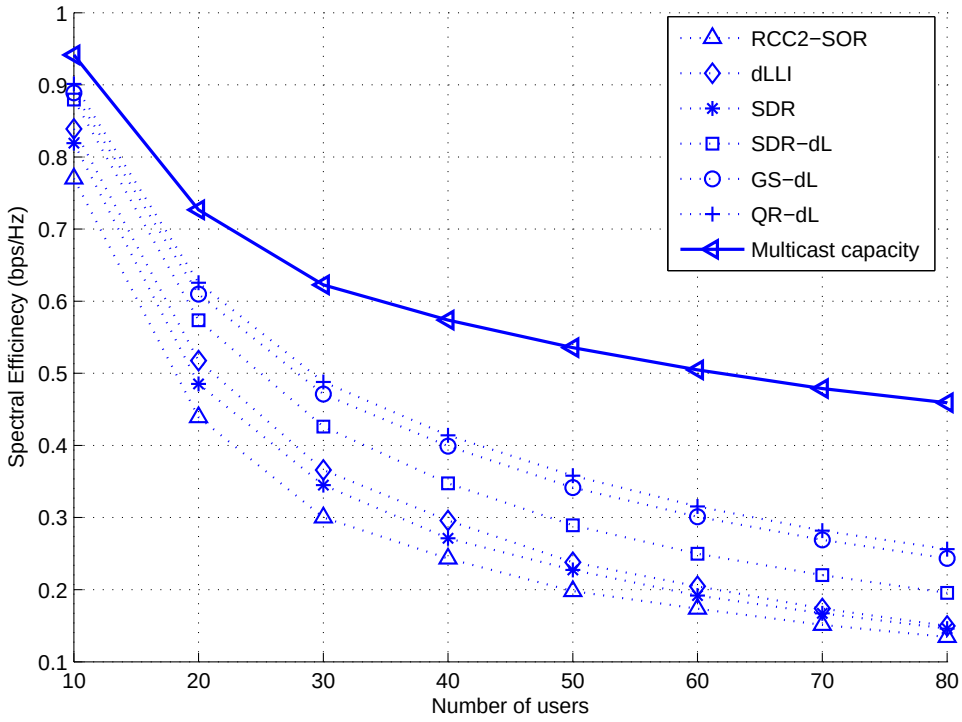

Figure 3.3: Achievable multicast rates versus number of users; second simulation example.

$N_s = 10$ and choose $N = 4$, and $M = [10, \ldots, 80]$. All the other parameters are the same as in the first example. We note that RCC2 and RCC2-SOR were implemented to be applied only in the case of instantaneous CSI, therefore, we compare the performance of our proposed algorithms only with SDR, SDR-dL and the dLLI techniques which can straightforwardly be applied in the covariance CSI case. Fig. 3.5 shows the average transmitted power required by the methods tested versus the number of users.

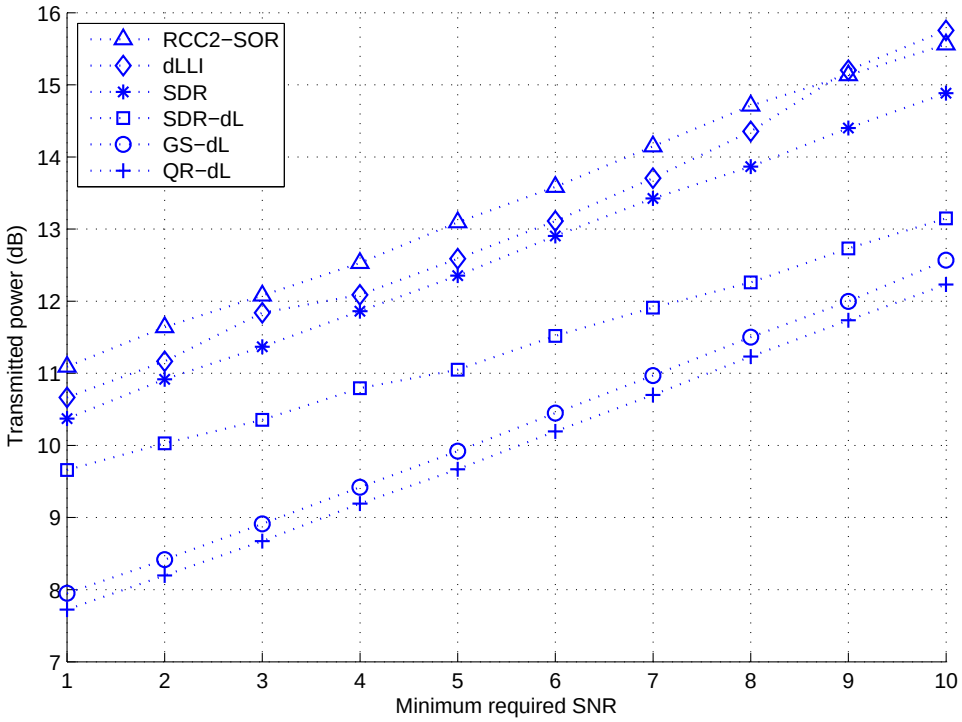

Figure 3.4: Total transmitted power versus minimum required SNR; third simulation example.

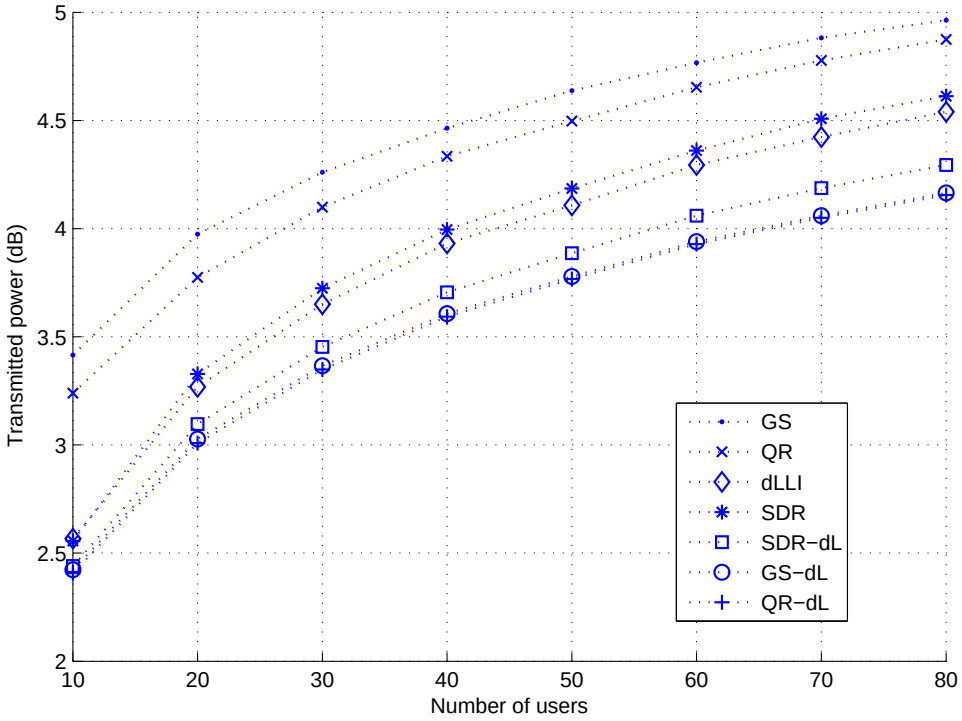

Figure 3.5: Total transmitted power versus number of users; fourth simulation example.

We observe from this figure that both GS-dL and QR-dL have an improved performance in terms of the transmitted power over the other techniques tested. The performance gap becomes significant as M increases. Also, interestingly, the gap in performance between GS-dL and QR-dL is reduced as compared to the gap in performance in the instantaneous CSI case.

3.7.3 Measured Indoor Data

To further compare the performance of the proposed and existing multicasting methods, we used measured channel data collected in the $902 - 928$ MHz ISM band by the iCORE HCDC Lab, University of Alberta in Edmonton [35]. The raw data and associated documentation files can be found at `http://www.ece.ualberta.ca/~mimo/`. Channel selection and preprocessing have been performed as detailed in [72]. The specific data set that we used here corresponds to the *indoor* scenario in [72].

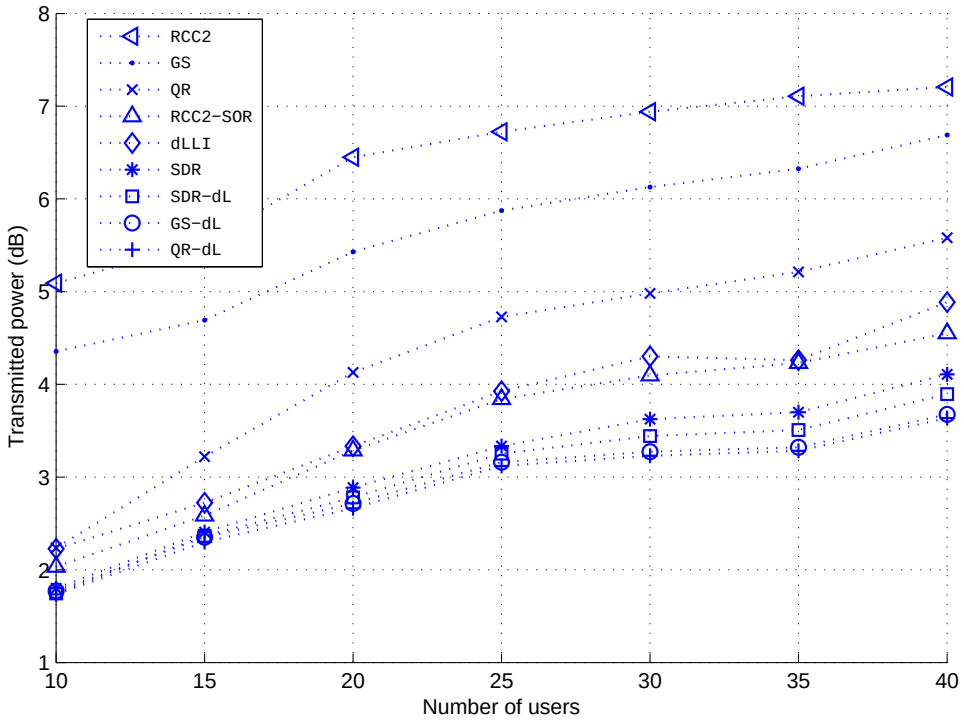

Figure 3.6: Total transmitted power versus number of users; measured channel data.

There are $N = 4$ transmit antennas, and $M = 12$ user channels, measured every 3 seconds for a total of 30 temporal snapshots. In order to test with a large number of users, we randomly selected and concatenated 4 out of 30 snapshots (there are 27405 possible combinations), and averaged the results over 1000 such draws. Fig. 3.6 shows the transmitted power versus the number of users M. The required minimum SNR has been set to 0 dB.
It can be seen that in this figure, the QR-dL and GS-dL techniques show comparable performance. Both of them outperform the remaining methods tested. These performance improvements become more significant when increasing M.

3.8 Conclusion

The problem of single-group multicasting has been considered in the case of the availability of instantaneous CSI and covariance CSI for all users. Two methods have been developed to approximately solve this problem using channel orthogonalization and a subsequent local refinement algorithm to further improve the beamformer weight vector. The results of our simulations and measured data processing clearly demonstrate an improved performance of the proposed QR-dL and GS-dL techniques with respect to the state-of-the-art multicasting methods such as the SDR, dLLI and RCC2-SOR algorithms. These improvements become especially pronounced when the number of users is large.

Chapter 4

Transmit Beamforming for Multi-Group Multicasting

The spatial multiplexing capabilities of a transmitter with multiple-antennas can be exploited by allowing multiple multicast groups, instead of a single-group, to share the same frequency band, thus increasing the number of accommodated users. This leads to a more efficient utilization of the available RF spectrum which is indeed a strong motivation for multi-group multicasting. On the other hand, multi-group multicasting will result in MAI since the signal intended to a certain multicast group is an undesired signal for the other groups. Therefore, efficient algorithms are required to reap the merits of multi-group multicasting while suppressing the effects of undesired MAI. In the present chapter, the transmit beamforming problem for multi-group multicasting is considered. Several existing techniques which solve the beamforming problem are briefly introduced in Section 4.1. In Section 4.2, the problem of minimizing the transmitted power subject to individual SINR constraints is formulated and the SDR-based technique is explained. A modification to the SDR-based technique which reduces the computational complexity while maintaining the same performance is also proposed in this section. In Section 4.3, we develop a novel approach to deal with the beamforming problem for multi-group multicasting. The proposed approach is based on broadcasting using hierarchical modulation. In contrast to the conventional

multicasting approaches, our proposed approach results in a problem formulation which is always feasible, has a significantly less computational cost, and achieves a better performance in terms of transmitted power. Furthermore, the approach naturally incorporates the reception of multiple datastreams while meeting the QoS requirement for each datastream. In Section 4.4, we compare the proposed techniques with existing state-of-the-art techniques and verify the improved performance via simulations.

4.1 Motivation and Preliminary Work

As a result of being a natural extension to the single-group multicasting and multi-user unicasting problems, the beamforming problem for multi-group multicast networks has gained enormous interest over the last decade. In this context, several problem formulations were proposed and some existing techniques were extended or modified as well as several others were developed particularly to solve this problem [8], [13], [14], [30], [31], [34], [46], [50], [51], [52], [53], [62], [70], [72], [75], [102], [103], [104]. The multi-group multicasting problem was first discussed by Lopez in his PhD thesis [62]. In his work, he suggested using the null-space projection technique to eliminate the MAI at the receivers. The main advantage of this technique is its reduced computational complexity. However, this technique is a good candidate only for scenarios where the number of users and multicast groups is relatively small compared to the number of transmit antennas.

Null-space-based methods have inspired several other works such as the methods in [102], [103], [104], [105], and [106]. In [105] and [106], a null-space-based method, referred to as the block diagonalization (BD) method, was developed to solve the sum-rate maximization problem in MIMO multi-user unicast networks, where it is assumed that each user has multiple receive antennas. In [104], Silva and Klein exploited the analogy between the multi-group multicast scenario and the MIMO multi-user unicast

scenario[1] to propose the so-called multicast-aware zero-forcing technique. The idea is to stack the symbols received at all the receivers in a vector $\mathbf{v}$ and then design the beamformers at the transmitter in order to minimize the mean square estimation error (MSE) of $\mathbf{v}$ subject to a total transmit power constraint and a zero-forcing constraint which forces the estimation error to be equal to zero in the absence of noise. The solution to this problem was found by using the multicast variant of the BD algorithm [105], [106]. Moreover, several linear and non-linear precoding techniques, such as vector precoding or Tomlinson Harashima precoding [29], [112], have been proposed using the MSE and the minimum MSE (MMSE) as optimization criteria in [102], [103], and [104].

In [53], a precoding strategy which employs dirty paper coding (DPC) [20] was proposed to maximize the sum-rate in multi-group multicast networks. This optimization criterion is not essentially fair in terms of the individual SINRs achieved at the receivers, since the power allocation in sum-rate maximization problems is the water filling algorithm [79] which favors the users with strong channels.

Other beamforming designs which promote fairness among the users are based on the power minimization subject to individual SINR constraints as well as the maximization of the minimum SINR problem, which is also known as the max-min fair beamforming design. Both beamforming designs were first formulated for multi-group multicasting by Karipidis et al. in [50] and [51]. The authors in [51] used the SDR approach to obtain approximate solutions to both problems. Moreover, a through analysis of both problems and an explanation of their relation to each other was provided in [51] . Similar to the single-group case, the SDR-based technique serves as a non-achievable performance bound and will be discussed later in more detail in Section 4.2.1. Note that the SDR approach for solving the beamforming problem for multi-group multicasting is, in fact, a generalization of the multi-user unicasting case which was studied by Bengtsson and Otterson in [10] and was solved using the same approach.

[1]The analogy comes from the fact that the receive antenna of a particular user in MIMO unicasting can be thought of as single-antenna users which are members of the same multicast group.

In [30] and [31], a technique based on DPC was proposed to solve the power minimization problem. By applying such a precoding strategy, the MIMO channel matrix, which is constructed by stacking the individual channel vectors of all users is transformed into a matrix with a block triangular structure. This structure allows designing the beamformers on a group-by-group basis since in each step, the interference from all previous groups is known. The authors in [30] and [31] designed the beamformer for each group using the SDR-based technique for single-group multicasting [97].

More recently, Bornhorst and Pesavento proposed a technique based on iterative second-order cone programming (SOCP) to solve the power minimization problem in [12]. The idea is to approximate the original problem as a SOCP problem. Then, through an iterative feasibility search procedure, the problem approximation is successively improved. In each iteration, the feasibility search problem is formulated as a SOCP problem. The iterative SOCP technique outperforms the SDR-based technique in terms of transmitted power and enjoys a relatively small computational complexity. Moreover, the computational complexity of the iterative SOCP technique becomes less than that of the SDR-based method as the total number of users increases.

4.2 Problem Formulation

Consider the wireless multicast network of Section 2.2.1 in the case where the transmitter is sending L datastreams simultaneously to M users. Each user is equipped with a single antenna and can choose to receive one or several datastreams out of the available L datastreams. The users are assumed to be randomly located within a certain coverage area of the transmitter as shown in Fig. 4.1. Due to the random distribution of the users, it is possible that the downlink channels of users belonging to different multicast groups are strongly correlated. This leads to the reception of undesired signals with fairly high powers at each user.

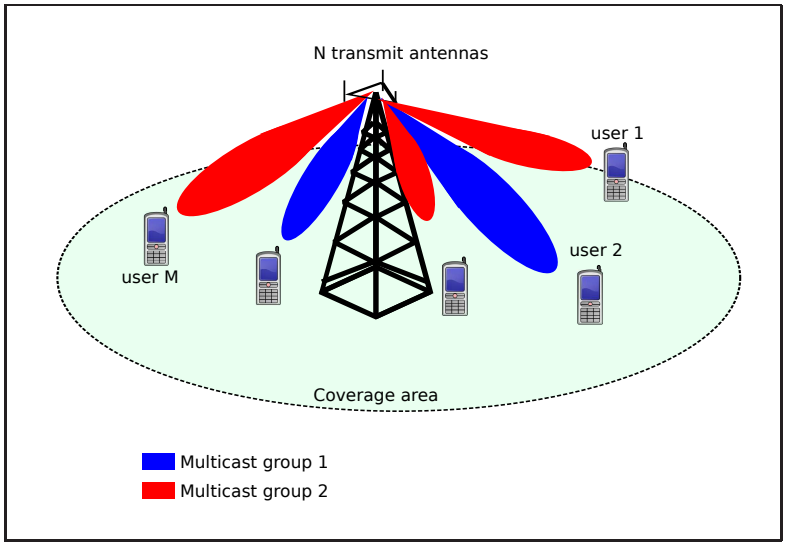

Figure 4.1: Transmit beamforming for a multicast scenario with two multicast groups.

In conventional multi-group multicasting networks, it is assumed that each user receives only one datastream, i.e., $\mathcal{G}_i \cap \mathcal{G}_j = \emptyset$, for all $i, j = 1, \ldots, L$ [51]. If we consider the input side of the transmitter, Fig. 4.2 shows the L parallel datastreams in their bitstream format before mapping the bits to complex information symbols. The kth bitstream represents a multicast service offered to the corresponding multicast group $\mathcal{G}_k$, $k = 1, \ldots, L$. Based on the multicast service specifications, the transmitter determines the number of bits m_k to be transmitted to the kth multicast group in one symbol duration and forms a binary codeword b_k of length m_k bits out of the kth bitstream, $k = 1, \ldots, L$. It is assumed that QAM schemes are used such that, the codeword b_k is mapped to a symbol s_k using QAM of order 2^{m_k}, $k = 1, \ldots, L$. The symbols $\{s_k\}_{k=1}^{L}$ are then fed to the transmitter.

The objective is to design L beamformers at the transmitter so that the resulting beam-pattern for each datastream is directed towards the intended users while minimizing the leakage in other directions. The benefit of this design is two-fold: First, the transmitted power is reduced significantly compared to isotropic radiation patterns. Second, the MAI is limited and the transmitter is able to provide a high QoS to each

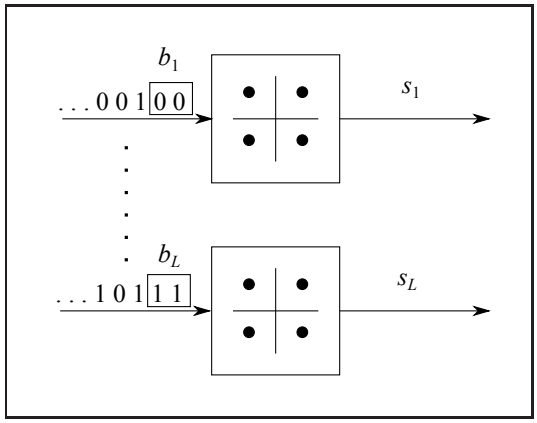

Figure 4.2: The input side of the transmitter in conventional multi-group multicasting.

user. In this context, two optimization problems for the design of the beamformers are presented. Taking into account the system model of Section 2.2.1 and assuming that the symbols s_k, $k = 1, \ldots, L$, are mutually uncorrelated with average power per symbol is equal to one, i.e., $E\{|s_k|^2\} = 1$, the total transmitted power is given as

$$P_T = E\{\mathbf{x}^H \mathbf{x}\} = \sum_{k=1}^{L} \|\mathbf{w}_k\|^2. \tag{4.1}$$

Using equation (2.9) and assuming that the transmitter knows the instantaneous CSI of all users, the SINR of the ith user γ_i is computed at the transmitter as

$$\gamma_i = \frac{|\mathbf{w}_k^H \mathbf{h}_i|^2}{\sum_{j \neq k} |\mathbf{w}_j^H \mathbf{h}_i|^2 + \sigma_i^2} \quad , \text{ for all } i \in \mathcal{G}_k \text{ and } j, k = 1, \ldots, L. \tag{4.2}$$

The problem of finding the beamforming weight vectors $\{\mathbf{w}_k\}_{k=1}^L$ which minimize the total transmitted power subject to satisfying the SINR constraint of the ith user can be written as

$$\begin{aligned} \min_{\{\mathbf{w}_k\}_{k=1}^L} \quad & \sum_{k=1}^{L} \|\mathbf{w}_k\|^2 \\ \text{s.t.} \quad & \gamma_i \geq \gamma_{\min,i} \quad , \; i = 1, \ldots, M \end{aligned} \tag{4.3}$$

where $\gamma_{\min,i}$ is the minimum SINR which guarantees the QoS of the ith user. The problem in (4.3) is a QCQP with non-convex constraints [16], which becomes infeasible if the SINR requirements are high or if the number of users is significantly larger than the number of transmit antennas, i.e., $M \gg N$ [51]. A similar beamforming design is the max-min fair optimization aiming at maximizing the worst SINR subject to a constraint on the maximum transmitted power. In this case, the transmitter serves the users on a "best effort" basis with no QoS guarantees. The optimization problem can be expressed as

$$\begin{aligned} \max_{\{\mathbf{w}_k\}_{k=1}^{L}} \quad & \min_{i} \quad \gamma_i \quad , \; i = 1, \ldots, M \\ \text{s.t.} \quad & \sum_{k=1}^{L} \|\mathbf{w}_k\|^2 \leq P_0 \end{aligned} \tag{4.4}$$

where P_0 denotes the maximum allowed transmit power. Similar to (4.3), the problem in (4.4) is a QCQP with a non-convex constraint. The main difference between the two problems is that the max-min fair problem in (4.4) is always feasible. Moreover, the inequality constraint in (4.4) will be always met with equality at the optimum. This can be proved by contradiction: Let us assume that the optimum beamformers do not satisfy the power inequality constraint with equality. This means that there is some power left in the power budget. This remaining power can be distributed, e.g., evenly among all the beamformers by multiplying each one with a constant $\alpha > 1$. This leads to an increase in the minimum SINR, thus contradicting optimality. Therefore, the problem can be equivalently rewritten by substituting the inequality constraint with equality. The resulting problem is given as

$$\begin{aligned} \max_{\{\mathbf{w}_k\}_{k=1}^{L}} \quad & t \\ \text{s.t.} \quad & \frac{\gamma_i}{\gamma_{\min,i}} \geq t \quad , \; i = 1, \ldots, M \\ & \sum_{k=1}^{L} \|\mathbf{w}_k\|^2 = P_0, \quad \text{and} \quad t \geq 0 \end{aligned} \tag{4.5}$$

where t is a positive real variable denoting a lower bound on the minimum of the weighted SINRs, i.e., $\min_i \frac{\gamma_i}{\gamma_{\min,i}}$, $i = 1, \ldots .M$. In (4.5) the weighted SINR of the

"worst user" is maximized, thus ensuring a weighted fairness among all users. If we define $\mathbf{d} \triangleq [\gamma_{\min,1}, \ldots, \gamma_{\min,M}]$ and t_0 as the optimum value of the problem in (4.5), then the SINR levels provided by the optimum beamformers are shown to be equal to $t_0\mathbf{d}$, i.e., all the weighted SINR constraints are active at the optimum [51]. In other words, if $t_0\mathbf{d}$ is regarded as a vector of target SINRs for the problem in (4.3), then the total transmitted power required to optimally satisfy these constraints is P_0. This interesting fact, which relates the problems in (4.3) and (4.5) can be used to obtain the solution of one problem from the other. For the problem in (4.5), the optimum value, t_0, can be found by iteratively solving the problem in (4.3), where $t\mathbf{d}$ is taken as the vector of SINR targets and the value of t is gradually increased until the power approaches the limit value P_0. Similarly, the problem in (4.3) can be solved by applying the bisection technique to the problem in (4.5) over P_0, provided that the problem in (4.3) can be solved optimally [51].

Another interesting feature of these two problem formulations is that they contain the single-group and the multi-user unicast beamforming problems as special cases. In the case where $L = 1$, the problems in (4.3) and in (4.5) reduce to the power minimization problem and the max-min fair problem in (3.2) and in (3.34), respectively. The latter problems were proved to be NP-hard in [97], which motivated the claim by Karipidis et al. in [51] that the problems in (4.3) and (4.5) are NP-hard in general. On the other hand, if $L = M$, i.e., each multicast group has only one user, both problems represent the popular multi-user unicasting problem which has been extensively explored in the literature, see [11], [24], [34], [65], [75], [124], and references therein. In [11], the authors showed that the SDP relaxation of the multi-user unicasting problem is guaranteed to have at least one optimal solution which is rank-one. In [90] and [91], computationally efficient iterative techniques were developed based on the uplink-downlink duality approach and it was proved that the algorithm always converges to the optimal value. These surprising results to this seemingly non-convex problem were confirmed by a solid equivalent reformulation of the problem as a convex SOCP problem in [124].

4.2.1 SDR-Based Technique

Following the same approach of the single-group case, the authors in [51] define the matrices:

$$\mathbf{Q}_i \triangleq \mathbf{h}_i\mathbf{h}_i^H, \quad \mathbf{X}_k \triangleq \mathbf{w}_k\mathbf{w}_k^H, \quad i = 1, \ldots, M, \quad k = 1, \ldots, L.$$

Using the fact that

$$|\mathbf{w}_k^H\mathbf{h}_i|^2 = \text{trace}\{\mathbf{w}_k\mathbf{w}_k^H\mathbf{h}_i\mathbf{h}_i^H\} = \text{trace}\{\mathbf{X}_k\mathbf{Q}_i\},$$

the problem in (4.3) can be rewritten as [51]

$$\begin{aligned} \min_{\{\mathbf{X}_k\}_{k=1}^L} \quad & \sum_{k=1}^{L} \text{trace}\{\mathbf{X}_k\} \\ \text{s.t.} \quad & \text{trace}\{\mathbf{X}_k\mathbf{Q}_i\} \geq \gamma_{\min,i} \sum_{j\neq k} \text{trace}\{\mathbf{X}_j\mathbf{Q}_i\} + \gamma_{\min,i}\sigma_i^2 \\ & \text{for all} \quad i \in \mathcal{G}_k, \quad \text{for all} \quad j, k \in \{1, \ldots, L\} \\ & \mathbf{X}_k \succeq \mathbf{0}, \quad \text{rank}\{\mathbf{X}_k\} = 1 \quad k = 1, \ldots, L. \end{aligned} \tag{4.6}$$

The L rank constraints in (4.6) are the only non-convex constraints. By dropping these constraints, the problem translates to a convex SDP problem which can be solved using available convex optimization tools [107], [36]. The resulting convex optimization problem reads

$$\begin{aligned} \min_{\{\mathbf{X}_k\}_{k=1}^L} \quad & \sum_{k=1}^{L} \text{trace}\{\mathbf{X}_k\} \\ \text{s.t.} \quad & \text{trace}\{\mathbf{X}_k\mathbf{Q}_i\} \geq \gamma_{\min,i} \sum_{j\neq k} \text{trace}\{\mathbf{X}_j\mathbf{Q}_i\} + \gamma_{\min,i}\sigma_i^2 \\ & \text{for all} \quad i \in \mathcal{G}_k, \quad \text{for all} \quad j, k \in \{1, \ldots, L\}. \\ & \mathbf{X}_k \succeq \mathbf{0} \quad k = 1, \ldots, L. \end{aligned} \tag{4.7}$$

If the solution of the convex problem in (4.7), denoted by $\{\mathbf{X}_{k,\text{opt}}\}_{k=1}^L$, contains only rank-one matrices, then the relaxation is tight and the optimal beamforming vectors $\{\mathbf{w}_{k,\text{opt}}\}_{k=1}^L$ are the principal components of $\{\mathbf{X}_{k,\text{opt}}\}_{k=1}^L$. If one of the matrices in

$\{\mathbf{X}_{k,\text{opt}}\}_{k=1}^{L}$ is not rank one, randomization techniques are used to generate multiple candidate weight vectors [51]. In every randomization, a random weight vector with unit-norm is generated from each matrix in $\{\mathbf{X}_{k,\text{opt}}\}_{k=1}^{L}$ which is not rank-one. For the rank-one matrices in $\{\mathbf{X}_{k,\text{opt}}\}_{k=1}^{L}$, the normalized principal component is used. For the so-obtained set of candidate weight vectors $\{\mathbf{w}_{k,\text{cand}}\}_{k=1}^{L}$, a set of optimal scaling coefficients $\{\sqrt{p_k}\}_{k=1}^{L}$ can be obtained by solving the following optimal power allocation problem [51]:

$$\begin{aligned} \min_{\{p_k\}_{k=1}^{L}} \quad & \sum_{k=1}^{L} p_k \\ \text{s.t.} \quad & \frac{p_k a_{k,i}}{\sum_{j\neq k} p_l a_{j,i} + \sigma_i^2} \geq \gamma_{\min,i} \quad , p_k \geq 0 \\ & \text{for all} \;\; i \in \mathcal{G}_k, \quad j,k = 1,\ldots,L, \end{aligned} \tag{4.8}$$

where $a_{k,i} \triangleq |\mathbf{w}_{k,\text{cand}}^H \mathbf{h}_i|^2$. The problem in (4.8) is a linear programming (LP) problem. If a solution $\{\tilde{p_k}\}_{k=1}^{L}$ exists, the candidate weight vectors are updated as $\{\tilde{\mathbf{w}}_{k,\text{cand}}\}_{k=1}^{L} = \{\sqrt{\tilde{p_k}}\mathbf{w}_{k,\text{cand}}\}_{k=1}^{L}$, otherwise they are discarded. After a number of randomizations n_{rand}, the set of candidate weight vectors with the least value of $\sum_{k=1}^{L} \|\tilde{\mathbf{w}}_{k,\text{cand}}\|^2$ is chosen.

Almost all modern SDP solvers use interior point methods to solve the problem in (4.7). For L variables of size $N \times N$ and M linear constraints, the interior point methods require $\mathcal{O}(\sqrt{LN}\log(1/\epsilon))$ iterations, where ϵ denotes the accuracy of the solution after termination. Each iteration requires in the worst case $\mathcal{O}(L^3N^6 + MLN^2)$ arithmetic operations [125]. For the LP program in (4.8), the optimal solution can be found using interior point methods which require $\mathcal{O}\big(\sqrt{L}\log(1/\epsilon)\big)$ iterations, where each iteration requires $\mathcal{O}(L^3 + ML)$ arithmetic operations at the most [125]. The overall computational complexity of the SDR-based technique involves solving the SDP in (4.7) and n_{rand} LP problems as in (4.8) for each of the candidate weight vector generated via randomizations. This resembles a relatively high computational cost especially for large-sized problems, i.e., when the problem parameters L, M, and N are large. In [12], it was shown that the iterative SOCP approach provides better

performance compared to the SDR-based technique at a reduced computational cost. The reason is that in the iterative SOCP approach, the randomization step and the accompanying LP problem are avoided altogether and are substituted by a SOCP problem, which can be solved within a few iterations. In the following section, a modification to the SDR-based technique is proposed in order to avoid solving the LP problem for the outcome of each randomization trial. This modification reduces the overall complexity of the SDR-based technique proposed in [51] while maintaining almost the same performance.

4.2.2 Modified SDR

In this section, we propose a modification to the SDR-based technique of [51], which reduces the overall computational complexity. The idea is to apply a simple test for each set of the randomly generated candidate weight vectors $\{\mathbf{w}_{k,\text{cand}}\}_{k=1}^{L}$ to verify if it admits a positive SINR at the ith user, $i = 1, \ldots, M$. If the set of candidate vectors passes this test, the LP problem in (4.8) is formulated and the optimal scaling coefficients $\{\sqrt{\widetilde{p}_k}\}_{k=1}^{L}$ are computed, otherwise, the set of vectors is discarded. We start by rewriting the problem in (4.3) by defining the $LN \times 1$ complex weight vector $\mathbf{w}_T$ as

$$\mathbf{w}_T \triangleq [\mathbf{w}_1^T, \ldots, \mathbf{w}_L^T]^T. \tag{4.9}$$

The total transmitted power P_T is then given as

$$P_T = \sum_{k=1}^{L} \|\mathbf{w}_k\|^2 = \|\mathbf{w}_T\|^2. \tag{4.10}$$

Similarly, for the ith user, $i = 1, \ldots, M$, the matrices $\underline{\mathbf{E}}_i$ and $\underline{\mathbf{H}}_i$ are defined as

$$[\underline{\mathbf{E}}_i]_{mn} \triangleq \begin{cases} 1 & , m = n = i \\ -\gamma_{\min,i} & , m = n, m \neq i \\ 0 & \text{otherwise} \end{cases} \tag{4.11}$$

and

$$\underline{\mathbf{H}}_i \triangleq \frac{1}{\sigma_i^2 \gamma_{\min,i}} \underline{\mathbf{E}}_i \otimes \mathbf{h}_i \mathbf{h}_i^H, \tag{4.12}$$

respectively, where $\otimes$ denotes the Kronecker product. The SINR constraint of the ith user can then be written as

$$\frac{1}{\sigma_i^2\gamma_{\min,i}}\left(|\mathbf{w}_k^H\mathbf{h}_i|^2-\gamma_{\min,i}\sum_{j\neq k}|\mathbf{w}_j^H\mathbf{h}_i|^2\right)=\mathbf{w}_T^H\underline{\mathbf{H}}_i\mathbf{w}_T\geq 1 \tag{4.13}$$

and the problem in (4.3) can be equivalently rewritten as

$$\begin{aligned}\min_{\mathbf{w}_T}\quad & \|\mathbf{w}_T\|^2\\ \text{s.t.}\quad & \mathbf{w}_T^H\underline{\mathbf{H}}_i\mathbf{w}_T\geq 1\\ & \text{for all}\ \ i\in\mathcal{G}_k,\quad k=1,\ldots,L.\end{aligned} \tag{4.14}$$

By definition, the matrix $\underline{\mathbf{H}}_i$ is of dimension $NL\times NL$, Hermitian, block-diagonal, and indefinite. The fact that $\underline{\mathbf{H}}_i$ is indefinite means that a vector $\mathbf{w}_T$ which satisfies all the SINR constraints in (4.14) might not exist. This is another way to explain why the problem in (4.3) could turn out to be infeasible. In order to check the feasibility of the problem, the SDR-based technique requires solving the LP in (4.8) for each of the randomly generated sets of candidate weight vectors $\{\mathbf{w}_{k,\text{cand}}\}_{k=1}^L$ for a large number of randomizations n_{rand} [51]. If no solution is found from all generated sets, the problem is considered infeasible. This is an inconclusive check since it depends on the number of randomizations to explore whether a solution exists or not. Another inconclusive check which requires less computations can be performed as follows: For each randomization, check if

$$\mathbf{w}_{T,\text{cand}}^H\underline{\mathbf{H}}_i\mathbf{w}_{T,\text{cand}}>0,\quad \text{for all } i=1,\ldots,M, \tag{4.15}$$

is satisfied, where $\mathbf{w}_{T,\text{cand}}\triangleq[\mathbf{w}_{1,\text{cand}}^T\ldots,\mathbf{w}_{L,\text{cand}}^T]^T$. If any of the inequalities in (4.15) is not satisfied, the candidate weight vectors are discarded. On the other hand, if all the inequalities in (4.15) are satisfied, then a set of candidates can be made feasible for (4.14) by simple scaling. This is similar to the single-group case. However, solving the LP in (4.8) may be more appropriate, since it computes the optimal scaling coefficients $\{\sqrt{p_k}\}_{k=1}^L$. This simple check allows to explore more random candidates while solving the LP only to those which satisfy the constraints in (4.15). Note that excluding the

candidate weight vectors which do not satisfy the constraints in (4.15) may damage the performance of the SDR-based technique. The reason is that the constraints in (4.15) are stricter than the constraints of the LP in (4.8). This makes it possible for some candidate weight vectors to be excluded via the check in (4.15), although they satisfy the constraints of the LP in (4.8) and have smaller cost functions than the ones which are considered. However, the simulation results show negligible reduction in performance compared to the SDR-based technique. Note that the computational complexity of the proposed check is $\mathcal{O}(MNL)$. Comparing with the complexity of solving the LP problem with a standard termination accuracy $\epsilon_0 = 0.01$, the proposed check has a much reduced complexity especially when $N < L^{2.5}$. The modified-SDR beamforming technique is summarized in the following table.

Table 4.1: Summary of the modified-SDR beamforming technique.

Step 1. Define $\mathbf{Q}_i = \mathbf{h}_i\mathbf{h}_i^H, \quad \mathbf{X}_k = \mathbf{w}_k\mathbf{w}_k^H, \quad i = 1, \ldots, M, \quad k = 1, \ldots, L.$

Step 2. Formulate the convex SDP problem as in (4.7) and find the solution $\{\mathbf{X}_{k,\text{opt}}\}_{k=1}^{L}$.

Step 3. **if** $\text{rank}\{\mathbf{X}_{k,\text{opt}}\} = 1$, $k = 1, \ldots, L$
The final solution is given as $\mathbf{w}_{k,\text{opt}} = \mathcal{PC}\{\mathbf{X}_{k,\text{opt}}\}, \quad k = 1, \ldots, L$
else

1. Generate a set of candidate weight vectors $\{\mathbf{w}_{k,\text{cand}}\}_{k=1}^{L}$ via randomizations.
2. Define $\mathbf{w}_{T,\text{cand}} = [\mathbf{w}_{1,\text{cand}}^T \ldots, \mathbf{w}_{L,\text{cand}}^T]^T$ and $\underline{\mathbf{H}}_i$ as in (4.12).
3. **if** $\mathbf{w}_{T,\text{cand}}^H \underline{\mathbf{H}}_i \mathbf{w}_{T,\text{cand}} > 0, \quad i = 1, \ldots, M$
Formulate the LP as in (4.8) and compute the scaling coefficients $\{\sqrt{p_k}\}_{k=1}^{L}$.
else Discard the candidate weight vectors $\{\mathbf{w}_{k,\text{cand}}\}_{k=1}^{L}$.
4. Repeat 1 to 3 for n_{rand} randomizations.

Step 4. Select the set of candidate weight vectors with the minimum $\sum_{k=1}^{L} \|\mathbf{w}_{k,\text{cand}}\|^2$ to be the final solution.

4.3 Multicasting Through Hierarchical Modulation

A novel approach to deal with the beamforming problem for multi-group multicasting is proposed in this section. The concept of hierarchical modulation, which is explained later in Subsection 4.3.1, is used to formulate the problem in (4.3) as a beamforming problem for single-group multicasting. The main advantage of the proposed approach is that the optimization problem for single-group multicasting, as discussed in the previous chapter, is always feasible, whereas, in case of conventional multi-group multicasting, the feasibility of the problem is limited due to the presence of MAI [51]. Furthermore, the proposed approach allows to naturally incorporate multiple service subscription (MSS) per user, where each user can receive multiple datastreams while meeting the QoS for each datastream. This is a generalization of the conventional multi-group multicasting scenario considered in section (4.2), since it is assumed here that $\mathcal{G}_i \cap \mathcal{G}_j \neq \emptyset$, for some $i, j \in \{1, \ldots, L\}, i \neq j$.

A practical application of the MSS scenario is a network providing two multicast services, such as different video and audio streaming programs. Each service is intended to a different multicast group and there are users, e.g., access points or high-end mobile devices, which are subscribed to both services simultaneously and receive both streams with high quality. Such a scenario was studied in the literature but with restrictions on the number of users per group or on the number of users in general. In [101], one multicast group was considered to have multiple users while the rest were restricted to have only one user per group. In [8], a technique based on a predetermined threshold was used to schedule either the multicast or the unicast traffic. In [94], the sum-rate maximization criterion was employed to find the beamforming weight vectors for simultaneous unicast and multicast services in the case of two users only.

4.3.1 Background

The basic idea of hierarchical modulation dates back to the early seventies when Cover in [21] performed an information-theoretical study on a strategy which guarantees a basic level of communication in broadcast channels. The idea is to divide the broadcast information into two or more classes with different degrees of protection, where the level of protection depends on the importance of the information. Then, the most important information, also known as "base layer or basic data", should be recovered by all receivers. Only the receivers which have better channels or better receive capabilities can recover the less important information or the "higher-layer data". From that time on, this study has triggered several research efforts which aimed at designing practical implementations of this strategy.

One practical implementation is based on hierarchical modulation [45], [74], [86], [109], [123]. This technique has been used since the early nineties for digital video broadcasting [45], [86] and has been included in various standards, such as digital video broadcasting-terrestrial (DVB-T) and ultra mobile broadband (UMB) for mobile communications. Recently, hierarchical modulation has gained a increasing interest in the initiative of upgrading the existing digital broadcast systems [45]. In contrast to traditional modulation schemes, hierarchical modulation uses several QAM schemes with variable constellation sizes based on the importance of the datastream. For the base layer, smaller constellation sizes are used, whereas for less important datastreams, higher QAM constellations are used. Fig. 4.3 shows how hierarchical modulation is applied in a broadcast network with one base layer and one enhancement layer. The more important bits of the base layer are mapped to QPSK symbols. The less important bits of the enhancement layer are used to increase the constellation size of QPSK symbols to 16 QAM such that the bits of the base layer are in the most significant bit locations (MSB) of the 16 QAM symbols. If the receive SNR at one particular user in the network is very low, the receiver can only distinguish in which quadrant the received symbol lies. Therefore, it can only extract the basic information in the bits of the base layer. On the other hand, if another user in

the network has a high receive SNR, the receiver will have more precise estimates of the phase and the amplitude of the received signal and will be able to extract the basic information and the enhancement information in the base layer bits and the enhancement layer bits, respectively.

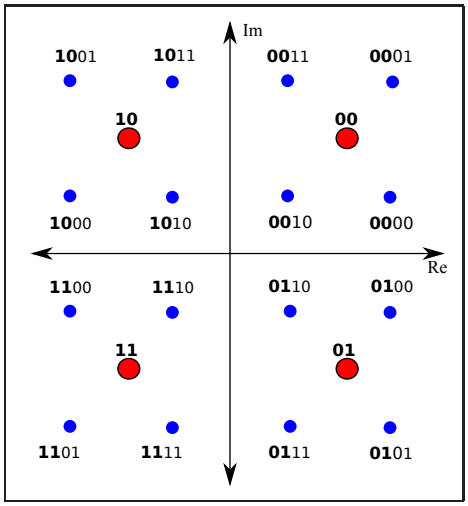

Figure 4.3: Example of QPSK and 16 QAM constellations in hierarchical modulation.

4.3.2 The Proposed Approach

The proposed approach is based on the hierarchical modulation scheme discussed in the previous subsection. The L parallel bitstreams available at the transmitter for the different groups are multiplexed to form a single bitstream. In one symbol duration, the multiplexer takes m_k successive bits from the kth bit stream, $k = 1, \ldots, L$, to construct a binary codeword b of length $m = \sum_{k=1}^{L} m_k$ bits as shown in Fig. 4.4. We assume that the indexing of the multicast groups and the corresponding bitstreams is predefined at the transmitter based on a certain criterion. A simple criterion is to perform the indexing to be equivalent to the order with which the multicast groups are admitted during the initialization phase of the system. Therefore, the bits b_1 intended to the first admitted multicast group $\mathcal{G}_1$ are multiplexed at the least significant bit (LSB) locations while the bits intended to the newly admitted multicast group $\mathcal{G}_L$

are multiplexed at the MSB locations of the codeword b:

$$b = \underbrace{b_L}_{MSB} \cdots \underbrace{b_1}_{LSB}$$

The codeword b is then mapped to a symbol s using the QAM scheme of order 2^m. The symbol s is then broadcasted to all M users. Note that, in contrast to the conventional hierarchical modulation scheme, the L bitstreams multiplexed at the transmitter do not belong to the same multicast service. Therefore, it is important that each user can demodulate and identify the bitstream intended to it. During the subscription phase of each user, the transmitter sends to the user the index of its multicast group k, the number of bits per symbol m_k, and the value $r_k = \sum_i^k m_i/m_k$ which is a multiple of 2 for $k > 1$. The order of the QAM scheme, which is used by the users of the kth multicast group to demodulate the received signal is given by

$$M_k = 2^{r_k m_k},\ k = 1, \ldots, L. \tag{4.16}$$

Based on this information, each user can demodulate the received signal and successfully select the m_k MSB bits out of the received codeword. For example, if $m_k = 2,\ k = 1, 2$, then the users of multicast groups $\mathcal{G}_1$ and $\mathcal{G}_2$ will use QAM schemes of order 4 and 16 to generate the received codewords $\tilde{b_1}$ and $\tilde{b_2}\tilde{b_1}$ and select $\tilde{b_1}$ and $\tilde{b_2}$ respectively. We note that this reception technique can be considered as a multi-user detection technique, since the users of the kth multicast group must successfully detect all the codewords intended to multicast groups of lower indices, i.e., $b_1, \ldots, b_{k-1}$, in order to detect the required codeword b_k.

Due to multiplexing the multiple bitstreams into one bitstream, the power minimization problem in (4.3) will now take the form of a single-group multicasting problem, i.e., $L = 1$. The power minimization problem is now written as

$$\begin{aligned} &\min_{\mathbf{w}} \ \|\mathbf{w}\|^2 \\ &\text{s.t.} \quad \frac{|\mathbf{w}^H \mathbf{h}_i|^2}{\sigma_i^2} \geq \beta_{\min,i},\ i = 1, \ldots, M \end{aligned} \tag{4.17}$$

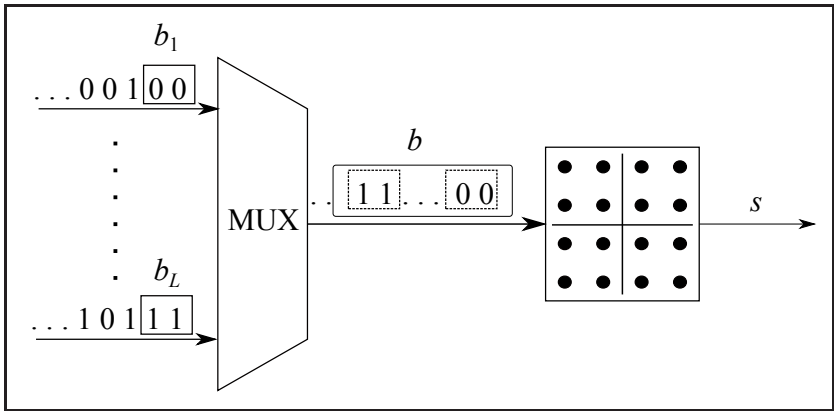

Figure 4.4: The input side of the transmitter using hierarchical modulation.

where $\mathbf{w}$ is $N \times 1$ beamforming vector and $\beta_{\min,i}$ is the minimum required SNR to guarantee the minimum QoS requirement of the ith user.

The main difference between the problem in (4.3) and the problem in (4.17) is that the former can easily become infeasible as the number of constraints increases or if the constraints become more strict, while the latter always admits a solution by scaling the transmitted power and therefore, it is always feasible [97]. Furthermore, approximate solutions to the problem in (4.17) can be obtained with significantly less computational complexity than the problem in (4.3), e.g., [4]. Similar to the procedure followed to obtain the relaxed problem in (4.7), we define $\mathbf{X} \triangleq \mathbf{w}\mathbf{w}^H$ and drop the rank constraint $\text{rank}\{\mathbf{X}\} = 1$ which results in a SDP problem. The final weight vector is obtained from the solution of the SDP, denoted by $\mathbf{X}_{\text{opt}}$, via randomization techniques [97]. Note that for $L = 1$, the problem in (4.8) boils down to a simple scaling problem and therefore, it is always feasible.

In (4.17), the value of $\beta_{\min,i}, i = 1, \ldots, M$, is chosen so that the same QoS is maintained as in the conventional multi-group multicasting case. In order to find the value $\beta_{\min,i}$, we note that for a given modulation scheme, the QoS requirement of the ith user expressed as $\gamma_{\min,i}$, is directly related to the maximum bit error rate (BER) tolerated at the receiver. Therefore, if a higher order modulation scheme is

used, $\beta_{\min,i}$ should be increased in order to achieve the same BER as that achieved by $\gamma_{\min,i}$, hence maintaining the same QoS.

The relation between $\gamma_{\min,i}$ and $\beta_{\min,i}$ for the Rayleigh fading channel model can be obtained from the BER curves for different QAM schemes in [61], [87]. In the high SNR region, the following relation holds

$$(\beta_{\min,i})_{\mathrm{dB}}^{2^{r_k m_k}} = (\gamma_{\min,i})_{\mathrm{dB}}^{2^{m_k}} + 10\log_{10}(r_k) + c_0(r_k - 1) \quad , k = 1, \ldots, L \tag{4.18}$$

where $c_0 \cong 3\mathrm{dB}$ and $(\cdot)_{\mathrm{dB}}^{2^m}$ denotes the SNR or the SINR in dB in case of 2^m QAM scheme. The term $10\log_{10}(r_k)$ is the power normalization term which guarantees a fair comparison between the different QAM schemes by fixing the energy per symbol at the transmitter for all QAM schemes. The value c_0 denotes the additional SNR that has to be invested to be able to transmit an extra bit per quadrature component, i.e., two extra bits per symbol, while maintaining the same BER. It was shown in [61] that the value of c_0 is about 3-4 dB. It is important to point out that the BER achieved with $\beta_{\min,i}$ refers to the error rate in the total number of bits received. Users of the kth multicast group, for $k > 1$, will select only one bitstream out of the multiple bitstreams they receive. Therefore, the actual BER will be less than the one provided using equation (4.18) and the QoS constraints will be oversatisfied. Nevertheless, for simplicity of comparison, we use equation (4.18) to compute $\beta_{\min,i}$ for the problem in (4.17).

One important aspect of our proposed approach is that it easily allows a single user to subscribe to multiple services and to receive multiple bitstreams with high SNR. Every time the ith user subscribes to a new service, the transmitter sends the subscription parameters mentioned previously and the ith user computes a new QAM order from these parameters as in (4.16). The user then selects the highest QAM order from all the ones it computed to demodulate the received signal. Another important property of the proposed scheme is that the process of adding/admitting users to the system does not alter the QoS experienced by the users that have already been

admitted in previous steps.

4.4 Simulation Results

Throughout our simulations, we assume a Rayleigh fading channel model, where the elements of each channel vector are i.i.d. circularly symmetric complex Gaussian random variables with zero mean and unit-variance. We consider the case where $N = 4$ and $\gamma_{\min,i} = \gamma_{\min}$ and $\sigma_i^2 = 1$, $i = 1, \ldots, M$. The users are considered to be evenly distributed among the multicast groups. The following techniques are compared:

- The SDR-based technique for multi-group multicasting (MGM) of Section 4.2.1, denoted by SDR-MGM.
- The modified SDR-based technique for MGM of Section 4.2.2, denoted by mSDR-MGM.
- the single-group multicasting (SGM) technique proposed in Section 4.3 based on hierarchical modulation, denoted by SDR-SGM.

We use the values $\sum_{k=1}^{L} \text{trace}\{\mathbf{X}_{k,\text{opt}}\}$ and $\mathbf{X}_{\text{opt}}$ as lower bounds on the transmitted power in the case of MGM and in the case of SGM and denote them as LB-MGM and LB-SGM, respectively.

In our first example, we compare the performance of the SDR-MGM technique with the mSDR-MGM technique in terms of the average transmitted power and the percentage of infeasible runs out of 1000 Monte-Carlo runs. We assume $L = 2$, $\gamma_{\min} = 6$ dB, and the number of users in each multicast group is increased from 2 to 8. For the randomization step, 300 randomization samples are generated and used for both techniques. Fig. 4.5 depicts the average of the total transmitted power of both techniques. Note that the average is taken only over the runs where *both* techniques generate a feasible solution. It can be observed from the figure that both technique show almost identical performance.

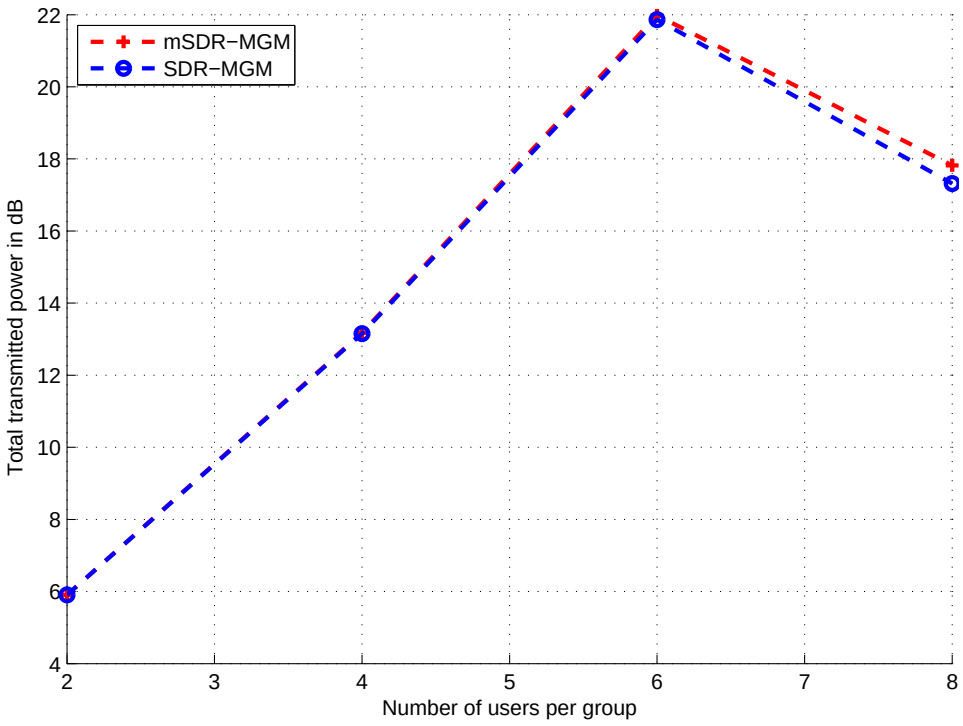

Figure 4.5: Total transmitted power versus number of users per multicast group; first simulation example.

A Similar observation can be made from Fig. 4.6, where the percentage of infeasible Monte-Carlo runs for both techniques is depicted. Table 4.2 shows the percentage of Monte-Carlo runs where the randomization with LP routine is employed, i.e., the relaxed problem is feasible and the solution contains matrices which are not rank-one. The average number of LP problems solved for each run in the case of mSDR-MGM is compared to 300 LPs for each run in the case of SDR-MGM. As it can be observed from the table, the mSDR-MGM technique requires solving significantly less number of LP problems, which results in a significant reduction in the total computational cost of the algorithm. This reduction becomes more evident as the number of users per group increases.

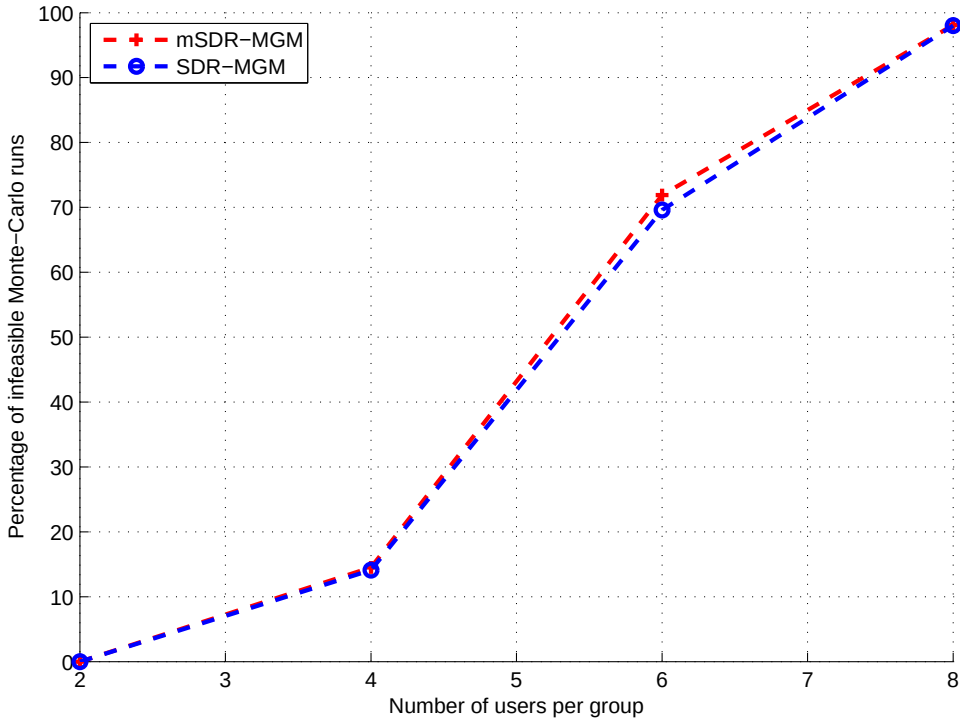

Figure 4.6: Percentage of infeasible runs versus number of users per multicast for group $N = 4$, $L = 2$, and $\gamma_{\min} = 6$ dB; first simulation example.

Number of users per group	2	4	6	8
Percentage of runs where LP is employed	0%	20%	22.2%	2.6%
Average number of LPs (mSDR)	0	47.7	11.3	3.00
Number of LPs (SDR)	0	300	300	300

Table 4.2: Average number of LPs in mSDR-MGM versus SDR-MGM for $N = 4$, $L = 2$, and $\gamma_{\min} = 6$ dB; first simulation example.

In our second example, we compare the performance of the SDR-MGM technique and its lower bound LB-MGM in terms of the average transmitted power with the SDR-SGM technique and its lower bound LB-SGM. We should remark that the average transmitted power is computed differently for each technique. This is due to the fact that in conventional MGM, feasibility is not always guaranteed. Therefore,

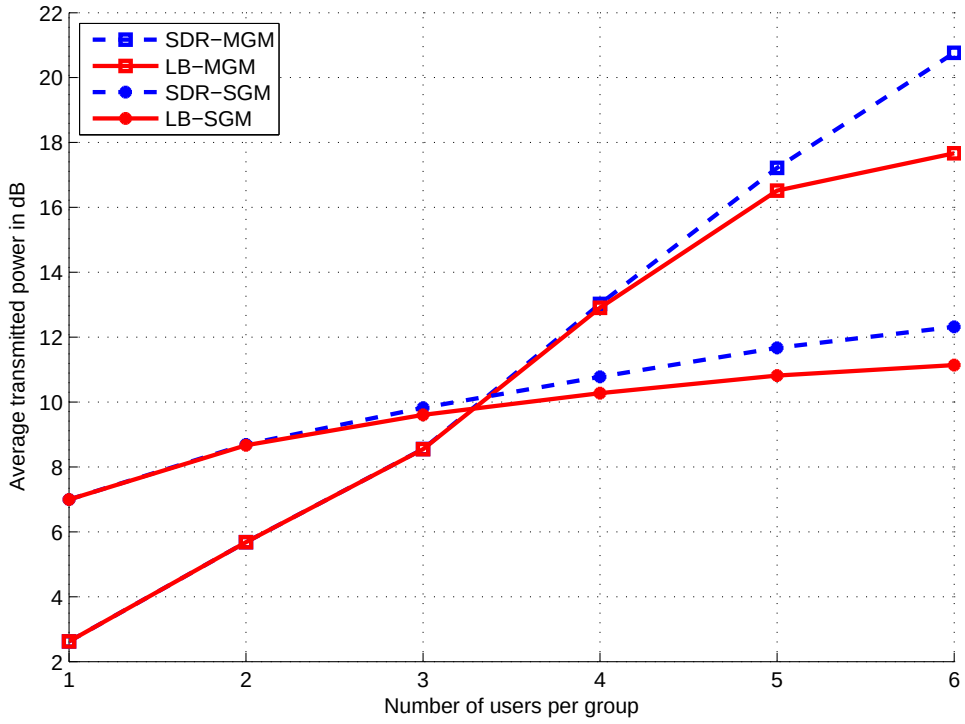

Figure 4.7: Total transmitted power versus number of users per multicast group for $N = 4$, $L = 2$, and $\gamma_{\min} = 6$ dB; second simulation example.

we average only over the runs where the SDR-MGM technique generates a feasible solution. For the SDR-SGM, we average over all runs since a feasible solution is always obtained. For both techniques, 300 randomizations are assumed and 1000 Monte-Carlo runs are performed. Fig. 4.7 shows the performance when $L = 2$ groups, $m_1 = m_2 = 2$ bits/symbol, and the number of users in each group is increased from 1 to 6 users. We assume $\gamma_{\min} = 6$ dB and $\beta_{\min}$ is computed as in equation (4.18) which is equal to 13 dB in this case. It can be observed from Fig. 4.7 that the SDR-SGM technique outperforms the SDR-MGM technique in terms of transmitted power, when the number of users per group exceeds 3. The performance gap between both techniques grows substantially as the number of users per group increases.

In Fig. 4.8 the same example is plotted in the case of $\gamma_{\min} = 14$ dB and $\beta_{\min} = 21$ dB. It can be observed that as the number of users per group exceeds 2, the SDR-SGM technique outperforms the SDR-MGM technique in terms of the transmitted power.

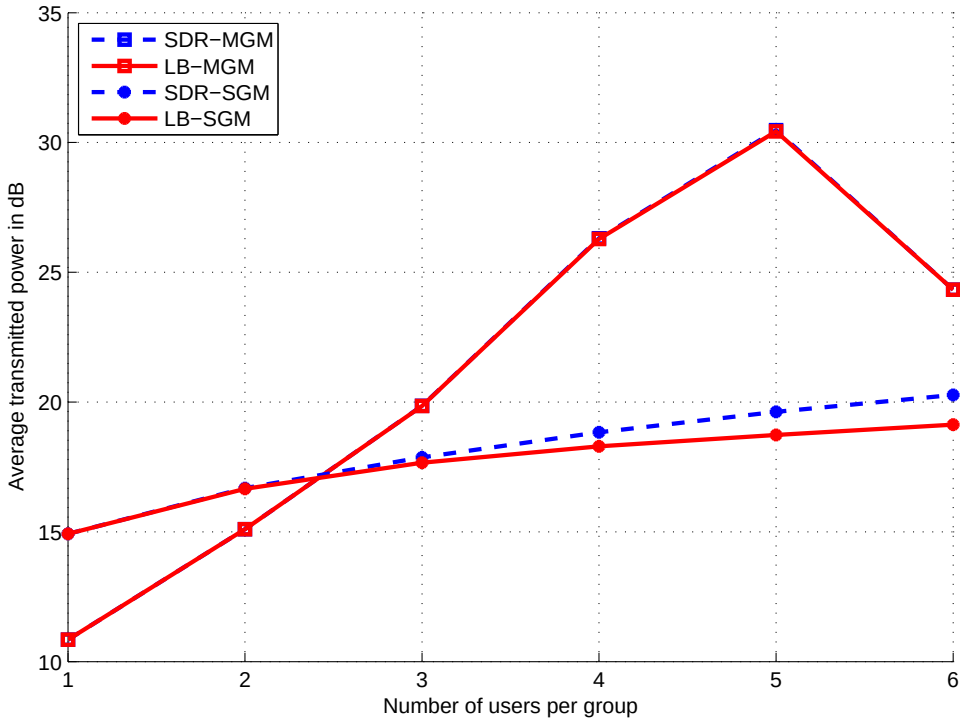

Figure 4.8: Total transmitted power versus number of users per group for $N = 4$, $L = 2$, and $\gamma_{\min} = 14$ dB; second simulation example.

In our third simulation example, we compare the performance of the SDR-MGM technique and its lower bound LB-MGM in terms of the average transmitted power with the SDR-SGM technique and its lower bound LB-SGM. We consider the case when $L = 3$ and $\gamma_{\min} = 6$ dB and the number of users in each groups is increased from 1 to 6 users. It can be observed from the figure that the SDR-SGM outperforms the SDR-MGM as the number of users per multicast group exceeds one. Furthermore, as the number of users per group increases and the SDR-MGM technique fails to provide a solution while the SDR-SGM technique only suffers a relatively small increase in the transmitted power. The same observations can be made on the behavior of the theoretical lower bounds which suggests that the problem formulation as a single-group multicasting problem is more power efficient than the multi-group multicasting formulation in case of large number of users per group.

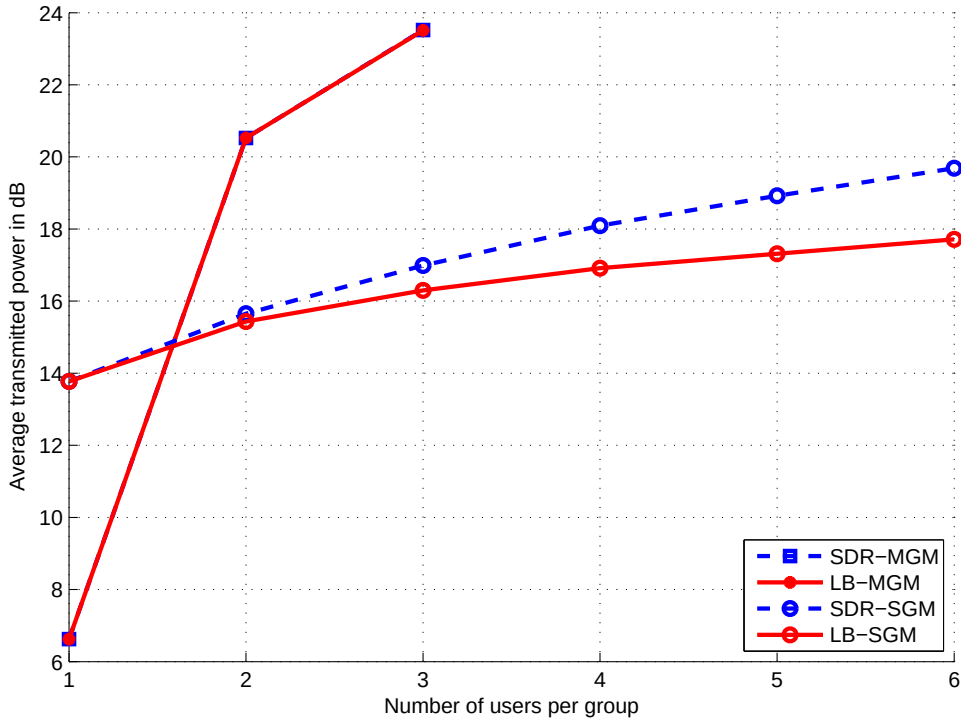

Figure 4.9: Total transmitted power versus number of users per group for $N = 4$, $L = 3$, and $\gamma_{\min} = 6$ dB; third simulation example.

4.5 Conclusion

We proposed a modification to the SDR-based technique to reduce its computational complexity while maintaining the same performance in terms of the total transmitted power and maintaining the ability to provide a feasible solution, if one exists. The reduction in complexity becomes more pronounced in the scenarios where the number of multicast groups is large. We also proposed a multicasting approach based on hierarchical modulation, where we showed via simulations that for a large number of users per group, our proposed approach outperforms the conventional multi-group multicasting approach in terms of transmitted power and computational complexity. Although an additional overhead is introduced during the subscription phase, our approach easily allows multiple service subscription, where users can receive multiple datastreams.

Chapter 5

Distributed Beamforming in Cooperative Relay Networks

In this chapter, we consider the distributed beamforming problem in AF relay networks with an emphasis on single-group multicasting scenarios. In Section 5.1, the channel orthogonalization techniques which were developed in Chapter 3 for conventional single-group multicasting are extended to approximately solve the distributed beamforming problem in AF relay networks. We examine the cases where perfect CSI or covariance CSI is available. Simulation results show that the proposed technique outperforms the popular SDR-based technique and provides a better performance to complexity trade-off over a large range of QoS constraints as compared to other existing techniques. The distributed beamforming problem relies on the assumption that all the relays in the network are fully synchronized at the symbol level. This assumption is valid only if the delay spread across different relaying paths is small compared to the symbol duration. In Section 5.2, we deal with the problem of distributed beamforming in AF relay networks with large delay spreads. We propose an OFDM-based transmission scheme which alleviates the requirement for relay synchronization. The performance of our proposed algorithms is analyzed in Section 5.3 via simulations. Finally, the main conclusions are drawn in Section 5.4.

5.1 Single-Group Multicasting in Synchronous Relay Networks

In modern subscription-based multicast networks, several users connect to the network to receive a single or multiple datastreams with acceptable QoS requirements. In order to guarantee these requirements, the transmitter relies on the CSI which it typically acquires from each subscriber via a feedback channel. In this context, the problem of transmit beamforming for single-group multicasting has been solved in [4], [42], [49], [62], [63], [77], [96], [97], [99], [100], [101], [108], [126], [127]. A common approach is to design the beamformer based on the CSI, such that the total transmitted power is minimized while satisfying the QoS requirement of each user [4], [42], [97], [108].

In some cases, conventional multicasting may lead to inefficient solutions and relaying in the form of fixed infrastructure or cooperating users may be required. Among the available relaying schemes, the AF relaying protocol is particularly popular due to its low processing complexity at the relays [5], [13], [14], [27], [28], [38], [39], [40], [48], [80], [81], [92], [93]. The problem of distributed beamforming for single-group as well as multi-group multicasting in AF relay networks was first introduced in [14] where the objective is to minimize the total relay transmitted power subject to the QoS constraints at the receivers. Based on the system model introduced in Section 2.3.1 and expressing the QoS constraints as SNR constraints at the intended receivers, the problem of total relay power minimization can be written as

$$\min \; P_t \quad \text{s.t.} \quad \frac{P_{s_j}}{P_{n_j}} \geq \gamma_j \quad j = 1, \ldots, M, \tag{5.1}$$

where γ_j denotes the minimum required SNR to satisfy the QoS constraint of the jth user. Using (2.17), (2.18), and (2.19) to substitute for the values of P_{s_j}, P_{n_j} and P_t,

respectively, (5.1) can be rewritten as

$$\begin{aligned} \min_{\mathbf{w}} \quad & \mathbf{w}^H \mathbf{D}_f \mathbf{w} \\ \text{s.t.} \quad & \frac{P_0 \mathbf{w}^H \mathbf{R}_{h_j} \mathbf{w}}{\sigma_n^2 \mathbf{w}^H \mathbf{D}_{g_j} \mathbf{w} + \sigma_\nu^2} \geq \gamma_j, \quad j = 1, \ldots, M, \end{aligned} \tag{5.2}$$

where the optimization variable $\mathbf{w}$ denotes the $R \times 1$ vector of beamforming coefficients applied at the relays. The problem in (5.2) is NP-hard [14], therefore, efficient suboptimal algorithms which can provide good approximate solutions in polynomial runtime are required. In order to convert problem (5.2) into a more convenient form, we define

$$\tilde{\mathbf{w}} \triangleq \mathbf{D}_f^{\frac{1}{2}} \mathbf{w} \tag{5.3}$$

and

$$\mathbf{R}_j \triangleq \frac{\mathbf{D}_f^{-\frac{1}{2}} (P_0 \mathbf{R}_{h_j} - \gamma_j \sigma_n^2 \mathbf{D}_{g_j}) \mathbf{D}_f^{-\frac{1}{2}}}{\sigma_\nu^2 \gamma_j} \tag{5.4}$$

Inserting (5.3) and (5.4) in (5.2) we have

$$\begin{aligned} \min_{\tilde{\mathbf{w}}} \quad & \|\tilde{\mathbf{w}}\|^2 \\ \text{s.t.} \quad & \tilde{\mathbf{w}}^H \mathbf{R}_j \tilde{\mathbf{w}} \geq 1, \ j = 1, \ldots, M. \end{aligned} \tag{5.5}$$

By definition, the matrix $\mathbf{R}_j$ in (5.3) is indefinite and a solution to problem (5.5) satisfying all M constraints might not exist, which renders the problem infeasible. This is the fundamental difference between the problem in (5.5) and the conventional transmit beamforming problem for single-group multicasting of Section 3.2, where a feasible solution can always be obtained, e.g., by increasing the transmitted power. However, in the special case where no noise is present at the receivers of the relays, the term $\gamma_j \sigma_n^2 \mathbf{D}_{g_j}$ in (5.5) vanishes and $\mathbf{R}_j$ becomes positive semi-definite and the problem becomes equivalent to the transmit beamforming problem in case of covariance CSI, which was discussed in Section 3.5.4. The similarity between both problems motivates the extension of the orthogonalization techniques [4] and the SDR-based technique [97], which were originally developed in the context of single-group multicasting to approximately solve the problem of distributed beamforming in relay networks.

The SDR-based technique for distributed beamforming can be obtained by following the approach of [97] and performing the variable transformation $\mathbf{X} \triangleq \tilde{\mathbf{w}}\tilde{\mathbf{w}}^H$. Then, using the property $\tilde{\mathbf{w}}^H\mathbf{R}_j\tilde{\mathbf{w}} = \text{trace}\{\tilde{\mathbf{w}}\tilde{\mathbf{w}}^H\mathbf{R}_j\}$, the problem in (5.5) can be converted into the following equivalent form:

$$\begin{aligned} \min_{\mathbf{X}} \quad & \text{trace}\{\mathbf{X}\} \\ \text{s.t.} \quad & \text{trace}\{\mathbf{X}\mathbf{R}_j\} \geq 1, \quad j = 1, \ldots, M \\ & \mathbf{X} \succeq 0, \quad \text{rank}\{\mathbf{X}\} = 1. \end{aligned} \tag{5.6}$$

The problem in (5.6) is then relaxed by dropping the rank constraint $\text{rank}\{\mathbf{X}\} = 1$ which results in a SDP problem which can be solved using convex optimization tools. If the solution of the SDP, denoted by $\mathbf{X}_{\text{opt}}$, is rank-one, problem (5.5) has its global optimum $\tilde{\mathbf{w}}_{\text{opt}}$ which is the principal component of $\mathbf{X}_{\text{opt}}$. For higher rank cases, the final weight vector is obtained from $\mathbf{X}_{\text{opt}}$ via randomization techniques combined with proper power scaling to ensure that the SNR constraints of all users are satisfied, as explained in Section 3.3. The $\text{trace}\{\mathbf{X}_{\text{opt}}\}$ in this case marks a strictly lower bound on P_t. This lower bound, which is generally not achievable is used in the simulations section to assess the performance of all techniques.

5.1.1 The Proposed Orthogonalization Technique

Consider the SNR constraint of the jth user in (5.5):

$$\tilde{\mathbf{w}}^H\mathbf{R}_j\tilde{\mathbf{w}} = \sum_{k=1}^{r_j} \lambda_{k,j}|\tilde{\mathbf{w}}^H\mathbf{u}_{k,j}|^2 \geq 1, \; r_j = \text{rank}\{\mathbf{R}_j\} \tag{5.7}$$

where $\lambda_{1,j}, \ldots, \lambda_{r_j,j}$ and $\mathbf{u}_{1,j}, \ldots, \mathbf{u}_{r_j,j}$ are the nonzero eigenvalues and the corresponding eigenvectors of $\mathbf{R}_j$, respectively, and it is assumed that the eigenvalues are indexed based on the descending of their values, i.e., $\lambda_{1,j} > \ldots > \lambda_{r_j,j}$. Note that from the definition in (5.3), the matrix $\mathbf{R}_j$ is generally indefinite, i.e., some of the eigenvalues $\lambda_{k,j}$, $k = 1, \ldots, r_j$, may be negative. Let $\tilde{r}_j$ denote the index of the smallest non-negative eigenvalue of $\mathbf{R}_j$, $j = 1, \ldots, M$. In order to satisfy the constraints in

(5.5), it is required that at least one eigenvalue of $\mathbf{R}_j$ is positive, i.e., $r_j \geq \tilde{r}_j \geq 1$, $j = 1, \ldots, M$. Hereafter, only this case will be considered. If $\tilde{r}_j = r_j$, $j = 1, \ldots, M$, the problem in (5.5) becomes equivalent to the conventional single-group multicasting problem in (3.26) and the technique proposed in Section 3.5.4 can be directly applied to solve the problem in (5.5). However, in the case where $1 \leq \tilde{r}_j < r_j$ for $j \in \{1, \ldots, M\}$, a slightly modified version of the technique proposed in Section 3.5.4 is used. Similar to the stricter approximation made in (3.29), the jth constraint is approximated by $\tilde{r}_j$ separate constraints, one constraint for each positive eigenvalue of $\mathbf{R}_j$. The approximation is given as

$$|\tilde{\mathbf{w}}^H \mathbf{u}_{l,j}|^2 \geq \frac{1}{\max\{\epsilon, \sum_{k=1}^{\tilde{r}_j} \lambda_{k,j}\}}, \quad l = 1, \ldots, \tilde{r}_j, \quad j = 1, \ldots, M, \tag{5.8}$$

where ϵ denotes a small positive value which we define to guarantee that the right part of the inequality does not approach infinity. The reason behind the above approximation is the following: As the number of positive eigenvalues of $\mathbf{R}_j$ decreases, the jth user becomes spatially more selective which makes the design of the beamformer more challenging. This fact is captured in the approximated constraints in (5.8), since the value of $\sum_{k=1}^{\tilde{r}_j} \lambda_{k,j}$ decreases with the decreasing number of positive eigenvalues of $\mathbf{R}_j$, thus strengthening the approximated constraints. If we define $\tilde{\mathbf{u}}_{l,j} \triangleq \sqrt{\max\{\epsilon, \sum_{k=1}^{\tilde{r}_j} \lambda_{k,j}\}}\mathbf{u}_{l,j}$, the approximated problem can be written as

$$\begin{aligned} &\min_{\tilde{\mathbf{w}}} \ \|\tilde{\mathbf{w}}\|^2 \\ &\text{s.t. } |\tilde{\mathbf{w}}^H \tilde{\mathbf{u}}_{l,j}|^2 \geq 1, \quad l = 1, \ldots, \tilde{r}_j, \quad j = 1, \ldots, M. \end{aligned} \tag{5.9}$$

It is important to note that unlike the approximation (3.29) for the constraint set of problem (3.26), a weight vector which satisfies the approximate constraints in (5.9) is not necessarily feasible for the original problem in (5.5). Nevertheless, this approach provides good candidate weight vectors as will be shown in the simulation results. Since the constraints in (5.9) exhibit exactly the same structure as the conventional single-group multicasting problem in (3.32), the orthogonalization-based procedure in Section 3.5.4 can be directly applied. For the technique based on the Gram-Schmidt

orthogonalization procedure, let the matrix $\tilde{\mathbf{U}}_j \triangleq [\tilde{\mathbf{u}}_{1,j}, \ldots, \tilde{\mathbf{u}}_{\tilde{r}_j,j}]$, $j = 1, \ldots, M$. Similar to the procedure in section 3.5.2, the initial vector in the Gram-Schmidt procedure denoted as $\mathbf{v}_1$ is chosen arbitrarily from one of the principal eigenvectors of the matrices $\tilde{\mathbf{U}}_1, \ldots, \tilde{\mathbf{U}}_M$. The first intermediate weight vector $\mathbf{w}_1$ is computed as in (3.23), where $\mathbf{q}_1$ and c_1 are given by equations (3.22) and (3.24), respectively, by substituting $k = 1$. Then, the respective column of the matrix from which $\mathbf{v}_1$ is chosen, is discarded. Using $\mathbf{w}_1$, we find the index, η, of the user with the "most violated" SNR constraint, i.e., $\eta = \arg\ \min_i \mathbf{w}_1^H \mathbf{R}_i \mathbf{w}_1$, $i = 1, \ldots, M$. The second vector in the Gram-Schmidt procedure, denoted as $\mathbf{v}_2$, is taken as the first column vector in $\tilde{\mathbf{U}}_\eta$ and the coefficient c_2 is computed as in (3.24) to satisfy the constraint corresponding to $\mathbf{v}_2$ in (3.32) with equality. Since the order of the vectors in $\tilde{\mathbf{U}}_\eta$ is based on the decreasing value of their respective eigenvalue, satisfying the constraint of the first vector with equality provides the strongest contribution to the SNR of the ηth user. This strategy follows a greedy approach in satisfying the SNR constraints. The matrix $\tilde{\mathbf{U}}_\eta$ is then updated by dropping the vector $\mathbf{v}_2$ and the second intermediate weight vector $\mathbf{w}_2$ is computed as in (3.23). The above routine is repeated in every step of the remaining $R-2$ steps of the Gram-Schmidt procedure in order to generate a candidate weight vector. The entire orthogonalization process is repeated M times, where each time a different eigenvector is chosen as the initial vector $\mathbf{v}_1$ for the Gram-Schmidt procedure. After generating M candidate weight vectors $\{\mathbf{w}_{\text{cand},j}\}_{j=1}^{M}$, the norm constrained local search step explained in Section 3.5.3 is performed in order to find a solution in the neighborhood of each of the candidate vectors or. If no solution is found, the problem is considered infeasible.

Table 5.1: Summary of the orthogonalization-based beamforming technique in single-group multicasting relay networks.

for $j = 1, \ldots, M$

Step 1. Define $\mathcal{U} = \{\tilde{\mathbf{u}}_{1,i}\}_{i=1}^{M}$ and select $\mathbf{v}_1 = \tilde{\mathbf{u}}_{1,j}$.

Step 2. Compute $\mathbf{q}_1 = \mathbf{v}_1/\|\mathbf{v}_1\|$.

Step 3. Compute c_1 using (3.18) and obtain $\mathbf{w}_1 = c_1\mathbf{q}_1$.

Step 4. For $k = 2, \ldots, N$

1. Compute $\mathbf{w}_{k-1}^H \mathbf{R}_i \mathbf{w}_{k-1}$, $i = 1, \ldots, M$.
2. Select $\mathbf{v}_k = \tilde{\mathbf{U}}_\eta^{(1)}$ where $\eta = \arg\ \min_i \mathbf{w}_{k-1}^H \mathbf{R}_i \mathbf{w}_{k-1}$, $i = 1, \ldots, M$ and $\tilde{\mathbf{U}}_\eta^{(1)}$ is first column vector of the corresponding matrix $\tilde{\mathbf{U}}_\eta$.
3. Update $\tilde{\mathbf{U}}_\eta$ by discarding $\tilde{\mathbf{U}}_\eta^{(1)}$.
4. Compute c_k using (3.21) and $\mathbf{q}_k$ using (3.22).

Step 5. Compute the candidate weight vector $\tilde{\mathbf{w}}_j$ using (3.12).

Step 6. Perform a norm-constrained local search in the neighborhood of $\tilde{\mathbf{w}}_j$.

Step 7. Rescale so that the most violated from all the M constraints in (5.5) is satisfied with equality, otherwise discard.

end for

Step 8. From the remaining vectors, select the vector with the minimum norm to be the final solution.

5.2 Joint Power Loading and Distributed Beamforming in Asynchronous Relay Networks

5.2.1 Background

In the previous section, we considered the problem of distributed beamforming in synchronous AF relay networks for single-multicasting. Assuming that the relays are

fully synchronized at the symbol level is only valid in the case where the delay spread across different source-to-destination paths is small compared to the symbol duration. However, in practice one can expect scenarios with large delay spreads.

There are several approaches to combat substantial propagation delays. One most straightforward approach is to directly compensate the delays at the relay nodes. However, in such a synchronous scheme the relays have to know their corresponding source-to-destination delays as well as the maximum delay in the network; otherwise, differently delayed replicas of the signal will cause ISI at the destination. Moreover, the relays should deploy a variable-length memory block to enable delay compensation over a wide range of possible delays. This significantly increases the relay complexity and cost and requires extra destination-to-relay feedback.

A natural alternative way to combat ISI caused by unknown delays is to apply the OFDM) approach at all nodes including the relays [60]. However, this approach may be limited by the necessity to implement the OFDM processing at all the relay nodes, which substantially increases their overall cost.

We propose a different OFDM-based approach to ISI removal at the destination node. In our approach, the OFDM processing will be used only at the source and destination nodes, while the relays will use the simple AF scheme. Therefore, the relays remain simple and inexpensive in our technique. According to our developed model, the network can be viewed as an artificial "multipath" channel where each path corresponds to a different relay. Unlike the traditional multipath channel models where there is no control of the channel impulse response, in our model the channel taps can be controlled by adjusting the relays complex weights. This additional degree of freedom in controlling the properties of the relay channel impulse response has been our motivation in this work. In fact, the proposed scheme can be viewed as a distributed equalizer applied to the artificial "multipath" channel.

5.2.2 System Model

Consider a network of a source, a destination, and R single-antenna relays which establish a connection between the source and the destination as shown in Fig. 5.1. Note that we consider here a simple case of single-group multicasting with only one user. The signal transmitted from the source node and arriving at the destination through the ith relay is assumed to have the delay τ_i and all channels from the source to the relays and from the relays to the destination are assumed to be flat fading channels. With these assumptions, the relay channel can be modeled as the following

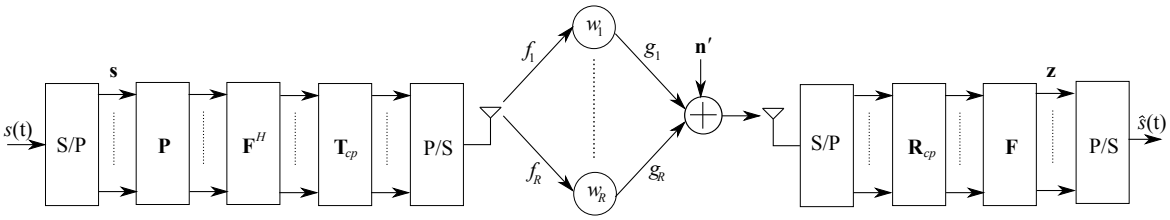

Figure 5.1: System model for distributed beamforming in OFDM-based asynchronous AF relay networks.

artificially generated finite impulse response (FIR) "multipath" channel:

$$h(t) = \sum_{i=0}^{R-1} \alpha_i \delta(t - \tau_i) \tag{5.10}$$

where $\alpha_i \triangleq w_i f_i g_i$ is the ith tap of the equivalent FIR channel model, w_i is the relay complex weight, while f_i and g_i are the source-to-relay and relay-to-destination flat fading channel coefficients. The signal transmitted from the source node to the relays can be written as

$$s(t) = \sum_{k=-\infty}^{\infty} s_k p(t - kT_s) \tag{5.11}$$

where $p(t)$ is the pulse shaping filter response of the duration T_s, s_k is the kth transmitted symbol, and T_s is the symbol length. Hence, the signal component at the destination node can be expressed as

$$r(t) = s(t) * h(t) = \sum_{k=-\infty}^{\infty} s_k \sum_{i=0}^{R-1} \alpha_i p(t - kT_s - \tau_i) \tag{5.12}$$

where $*$ denotes the convolution. Sampling $r(t)$ at the symbol rate $1/T_s$, we express the discrete-time received sequence $r[n]$ as

$$\begin{aligned} r[n] &= r(t)\Big|_{t=nT_s} \\ &= \sum_{k=-\infty}^{\infty} s_k \sum_{i=0}^{R-1} \alpha_i p\big((n-k)T_s - \tau_i\big) \\ &= s_n * h_n \end{aligned} \tag{5.13}$$

where

$$h_n \triangleq \sum_{i=0}^{R-1} \alpha_i p(nT_s - \tau_i). \tag{5.14}$$

This channel model will result in ISI at the destination, and exploiting the OFDM scheme is a natural approach to suppress such ISI components [41], [55]. Therefore, it is assumed that the source uses the OFDM transmitter while the destination deploys the corresponding OFDM receiver, see Fig. 5.1. In this figure, "S/P" and "P/S" stand for "serial to parallel" and "parallel to serial", respectively, $\mathbf{F}$ and $\mathbf{F}^H$ are the fast Fourier transform (FFT) and the inverse FFT (IFFT) matrices [121]. The matrix $\mathbf{T}_{cp}$ inserts the cyclic prefix and is defined as $\mathbf{T}_{cp} \triangleq [\mathbf{I}_{N_{cp}}^T, \mathbf{I}_{N_c}^T]^T$, which is a concatenation of the last N_{cp} rows of an $N_c \times N_c$ identity matrix $\mathbf{I}_{N_c}$, denoted here as $\mathbf{I}_{N_{cp}}$, and the identity matrix $\mathbf{I}_{N_c}$ itself. Similarly, the matrix $\mathbf{R}_{cp}$ removes the cyclic prefix at the receiver and is defined as $\mathbf{R}_{cp} \triangleq [\mathbf{O}_{N_{cp}}, \mathbf{I}_{N_c}]$, where $\mathbf{O}_n$ is the $n \times n$ all-zero matrix [121]. Let $\mathbf{h} \triangleq [h_0, \ldots, h_{L_n-1}, \mathbf{0}]^T$ be $N_c \times 1$ zero-padded vector, where L_n is the length of the discrete channel sequence h_n. Note that the length of the cyclic prefix N_{cp} should greater than or equal to $L_n - 1$ to guarantee ISI-free transmission [121], therefore, we assume hereafter that $N_{cp} = L_n - 1$. We can express (5.14) in the vector notation as

$$\mathbf{h} = \mathbf{A}_s \mathbf{w} \tag{5.15}$$

where $\mathbf{w} \triangleq [w_1, \ldots, w_R]^T$ is $R \times 1$ vector of the relay complex weights and $\mathbf{A}_s$ is $N_c \times R$ matrix whose (k, i)th element describes the contribution of the ith relay to the kth tap of h_n. Similarly for the noise, let $\psi_i(t)$ denote the spatially and temporally white

noise at the ith relay. This noise is multiplied by $w_i g_i$ and arrives at the destination simultaneously with the signal component coming from the ith relay. Therefore, similar to (5.15), we define the $N_c \times 1$ vector $\mathbf{n}$ as

$$\mathbf{n} = \mathbf{A_n}\mathbf{w} \tag{5.16}$$

where $\mathbf{A_n}$ is $N_c \times R$ matrix whose (k,i)th element describes the contribution of the ith relay to the kth element of $\mathbf{n}$. At the output of the FFT block, the vector of received signals over all subcarriers is given by

$$\mathbf{z} = \mathbf{P}\mathcal{D}\mathbf{s} + \mathbf{F}\mathbf{n} + \mathbf{F}\mathbf{R}_{cp}\mathbf{n}' \tag{5.17}$$

where $\mathcal{D} \triangleq \text{diag}\{\mathbf{F}\mathbf{h}\}$, $\mathbf{P} \triangleq \text{diag}\{\sqrt{p_1}, \ldots, \sqrt{p_{N_c}}\}$, p_j is the power allocated to the ith subcarrier, $\mathbf{F}$ is the N_c-point FFT matrix, and $\mathbf{n}'$ is $(N_{cp} + N_c) \times 1$ vector of AWGN receiver noise of variance σ^2. The received signal power at the jth subcarrier can be expressed as

$$\begin{aligned} P_{s_j} &= p_j E\{|s_j|^2\}\mathbf{h}^H \mathbf{e}_j \mathbf{e}_j^H \mathbf{h} \\ &= p_j |\mathbf{h}^H \mathbf{e}_j|^2 \\ &= p_j |\mathbf{e}_j^H \mathbf{A}_s \mathbf{w}|^2 \end{aligned} \tag{5.18}$$

where $\mathbf{e}_j$ is the jth Vandermonde column vector of $\mathbf{F}^H$ and we have used the fact that $E\{|s_j|^2\} = 1$. Using (5.17), the noise power at the jth subcarrier can be written as

$$P_{n_j} = E\{\mathbf{w}^H \mathbf{A}_n^H \mathbf{e}_j \mathbf{e}_j^H \mathbf{A}_n \mathbf{w}\} + E\{\mathbf{n'}^H \mathbf{R}_{cp}^H \mathbf{e}_j \mathbf{e}_j^H \mathbf{R}_{cp} \mathbf{n}'\} \tag{5.19}$$

$$= \mathbf{w}^H \mathbf{D} \mathbf{w} + \sigma^2, \tag{5.20}$$

where $\mathbf{D}$ is the diagonal matrix with the elements

$$[\mathbf{D}]_{ii} = \sigma_i^2 |g_i|^2, \quad i = 1, \ldots, R. \tag{5.21}$$

and σ_i^2 is the noise variance per subcarrier at the ith relay. From (5.18) and (5.19), the SNR at the jth subcarrier can be written as

$$\text{SNR}_j = \frac{p_j |\mathbf{e}_j^H \mathbf{A}_s \mathbf{w}|^2}{\mathbf{w}^H \mathbf{D} \mathbf{w} + \sigma^2}. \tag{5.22}$$

It can also be shown that the transmitted power of the ith relay can be written as

$$\begin{aligned}\tilde{p}_i &= |w_i|^2 \left(N_c \sigma_i^2 + |f_i|^2 \left(\sum_{j=1}^{N_c} p_j \right) \right) \\ &= |w_i|^2 \left(N_c \sigma_i^2 + |f_i|^2 \mathbf{1}^T \mathbf{p} \right) \end{aligned} \tag{5.23}$$

where $\mathbf{1}$ is a vector of all ones and $\mathbf{p} \triangleq [p_1, \ldots, p_{N_c}]^T$.

5.2.3 Joint Power Loading and Distributed Beamforming

Using the signal model developed in Section 5.2.2, we jointly optimize the beamformer weights $\{w_i\}_{i=1}^R$ and subcarrier powers $\{p_j\}_{j=1}^{N_c}$ by means of the max-min fair design approach. The idea is to maximize the worst of the subcarrier SNRs subject to the individual power constraints on the source and relay nodes. This problem can be written as

$$\begin{aligned} \max_{\mathbf{w},\, \mathbf{p} \geq \mathbf{0}} \quad & \min_j \frac{p_j |\mathbf{e}_j^H \mathbf{A}_s \mathbf{w}|^2}{\mathbf{w}^H \mathbf{D} \mathbf{w} + \sigma^2} \\ \text{s.t.} \quad & \mathbf{1}^T \mathbf{p} \leq P_{\text{Tx,max}} \\ & |w_i|^2 \left(N_c \sigma_i^2 + |f_i|^2 \mathbf{1}^T \mathbf{p} \right) \leq P_{\max,i}, \quad i = 1, \ldots, R, \end{aligned} \tag{5.24}$$

where $P_{\max,i}$ is the maximum allowed transmitted power of the ith relay and $P_{\text{Tx,max}}$ is the maximum allowed source transmitted power. Note that without any loss of generality, we can assume that all SNRs in (5.24) are balanced at the optimum, that is, $\text{SNR}_j = \text{SNR}_k$ for all $j, k = 1, \ldots, N_c$. Otherwise, if $\text{SNR}_j > \text{SNR}_k$ holds for some particular values of j and k, then the optimal value of p_j can be always reduced so that $\text{SNR}_j = \text{SNR}_k$. This new value of p_j does not alter the optimal value of the objective function and does not violate the constraints in (5.24). Therefore, it follows from the fact that the SNRs can be balanced that

$$p_j |\mathbf{e}_j^H \mathbf{A}_s \mathbf{w}|^2 = p_1 |\mathbf{e}_1^H \mathbf{A}_s \mathbf{w}|^2, \quad j = 2, \ldots, N_c \tag{5.25}$$

or, equivalently,

$$p_j = p_1 \frac{|\mathbf{e}_1^H \mathbf{A}_s \mathbf{w}|^2}{|\mathbf{e}_j^H \mathbf{A} \mathbf{w}|^2}. \tag{5.26}$$

Another important remark regarding the problem in (5.24) is that at the optimum, the second constraint in is active, that is,

$$\mathbf{1}^T\mathbf{p} = P_{\text{Tx,max}} \tag{5.27}$$

holds true. To prove this, let $\mathbf{p}^o$ and $\mathbf{w}^o$ denote the optimal values of the vectors $\mathbf{p}$ and $\mathbf{w}$, respectively. Let us also denote the jth SNR in (5.24) as $\phi_j(\mathbf{p}, \mathbf{w})$. If $z \triangleq P_{\text{Tx,max}}/\mathbf{1}^T\mathbf{p}^o > 1$, then

$$\phi_j\left(z\mathbf{p}^o, \frac{\mathbf{w}^o}{\sqrt{z}}\right) = \frac{p_j^o|\mathbf{e}_j^H\mathbf{A}_s\mathbf{w}^o|^2}{z^{-1}\mathbf{w}^{oH}\mathbf{D}\mathbf{w}^o + \sigma^2} > \phi_j(\mathbf{p}^o, \mathbf{w}^o). \tag{5.28}$$

Note also that $z\mathbf{p}^o$ and $\mathbf{w}^o/\sqrt{z}$ satisfy the ith relay power constraint in (5.24) as

$$\begin{aligned} z^{-1}|w_i^o|^2\left(N_c\sigma_i^2 + z|f_i|^2\mathbf{1}^T\mathbf{p}^o\right) = \\ |w_i^o|^2\left(z^{-1}N_c\sigma_i^2 + |f_i|^2\mathbf{1}^T\mathbf{p}^o\right) < \\ |w_i^o|^2\left(N_c\sigma_i^2 + |f_i|^2\mathbf{1}^T\mathbf{p}^o\right) < P_{\text{max},i}. \end{aligned} \tag{5.29}$$

It follows from (5.28) and (5.29) that $z\mathbf{p}^o$ and $\mathbf{w}^o/\sqrt{z}$ belong to the feasible set of (5.24) and achieve a larger value of the cost function than that achieved by $\mathbf{p}^o$ and $\mathbf{w}^o$. However, this contradicts the optimality of $\mathbf{p}^o$ and $\mathbf{w}^o$. Hence, z has to be equal to one, and (5.27) is proved. Inserting (5.26) into (5.27), we obtain that

$$p_1|\mathbf{e}_1^H\mathbf{A}_s\mathbf{w}|^2\mathbf{1}^T\mathbf{y}(\mathbf{w}) = P_{\text{Tx,max}} \tag{5.30}$$

where

$$\mathbf{y}(\mathbf{w}) \triangleq \left[\frac{1}{|\mathbf{e}_1^H\mathbf{A}_s\mathbf{w}|^2}, \ldots, \frac{1}{|\mathbf{e}_{N_c}^H\mathbf{A}_s\mathbf{w}|^2}\right]^T. \tag{5.31}$$

Noting that under SNR balancing, the objective function of (5.24) becomes

$$\min_j \frac{p_j|\mathbf{e}_j^H\mathbf{A}_s\mathbf{w}|^2}{\mathbf{w}^H\mathbf{D}\mathbf{w} + \sigma^2} = \frac{p_1|\mathbf{e}_1^H\mathbf{A}_s\mathbf{w}|^2}{\mathbf{w}^H\mathbf{D}\mathbf{w} + \sigma^2} \tag{5.32}$$

and using (5.30) in the right-hand side of (5.32), we rewrite the objective function as

$$\frac{P_{\mathrm{Tx,max}}}{\mathbf{1}^T\mathbf{y}(\mathbf{w})(\mathbf{w}^H\mathbf{D}\mathbf{w}+\sigma^2)}. \tag{5.33}$$

Maximizing (5.33) subject to the individual relay power constraints is equivalent to

$$\begin{aligned} \min_{\mathbf{w}} \quad & \mathbf{1}^T\mathbf{y}(\mathbf{w})(\mathbf{w}^H\mathbf{D}\mathbf{w}+\sigma^2) \\ \text{s.t.} \quad & |w_i|^2 \leq \beta_i, \quad i=1,\ldots,R \end{aligned} \tag{5.34}$$

where

$$\beta_i \triangleq \frac{P_{\max,i}}{(N_c\sigma_i^2+|f_i|^2P_{\mathrm{Tx,max}})}.$$

The max-min fair problem in (5.34) can then be rewritten as

$$\begin{aligned} \min_{\mathbf{w}} \quad & \sum_{j=1}^{N_c}\frac{\mathbf{w}^H\mathbf{D}\mathbf{w}+\sigma^2}{|\mathbf{e}_j^H\mathbf{A}_s\mathbf{w}|^2} \\ \text{s.t.} \quad & |w_i|^2 \leq \beta_i, \quad i=1,\ldots,R. \end{aligned} \tag{5.35}$$

The optimization problem in (5.35) can be interpreted as the minimization of the sum of the noise-to-signal ratios with the particular choice $p_j = 1$, $j = 1,\ldots,N_c$, subject to individual relay power constraints. This problem is non-convex and rather difficult to solve efficiently. Therefore, we will resort to the steepest descent algorithms to find a local optimum of this problem [16]. To ensure that we obtain the "best" local optimum, we solve the optimization problem in (5.35) several times, each time with a different random initial point, i.e., a randomly generated weight vector $\mathbf{w}$, and pick the solution that results in the smallest value of the objective function among all candidate solutions. We have used `fmincon` function from the Matlab Optimization Toolbox to find local solutions of the problem in (5.35). Note that there are several other techniques [89], [108] which can provide efficient solutions to the problem in (5.35). We remark that the contribution of our proposed approach is to avoid the synchronization problem of the relays in distributed beamforming relay networks.

5.3 Simulation Results

5.3.1 Part I: Single-Group Multicasting in Synchronous Relay Networks

In our numerical examples, we assume Rayleigh fading channels with i.i.d. circularly symmetric coefficients with unit-variance. We assume that $\gamma_j = \gamma_{\min}$, $j = 1, \ldots, M$, and $\sigma_n^2 = \sigma_\nu^2 = 1$. All our results are averaged over 1000 Monte-Carlo runs. We compare the SDR-based technique of [97], denoted as SDR, and the iterative SOCP algorithm of [14], denoted as Iter-SOCP, with the orthogonalization technique based on the Gram-Schmidt procedure, which is proposed in Section 5.1.1 and denoted here as GS-dL. The initial step-size μ_0 and the maximum number of iterations in the local refinement I were carefully chosen to achieve fast convergence and good performance ($\mu_0 = 1$ and $I \leq 40$). For the SDR technique we used three different randomization procedures in parallel, with 1000 randomizations for each [97]. In all our simulations, the lower bound corresponds to trace($\mathbf{X}_{\text{opt}}$).

In our first example, we consider a network with $R = 7$ relays and assume instantaneous CSI, i.e., $\mathbf{R}_{h_j} = \mathbf{h}_j \mathbf{h}_j^H$. Fig. 5.3.1 shows the average total transmitted relay power for $\gamma_{\min} = 1$ and number of users, $M = [4, \ldots, 20]$. We observe that the proposed technique outperforms all other techniques. In Table. 1, we compare the percentage of Monte-Carlo runs rendered infeasible by all techniques at different SNR thresholds $\gamma_{\min} = [-5, \ldots, 20]$ dB. In the low SNR region, GS-dL provides the least infeasible cases while the performance degrades in the high SNR region compared to iterative SOCP.

In the second example, we assume covariance CSI at the receiver. We model the channel coefficients, f_i, g_{ij} as:

$$f_i = \bar{f}_i + \tilde{f}_i, \quad g_{ij} = \bar{g}_{ij} + \tilde{g}_{ij}$$

where $\bar{f}_i$ is the mean of f_i and $\tilde{f}_i$ is a zero mean random variable. We choose $\bar{f}_i = \frac{e^{j\theta_i}}{\sqrt{1+\alpha}}$ and $\text{var}(\tilde{f}_i) = \frac{\alpha}{1+\alpha}$. Similarly, $\bar{g}_{ij} = \frac{e^{j\phi_{ij}}}{\sqrt{1+\beta}}$ and $\text{var}(\tilde{g}_{ij}) = \frac{\beta}{1+\beta}$, where θ_i and ϕ_{ij} are

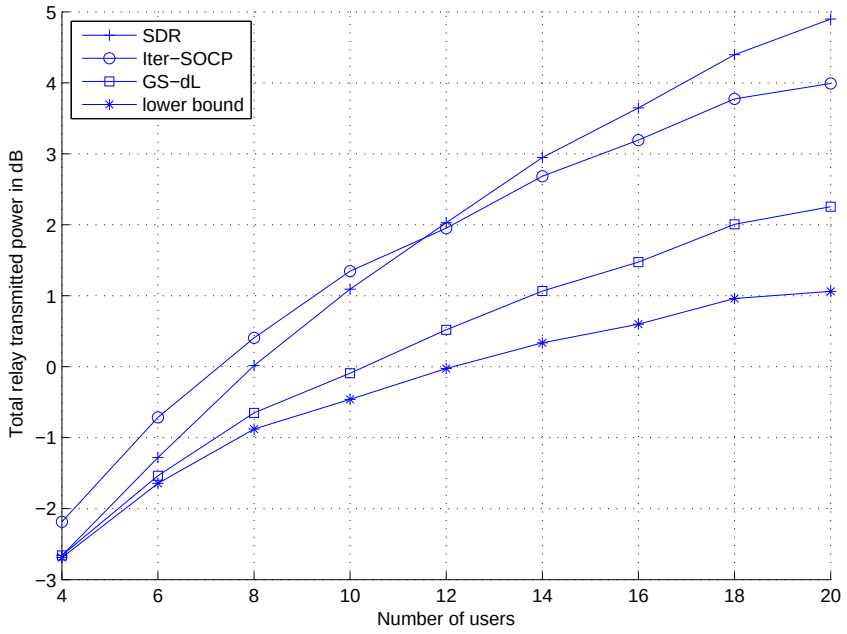

Figure 5.2: Average transmitted power for instantaneous CSI, $R = 7$, $P_0 = 10$ dB, $\gamma_{\min} = 1$.

uniformly distributed random variables chosen from the interval $[0, 2\pi]$. Based on this model, if we define $\mathbf{R}_f \triangleq \mathrm{E}\{\mathbf{f}\ \mathbf{f}^H\}$, $\mathbf{R}_{g_j} \triangleq \mathrm{E}\{\mathbf{g}_j\ \mathbf{g}_j^H\}$ then the (m,n)th entry of the matrices $\mathbf{R}_f$ and $\mathbf{R}_{g_j}$ are written respectively as:

$$[\mathbf{R}_f]_{m,n} = \left(\bar{f}_m \bar{f}_n^* + \frac{\alpha\delta_{mn}}{1+\alpha}\right), \ [\mathbf{R}_{g_j}]_{m,n} = \left(\bar{g}_{mj}\bar{g}_{nj}^* + \frac{\beta\delta_{mn}}{1+\beta}\right)$$

where δ_{mn} is the Kronecker delta and $\mathbf{R}_{h_j} = \mathbf{R}_f \odot \mathbf{R}_{g_j}$. As the values of α and β increase, the variance of the random components of f_i, g_{ij} increases and the matrix $\mathbf{R}_{h_j}$ becomes full rank. In Fig. 5.3.1, we show the average total transmitted relay power for $R = 4$, $\alpha = \beta = 1$, and $\gamma_{\min} = 1$. Note that iterative SOCP can not be applied here since $\mathbf{R}_{h_j}$ is full rank [14]. We observe that both GS-dL and SDR are close to the lower bound whereas GS-dL performs slightly better as the number of users increases.

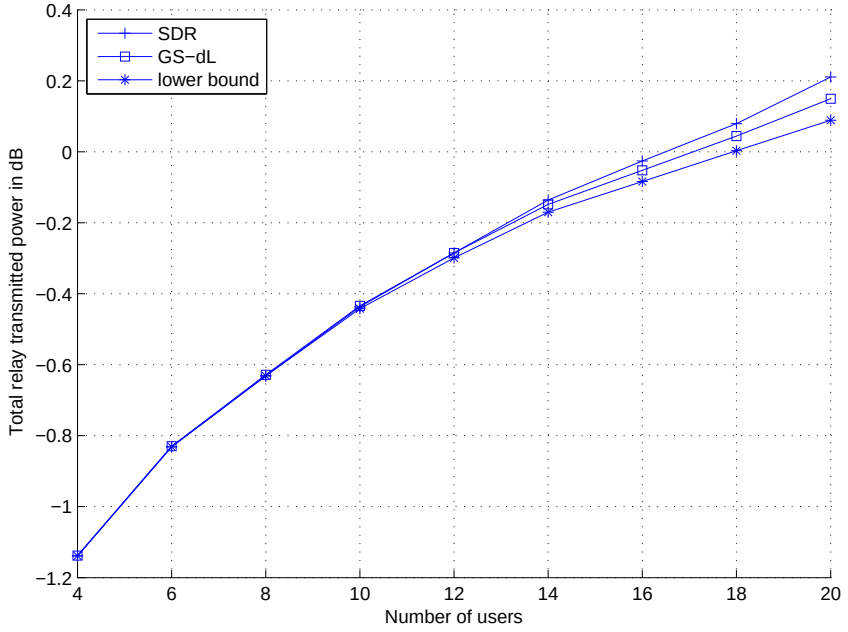

Figure 5.3: Average transmitted power for covariance CSI, $R = 4$, $P_0 = 10$ dB, $\gamma_{\min} = 1$, $\alpha = \beta = 1$.

Table 5.2: Percent of infeasible MC runs for instantaneous CSI, $R = 7$, $M = 20$, $P_0 = 10$ dB.

$\gamma_{\min}$ in dB	-5	0	5	10	15	20
SDR	0%	0%	3%	41%	77.6%	100%
Iter SOCP	0%	0%	0.8%	19.2%	76.0%	100%
GS-dL	0%	0%	0.1%	21.3%	89.5%	100%
Lower bound	0%	0%	0%	4.3%	72.4%	100%

5.3.2 Part II: Joint Power Loading and Distributed Beamforming in Asynchronous Relay Networks

We consider a network with $R = 10$ relays, $N_c = 16$ subcarriers, and $N_{cp} = 3$. In each simulation run, the delay of each relay is chosen randomly in the interval $[0, 4T_s]$. The channel coefficients $\{f_i\}_{i=1}^{10}$ and $\{g_i\}_{i=1}^{10}$ are modeled as zero-mean i.i.d. complex Gaussian random variables with unit variance. The relay and destination noises are assumed to have variances equal to one, i.e., $\sigma^2 = \sigma_i^2 = 1$ and we choose the ith

relay maximum transmit power, $P_{\max,i} = 0.5P_{\text{Tx,max}}$, $i = 1, \ldots, R$. For the `fmincon` function, we use 10 randomly generated initialization weight vectors. In Fig. 5.4, the performance of our proposed scheme is compared to that of the fully synchronized network in terms of average receive SNR versus the total transmit power consumed in the whole network, i.e., $P^{\text{sym}}_{\text{Tx,max}} = \frac{P_{\text{Tx,max}}}{N_c}$ and $P^{\text{sym}}_{\max,i} = \frac{P_{\max,i}}{N_c}$, where $P^{\text{sym}}_{\text{Tx,max}}$ and $P^{\text{sym}}_{\max,i}$ denote the maximum transmit power per symbol at the source and ith relay, respectively. The synchronous relay network is assumed to have the same transmission bandwidth and the same power constraints at the source and relay nodes. The problem in this case is a SNR maximization problem rather than a max-min fair problem and the solution was proposed in [48].

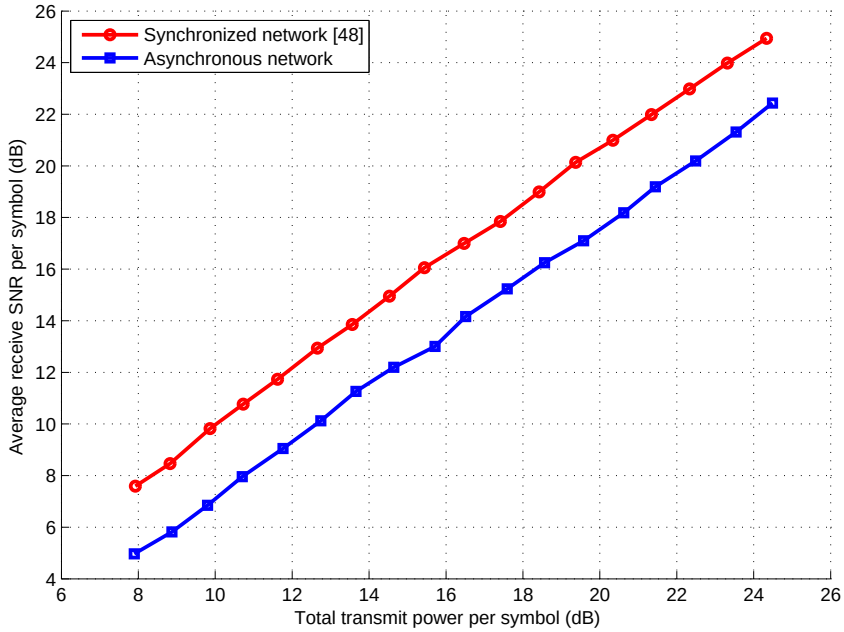

Figure 5.4: Average receive SNR per symbol versus total transmit power per symbol, $R = 10$.

As it can be seen from this figure, the proposed asynchronous scheme achieves SNRs which are only 2.3 dB lower than that achieved by the synchronous scheme proposed in [48]. We stress here that, in contrast to our asynchronous approach, in the synchronous scheme the relays have to know their corresponding delays τ_i as well as the

maximum delay $\max_i \tau_i$. Moreover, in the synchronous case the relays should deploy a variable-length memory block to enable delay compensation over a wide range of possible delays. This will impose extra complexity on the relay hardware and extra feedback overhead as compared to the proposed scheme.

5.4 Conclusion

We considered the problem of distributed beamforming in AF relay networks for single-group multicasting, where a single transmitter sends common information symbols to a group of users via cooperating relays. The objective is to design a computationally efficient beamforming scheme to minimize the total transmitted power at the relays subject to QoS constraints of all users. We extended the simple orthogonalization techniques, originally developed in the context of conventional single-group multicasting to solve the present problem in the case when instantaneous CSI or when second-order statistics of the channel is available. Simulation results show that our technique outperforms the popular SDR-based technique and provides an excellent performance to complexity trade-off over a large range of QoS constraint thresholds compared to the iterative SOCP technique. We also proposed an OFDM-based approach to combat the ISI in cooperative relay networks with large delay spread. By avoiding relay synchronization, this approach does not require each relay node to know its corresponding source-to-destination (total) path delay and the maximum delay in the network. Furthermore, the relay nodes do not need to artificially compensate for their delays, thus eliminating the additional cost of the variable-length storage at the relays.

Bibliography

[1] 3GPP, "Multimedia broadcast/multicast service (MBMS); architecture and functional description," TS 23.246, V8.0.0, June 2007.

[2] 3GPP, "Long Term Evolution, Evolved Universal Terrestrial Radio Access (EUTRA); Physical layer; General description," TS 36.201 v1.0.0, March 2007.

[3] A. Abdelkader, S. Shahbazpanahi, and A. B. Gershman, "Joint subcarrier power loading and distributed beamforming in OFDM-based asynchronous relay networks," *Proc. CAMSAP,* pp. 105-108, Aruba, December 2009.

[4] A. Abdelkader, A. B. Gershman, and N. D. Sidiropoulos, "Multiple-antenna multicasting using channel orthogonalization and local refinement," *IEEE Transactions on Signal Processing*, vol. 58, no. 7, pp. 3922-3927, July 2010.

[5] A. Abdelkader, M. Pesavento, and A. B. Gershman, "Orthogonalization techniques for single group multicasting in cooperative amplify-and-forward networks," *Proc. CAMSAP*, pp. 225-228 , San Juan, Puerto Rico, December 2011.

[6] S. J. Alabed, J .M. Paredes, and A. B. Gershman, "A simple distributed space-time coded strategy for two-way relay channels, " submitted to IEEE Transactions on Wireless Communications, December 2010.

[7] S. J. Alabed, M. Pesavento, and A. B. Gershman, "Distributed differential space-time coding techniques for two-Way wireless relay networks," *Proc. CAMSAP*, pp. 221-224, San Juan, Puerto Rico, December 2011.

[8] S. Y. Baek, Y. -J. Hong, and D. K. Sung, "Adaptive transmission scheme for mixed multicast and unicast traffic in cellular systems," *IEEE Transactions on Vehicular Technology*, vol. 58, no. 6, pp. 2899-2908, July 2009.

[9] M. Bakhuizen and U. Horn, "Mobile broadcast/multicast in mobile networks," Ericsson review, issue no. 01/2005, May 2005.

[10] M. Bengtsson and B. Otterson, "Optimal downlink beamforming using semidefinite optimization," *Proc. Annual Allerton Conference on Comm., Control, and Computing*, pp. 987-996, September 1999.

[11] M. Bengtsson and B. Otterson, "Optimal and suboptimpal transmit beamforming," in *Handbook of Antennas in Wireless Communications,* L. C. Godara, Ed. Boca Raton, FL: CRC, 2001.

[12] N. Bornhorst and M. Pesavento, "An iterative convex approximation approach for transmit beamforming in multi-group multicasting," *Proc. SPAWC*, pp. 411-415, San Francisco, CA, USA, June 2011.

[13] N. Bornhorst, M. Pesavento, and A. B. Gershman, "Distributed beamforming for multiuser peer-to-peer and multi-group multicasting relay networks," *Proc. ICASSP*, pp. 2800-2803, Prague, Czech Republic, May 2011.

[14] N. Bornhorst, M. Pesavento, and A. B. Gershman, "Distributed beamforming for multi-group multicasting relay networks," *IEEE Transactions on Signal Processing*, vol. 60, no. 1, pp. 221-232, January 2012.

[15] M. Bossert and M. Breitbach, *Digitale Netze*, 1st edition, Germany, Stuttgart, Teubner Verlag, 1999.

[16] S. Boyd and L. Vandenberghe, *Convex Optimization.* Cambridge, U.K. : Cambridge University Press, 2004.

[17] M. Butussi and M. Bengtsson, "Low complexity admission in downlink beamforming," *Proc. ICASSP*, pp. 261-264, Toulouse, France, May 2006.

[18] H. Chen and A. B. Gershman, "Robust adaptive beamforming for general-rank signal models using positive semi-definite covariance constraint," *Proc. ICASSP*, pp. 2341-2344, Las Vegas, USA, April 2008.

[19] H. Chen, A. B. Gershman, and S. Shahbazpanahi, "Filter-and-forward distributed beamforming for two-way relay networks with frequency selective channels," *Proc. GLOBECOM*, pp. 1-5 , Miami, FL, USA, December 2010.

[20] M. H. M. Costa, "Writing on dirty paper," *IEEE Transactions on Information Theory*, vol. IT-29, no. 3, pp. 439-441, May 1983.

[21] T. Cover, "Broadcast channels," *IEEE Transactions on Information Theory*, vol. 18, pp. 2-14. January 1972.

[22] E. Dahlman, S. Parkvall, and J. Sköld, *4G: LTE/LTE-Advanced for Mobile Broadband,* First edition, USA: Academic Press, 2011.

[23] G. Dimic and N. D. Sidiropoulos, "On downlink beamforming with greedy user selection: performance analysis and a simple new algorithm," *IEEE Transactions on Signal Processing*, vol. 53, no. 10, pp. 3857-3868, October 2005.

[24] F. R. Farrokhi, K. J. R. Liu, and L. Tassiulas, "Downlink power control and base station assignement," *IEEE communications Letters*, vol. 1, no. 4, pp. 102-104, July 1997.

[25] F. R. Farrokhi, L. Tassiulas, and K. J. R. Liu, "Joint optimal power control and beamforming in wireless networks using antenna arrays," *IEEE Journal on Selected Areas in Communications*, vol. 46, no. 10, pp. 1313-1324, October 1998.

[26] F. R. Farrokhi, K. J. R. Liu, and L. Tassiulas, "Transmit beamforming and power control for cellular wireless systems," *IEEE Journal on Selected Areas in Communications*, vol. 16, no. 8, pp. 1437-1450, October 1998.

[27] S. Fazeli-Dehkordy, S. Gazor, and S. Shahbazpanahi, "Distributed peer-to-peer multiplexing using ad hoc relay networks," *Proc. ICASSP*, pp. 2373-2376, Las Vegas, NV, USA, April 2008.

[28] S. Fazeli-Dehkordy, S. Shahbazpanahi, and S. Gazor, "Multiple peer-to-peer communications using a network of relays," *IEEE Transactions on Signal Processing*, vol. 57, no. 8, pp. 3053-3062, August 2009.

[29] R. F. H. Fischer, C. Windpassinger, A. Lampe, and J. B. Huber, "Space-time transmission using Tomlinson-Harashima precoding," *Proc. ITG SCC*, pp. 139-147, January 2002.

[30] Y. Gao and M. Schubert, "Group-oriented beamforming for multi-stream multicasting based on quality-of-service requirements," *Proc. CAMSAP*, pp. 193-196, Puerto Vallarta, December 2005.

[31] Y. Gao and M. Schubert, "Power allocation for multi-group multicasting with beamforming," *Proc. ITG/IEEE Workshop on Smart Antennas (WSA),* Ulm, Germany, March 2006.

[32] M. R. Garey and D. S. Johnson, *Computers and Intractability: A Guide to the Theory of NP-Completeness*, San Francisco, CA: Freeman, 1979.

[33] A. B. Gershman and N. D. Sidiropoulos, *Space-Time Processing for MIMO Communications*, UK: John Wiley and Sons, 2005.

[34] A. B. Gershman, N. D. Sidiropoulos, S.Shahbazpanahi, M. Bengtsson, and B. Otterson, "Convex optimization-based beamforming," *IEEE Signal Processing Magazine*, vol. 27, pp. 62-75, May 2010.

[35] P. Goud, Jr., R. Hang, D. Truhachev, and C. Schlegel, "A portable MIMO testbed and selected channel measurements," *EURASIP Journal on Applied Signal Processing*, vol. 2006, manuscript ID 51490, 2006. doi:10.1155/ASP/2006/51490

[36] M. Grant and S. Boyd, "CVX: Matlab software for disciplined convex programming," version 1.21, `http://cvxr.com/cvx`, January 2011.

[37] X. Guo and X.-G. Xia, "A distributed space-time coding in asynchronous wireless relay networks," *IEEE Transactions on Wireless Communications*, vol. 7, no. 5, pp. 18121816, May 2008.

[38] V. Havary-Nassab, S. ShahbazPanahi, A. Grami, and Z.-Q. Luo, "Distributed beamforming for relay networks based on second-order statistics of the channel state information," *IEEE Transactions on Signal Processing*, vol. 56, pp. 4306-4316, September 2008.

[39] V. Havary-Nassab, S. ShahbazPanahi, and A. Grami, "Optimal distributed beamforming for two-way relay networks," *IEEE Transactions on Signal Processing*, vol. 58, pp. 1238-1250, March 2009.

[40] V. Havary-Nassab, S. ShahbazPanahi, and A. Grami, "Joint transmit-receive beamforming for multi-antenna relaying schemes," *IEEE Transactions on Signal Processing*, vol. 58, pp. 4966-4972, September 2009.

[41] S. Haykin, *Communication Systems,* 3rd edition USA: John Wiley & Sons, 1994.

[42] R. Hunger, D. A. Schmidt, A. S. M. Joham, and W. Utschick, "Design of single-group multicasting beamformers," in *Proc. ICC*, pp. 2499-2505, Glasgow, Scotland, June 2007.

[43] H. Jafarkhani, *Space-Time Coding: Theory and Practice,* USA: Cambridge University Press, 2005.

[44] T. Jiang, W. Xiang, H.-H. Chen, and Q. Ni, "Multicast broadcast services support in OFDMA-based WiMax systems," *IEEE Communications Magazine*, vol. 45, no. 8, pp. 78-86, August 2007.

[45] H. Jiang and P. Wilford, "A hierarchical modulation for upgrading digital broadcast systems," *IEEE Transactions on Broadcasting*, vol. 51, pp. 223-229, June 2005.

[46] N. Jindal, Z.-Q. Luo, "Capacity limits of multiple antenna multicast," *Proc. ISIT*, pp. 1841-1845, Seattle, WA, USA, July 2006.

[47] Y. Jing and B. Hassibi, "Distributed space-time coding in wireless relay networks," *IEEE Transactions on Wireless Communications*, vol. 5, pp. 3524-3536, December 2006.

[48] Y. Jing and H. Jafarkhani, "Network beamforming using relays with perfect channel information," *Proc. ICASSP*, pp. 473-476, Honolulu, Hawaii, USA, April 2007.

[49] M. Jordan, M. Senst, G. Ascheid, and H. Meyr, "Evaluation of beamforming for broadcast applications in single frequency networks," *Proc. IST Mobile and Wireless Communication Summit*, pp. 1-5, Budapest, Hungary, July 2007.

[50] E. Karipidis, N. D. Sidiropoulos, and Z.-Q. Luo, "Transmit beamforming to multiple co-channel multicast groups," *Proc. CAMSAP*, pp. 109-112, Puerto Vallarta, Mexico, December 2005.

[51] E. Karipidis, N. D. Sidiropoulos, and Z.-Q. Luo, "Convex transmit beamforming for downlink multicasting to multiple co-channel groups," *Proc. ICASSP*, pp. 973-976, Toulouse, France, May 2006.

[52] E. Karipidis, N. D. Sidiropoulos, and Z.-Q. Luo "Quality of service and max-min fair transmit beamforming to multiple cochannel multicast groups," *IEEE Transactions on Signal Processing*, vol. 56, pp. 1268-1279, March 2008.

[53] A. Khisti, "Coding techniques for multicasting," Master thesis, Massachusetts Institute of Technology, Cambridge, MA, 2004.

[54] I. H. Kim, D. J. Love, and S. Y. Park,"Optimal and successive approaches to signal design for multiple antenna physical layer multicasting," *IEEE Transactions on Communications*, vol. 59, no. 8, pp. 2316-2327, August 2011.

[55] A. Klein, "Mobile Communication," *Lecture Script,* FB ETiT, TU-Darmstadt, 2005.

[56] V. Kühn, *Wireless Communications Over MIMO Channels: Applications to CDMA and Multiple Antenna Systems,* USA: Wiley-Blackwell, 2006.

[57] R. C. de Lamare, R. Sampaio-Neto, "Minimum mean-squared error iterative successive parallel arbitrated decision feedback detectors for DS-CDMA systems", *IEEE Transactions on Communications*, vol. 56, pp. 778-789, May 2008.

[58] J. Laneman, D. Tse, and G. Wornell, "Cooperative diversity in wireless networks: efficient protocols and outage behavior," *IEEE Transactions on Information Theory*, vol. 50, pp. 30623080, December 2004.

[59] Z. Li and X.-G. Xia, "A simple Alamouti space-time transmission scheme for asynchronous cooperative systems," *IEEE Signal Processing Letters*, vol. 14, no. 11, pp. 804807, November 2007.

[60] Y. Liang and R. Schober, "Cooperative amplify-and-forward beamforming for OFDM systems with multiple relays," *Proc. ICC*, pp. 1-6, Dresden, Germany, June 2009.

[61] W. T. A. Lopes, W. J. L. Queiroz, F. Madeiro and M. S. Alencar, "Exact bit error probability of M-QAM modulation over flat Rayleigh fading channels," *Proc. IEEE international microwave and optoelectronics conference,* Dec. 2007.

[62] M. J. Lopez, "Multiplexing, scheduling, and multicasting strategies for antenna arrays in wireless networks," Ph.D. Thesis, Department of Electrical Engineering and Computer Science, Massachusetts Institute of Technology, Cambridge, MA, 2002.

[63] A. Lozano, "Long-term transmit beamforming for wireless multicasting," *Proc. ICASSP*, pp. 417-420, Honolulu, Hawaii, USA, April 2007.

[64] Z. -Q. Luo, "Lecture notes for EE8950: Engineering Optimization," University of Minnesota, Minneapolis, Spring 2004.

[65] Z. -Q. Luo and W. Yu, "An introduction to convex optimization for communications and signal processing," *IEEE Journal on Selected Areas in Communications*, vol. 24, no. 8, pp. 1426-1438, August 2006.

[66] C. -G. Löf, "Power control in cellular radio systems with multicast traffic," *Proc. PIMRC*, vol. 2, pp. 910-914, Osaka, Japan, September 1998.

[67] W. -K. Ma, T. N. Davidson, K. M. Wong, Z. -Q. Luo, and P. -C. Ching, "Quasi-ML multiuser detection using semi-definite relaxation with application to synchronous CDMA," *IEEE Transactions on Signal Processing*, vol. 50, no. 4, pp. 912-922, April 2002.

[68] E. Matskani, N. D. Sidiropoulos, Z.-Q. Luo, and L. Tassiulas, "A Second-order cone deflation approach to joint multiuser downlink beamforming and admission Control," *Proc. SPAWC* , pp. 1-5, Helsinki, Finland, June 2007.

[69] E. Matskani, N. D. Sidiropoulos, Z.-Q. Luo, and L. Tassiulas, "Convex approximation techniques for joint multiuser downlink beamforming and admission control," *IEEE Transactions on Wireless Communications*, vol. 7, no. 7, pp. 2682-2693, July. 2008.

[70] E. Matskani and N. D. Sidiropoulos, "On multicast beamforming and admission control for UMTS-LTE," *Proc. ICASSP*, pp. 2361-2364, Las Vegas, NV, USA, April 2008.

[71] E. Matskani, N. D. Sidiropoulos, Z. -Q. Luo, and L. Tassiulas, "Convex approximation techniques for joint multiuser downlink beamforming and admission

control," *IEEE Transactions on Wireless Communications*, vol. 7, pp. 2682-2693, July 2008.

[72] E. Matskani, N. D. Sidiropoulos, Z.-Q. Luo, and L. Tassiulas, "Efficient batch and adaptive approximation algorithms for joint multicast beamforming and admission control," *IEEE Transactions on Signal Processing*, vol. 57, no. 12, pp. 4882-4894, December 2009.

[73] N. F. Mir, "A survey of data multicast techniques, architectures, and algorithms," *IEEE Communications Magazine*, vol. 39, no. 9, pp. 164-170, September 2001.

[74] M. Morimoto, M. Okada, and S. Komaki, "A hierarchical image transmission system in a fading channel," *Proc. ICUPC*, pp. 769-772, Tokyo, Japan, November 1995.

[75] A. Mutapcic, S.-J. Kim, and S. Boyd, "A Tractable method for robust downlink beamforming in wireless communications," *Proc. ACSSC*, pp. 1224-1228, Asilomar, CA, USA, November 2007.

[76] R. Nabar, H. Boelcskei, and F. Kneubuhler, "Fading relay channels: performance limits and space-time signal design," *IEEE Journal on Selected Areas in Communications*, vol. 22, no. 6, pp. 1099-1109, August 2004.

[77] A. Narula, M. J. Lopez, M. D. Trott, and G. W. Wornell, "Efficient use of side information in multiple-antenna data transmission over fading channels," *IEEE Journal on Selected Areas in Communications*, vol. 16, pp. 1423-1436, October 1998.

[78] J. Ogunbekun and A.Mendjeli, "MBMS service provision and its challenges," *Proc. Inter. Conf. on 3G Mob. Comm. Tech.*, pp. 128-133, June 2003.

[79] D. P. Palomar and J. R. Fonollosa, "Practical algorithms for a family of water-filling solutions," *IEEE Transactions on Signal Processing*, vol. 53, pp. 686-695, February 2005.

[80] J. M. Paredes, A. B. Gershman, "Relay network beamforming and power control using maximization of mutual information," *IEEE Transactions on Wireless Communications*, pp. 4356-4365, December 2011.

[81] J. M. Paredes and A. B. Gershman, "Relay network beamforming and power control using maximization of mutual information," *Proc. GLOBECOM*, Miami, FL, USA, December 2010.

[82] S. Y. Park and D. J. Love, "Capacity limits of multiple antenna multicasting using antenna subset selection," *IEEE Transactions on Signal Processing*, vol. 56, pp. 2524-2534, June 2008.

[83] A. Paulraj, R. Nabar, and D. Gore, *Introduction to Space-Time Wireless Communications,* 1st edition, USA: Cambridge University Press, 2003.

[84] J. G. Proakis, *Digital Communications,* 4th edition USA: McGraw-Hill, 2000. [4] Proakis

[85] M. B. Pursley and J. M. Shea, "Nonuniform phase-shift-key modulation for multimedia multicast transmission in mobile wireless networks," *IEEE Journal on Selected Areas in Communications*, vol. 17, pp. 774-783, May 1999.

[86] K. Ramachandran, A. Ortega, K. M. Uz, and M. Vetterli, "Multiresolution broadcast for digital HDTV using joint source/channel coding," *IEEE Journal on Selected Areas in Communications*, vol. 11, pp. 6-23, January 1993.

[87] T. Rappaport, *Wireless communications - principles and practice.*, 2nd Edition, Prentice Hall, 2001.

[88] M. Rossi, M. Zorzi, and F. H. P. Fitzek, "Investigation of link layer algorithms and play-out buffer requirements for efficient multicast services in 3G cellular systems," *Proc. PIMRC*, vol. 3, pp. 2256-2261, Barcelona, Spain, September 2004.

[89] A. Schad, and M. Pesavento, "Multiuser bi-directional communications in cooperative relay networks," *Proc. CAMSAP*, pp. 217-220, San Juan, Puerto Rico, December 2011.

[90] M. Schubert and H. Boche, "Solution of multiuser downlink beamforming problem with individual SINR constraints," *IEEE Transactions on Vehicular Technology*, vol. 53, no. 1, pp. 18-28, January 2004.

[91] M. Schubert and H. Boche, "Iterative multiuser uplink and downlink beamforming under SINR constraints," *IEEE Transactions on Signal Processing*, vol. 53, no. 7, pp. 2324-2334, July 2005.

[92] A. Sendonaris, E. Erkip, and B. Aazhang, "User cooperation diversity Part-I: system description," *IEEE Transactions on Communications*, vol. 51, no. 11, pp. 1927-1938, November 2003. [100] Sendonaris

[93] A. Sendonaris, E. Erkip, and B. Aazhang, "User cooperation diversity Part-II: Implementation aspects and performance analysis," *IEEE Transactions on Communications*, vol. 51, no. 11, pp. 1939-1948, November 2003.

[94] U. Sethakaset and S. Sun, "Sum-rate maximization in the simultaneous unicast and multicast services with two Users," *Proc. PIMRC*, pp. 672-677, Istanbul, Turkey, September 2010.

[95] C. E. Shannon, "A mathematical theory of communication," *Bell System Technical Journal*, vol. 27, pp. 379-423, July 1948.

[96] M. Sharif and B. Hassibi, "A comparison of time-sharing, DPC, and beamforming for MIMO broadcast channels with many users," *IEEE Transactions on Communications*, vol. 55, no. 1, pp. 1115, January 2007.

[97] N. D. Sidiropoulos, T. N. Davidson, and Z.-Q. Luo, "Transmit beamforming for physical-layer multicasting," *IEEE Transactions on Signal Processing*, vol. 54, pp. 2239-2251, June 2006.

[98] N. D. Sidiropoulos and Z.-Q. Luo, "A semidefinte relaxation approach to MIMO detection for high-order QAM constellations," *IEEE Signal Processing Letters*, vol. 13, pp. 525-528, September 2006.

[99] Y. C. B. Silva and A. Klein, "Multicast transmission performance improvement through adaptive antenna arrays," Karlsruhe Workshop on Software Radios (WSR), March 2006.

[100] Y. C. B. Silva and A. Klein, "Adaptive antenna techniques applied to multicast services," *Frequenz-Journal of RF-Engineering and Telecommunications*, vol. 60, pp. 199-202, September 2006.

[101] Y. C. B. Silva and A. Klein, "Adaptive beamforming and spatial multiplexing of unicast and multicast services," *Proc. PIMRC*, pp. 1-5, Helsinki, Finland, September 2006.

[102] Y. C. B. Silva and A. Klein, "Downlink beamforming and SINR balancing for the simultaneous provision of unicast/multicast services," *Proc. IST Mobile Wireless Commun. Summit*, pp. 15, Budapest, Hungary, July 2007.

[103] Y. C. B. Silva and A. Klein, "Analysis of linear and non-linear precoding techniques for spatial separation of unicast and multicast users," *Proc. PIMRC*, pp. 1-5, Athens, Greece, September 2007.

[104] Y. C. B. Silva and A. Klein, "Linear Transmit Beamforming Techniques for the Multigroup Multicast Scenario", *IEEE Transactions on Vehicular Technology*, vol. 58, no. 8, October 2009.

[105] Q. H. Spencer and M. Haardt, "Capacity and downlink transmission algorithms for a multi-user MIMO channel," *Proc. Asilomar*, vol. 2, pp. 1384-1388, Pacific Grove, CA, November 2002.

[106] Q. H. Spencer, A. L. Swindlehurst, and M. Haardt, "Zero-forcing methods for downlink spatial multiplexing in multiuser MIMO channels," *IEEE Transactions on Signal Processing*, vol. 52, pp. 461-471, February 2004.

[107] J. F. Sturm, "Using SeDuMi 1.02, a MATLAB toolbox for optimization over symmetric cones," *Optim. Meth. Software*, vol. 11-12, pp. 625-653, August 1999.

[108] Y. Sun and K. J. R. Liu, "Transmit diversity techniques for multicasting over wireless networks," *Proc. WCNC,* vol. 1, pp. 593-598, March 2004. [39] Liu

[109] C. -E. W. Sundberg, W. C. Wong, and R. Steele, "Logarithmic PCM weighted QAM transmission over Gaussian and Rayleigh fading channels," *IEE Proceedings-F*, vol. 134, pp. 557-570, October 1987.

[110] A. Tajer, N. Parsad, and X. Wang, "Robust transceiver design for the multi-user interference channel," *Proc. ICC*, pp. 1-5, Cape Town, South Africa, May 2010. [12] Tajer

[111] S. Talwar, Y. Jing, and S. Shahbazpanahi, "Joint relay selection and power allocation for two-way relay networks," *IEEE Signal Processing Letters*, vol. 18, pp. 91-94, February 2011. [114] Talwar

[112] M. Tomlinson, "New automatic equalizer employing modulo arithmetic," *Electronic Letters*, vol. 7, pp. 138-139, March 1971.

[113] D. Tse and P. Viswanath, *Fundamentals of wireless communication,* USA: Cambridge University Press, 2005.

[114] P. Tseng, "Further results on approximating nonconvex quadratic optimization by semidefinite programming relaxation," *SIAM J. Optim.,* vol. 14, no. 1, pp. 268-283, July 2003.

[115] B. D. Van Venn, and K. M. Buckley, "Beamforming: A versatile approach to spatial filtering,"*IEEE ASSP Magazine,* pp. 4-24, April 1988.

[116] U. Varsheny, "Multicast over wireless networks," *Communications of ACM*, vol. 45, no. 12, pp. 31-37, December 2002. [24] Var

[117] S. A. Vorobyov, A. B. Gershman, and Z.-Q. Luo, "Robust adaptive beamforming using worst-case performance optimization: A solution to the signal mismatch problem," *IEEE Transactions on Signal Processing*, vol. 51, pp. 313-324, February 2003.

[118] I. Wajid, A. B. Gershman, S. A. Vorobyov, and Y. A. Karanouh, "Robust multiantenna broadcasting with imperfect channel state estimation," *Proc. CAMSAP,* pp. 213-216, Virgin Islands, USA, December 2007.

[119] S. Wang, S. Kwon. and B.K. Yi, "On enhancing hierarchical modulation," *Proc. BMSB*, pp. 1-6, Las Vegas, NV, USA, March 2008.

[120] J. Wang, M. D. Zoltowski, and D. J. Love, "Improved space-time coding for multiple antenna multicasting," in *Proc. IEEE Int. Waveform Diversity Design Conf.,* January 2006.

[121] Z. Wang and G. B. Giannakis, "Wireless Multicarrier Communications: where Fourier Meets Shannon," *IEEE Signal Processing Magazine*, vol. 17, no. 3, pp. 29-48, May 2000.

[122] S. Wei, D. L. Goeckel, and M. Valenti, "Asynchronous cooperative diversity," *IEEE Transactions on Wireless Communications*, vol. 5, no. 6, pp. 1547-1557, June 2006.

[123] L. -F. Wei, "Coded modulation with unequal error protection," *IEEE Transactions on Communications*, vol. 41, pp. 1439-1449, October 1993.

[124] A. Wiesel. Y. C. Eldar, and S. Shamai, "Linear precoding via conic optimization for fixed MIMO receivers," *IEEE Transactions Signal Processing*, vol. 54, no. 3, pp. 161-176, January 2006.

[125] Y. Ye, *Interior Point Algorithms: Theory and Analysis*, New York: Wiley, 1997.

[126] J. Zhang, A. M. Sayeed, and B. D. V. Veen, "Optimal transceiver design for selective wireless broadcast with channel state information," *Proc. ICASSP*, vol. 3, pp. 2153-2156, Orlando, Florida, USA, May 2002.

[127] J. Zhang, A. M. Sayeed, and B. D. V. Veen, "Optimal transceiver design for selective wireless broadcast with channel state infromation," *IEEE Transactions on Wireless Communications*, vol. 3, pp. 2040-2050, November 2004.

[128] S. Zhang, "Quadratic maximization and semidefinite relaxation," *Mathematical Programming*, ser. A, vol. 87, pp. 453-465, 2000.

Wissenschaftlicher Werdegang

Studium

- Promotion, "Multiple-Antenna multicasting and Relay Beamforming in Multi-user Networks", Technische Universität Darmstadt, April 2008 - 2012.
- Master in Information- and Communication Engineering, Technische Universität Darmstadt, Oktober 2004 - April 2008.
  Notendurchschnitt: Gut (1,75).
- Masterarbeit, " Downlink Transmit Beamforming for Wireless Multicast Networks",Technische Universität Darmstadt, März 2007 - Oktober 2008.
  Note: Sehr gut (1,0).
- Bachelor in Elektro- und Nachrichtentechnik, Universität Alexandria, Ägypten, September 1997 - September 2002.
  Notendurchschnitt: Sehr gut.
- Bachelorarbeit, "Bluetooth Drahtlose Technoligie und ihre Anwendungen", Universität Alexandria, Ägypten, März 2002 - July 2002.
  Note: Sehr gut.

Berufserfahrung

- Wissenschaftlicher Mitarbeiter am Institut für Nachrichtentechnik-Fachgebiet Nachrichtentechnische Systeme, Technische Universität Darmstadt, März 2011 - März 2012.
- Wissenschaftliche Hilfskraft am Institut für Kommunikationstechnik-Fachgebiet Nachrichtentechnische Systeme, Technische Universität Darmstadt, Juni 2007 - August 2007.

Publikationen

- A. Abdelkader, A. B. Gershman, and N. D. Sidiropoulos, "Multiple-Antenna Multicasting Using Channel Orthogonalization and Local Refinement," *IEEE Transactions on Signal Processing*, vol. 58, no. 7, pp. 3922-3927, July 2010.
- Abdelkader, I. Wajid, A. B. Gershman, and N. D. Sidiropoulos, "Transmit beamforming for wireless multicasting using channel orthogonalization and local refinement," *Proceedings of the IEEE International Conference on Acoustics, Speech and Signal Processing (ICASSP'09)*, pp. 2281-2284, Taipei, Taiwan, April 2009.
- A. Abdelkader, S. Shahbazpanahi, and A. B. Gershman, "Joint Subcarrier Power Loading and Distributed Beamforming in OFDM-Based Asynchronous Relay Networks," *Proceedings of the Fourth International Workshop on Computational Advances in Multi-Sensor Adaptive Processing (CAMSAP2009)*, pp. 105-108, Aruba, December 2009.
- A. Abdelkader, M. Pesavento, and A. B. Gershman, "Orthogonalization Techniques for Single Group Multicasting in Cooperative Amplify-And-Forward Networks," *Proceedings of the Fourth International Workshop on Computational Advances in Multi-Sensor Adaptive Processing (CAMSAP2011)*, pp. 225-228, San Juan, Puerto Rico, December 2011.